

Dissertation zur Erlangung des Doktorgrades  
der Fakultät für Chemie und Pharmazie  
der Ludwig-Maximilians-Universität München



siRNA Therapy for Cancer: Evaluation of Oligomers  
for the *in vitro* and *in vivo* Delivery

vorgelegt von

Daniel Edinger

aus München

2013

### Erklärung

Diese Dissertation wurde im Sinne von § 7 der Promotionsordnung vom 28. November 2011 von Herrn Prof. Dr. Ernst Wagner betreut.

### Eidesstattliche Versicherung

Diese Dissertation wurde eigenständig und ohne unerlaubte Hilfe erarbeitet.

München, den 25.04.2013

.....  
(Unterschrift des Autors)

Dissertation eingereicht am: 25.04.2013

1. Gutachter: Prof. Dr. Ernst Wagner

2. Gutachter: Prof. Dr. Gerhard Winter

Mündliche Prüfung am: 19.06.2013

---

## TABLE OF CONTENTS

<b>1</b>	<b>INTRODUCTION .....</b>	<b>1</b>
1.1	Nucleic Acid Therapy .....	1
1.2	siRNA Design .....	3
1.3	Polymers and Oligomers for siRNA Delivery .....	4
1.3.1	siRNA Packaging .....	5
1.3.2	Endosomal Escape .....	8
1.3.3	Polyplex Shielding.....	9
1.3.4	Receptor Targeting .....	10
1.4	Target Genes .....	12
1.5	Aims of the Thesis.....	14
<b>2</b>	<b>MATERIALS AND METHODS .....</b>	<b>16</b>
2.1	Materials.....	16
2.2	siRNAs .....	16
2.3	Oligomers .....	17
2.4	Polyplex Formation .....	18
2.5	Biophysical Characterization .....	18
2.5.1	Particle Size and Zeta Potential Measurement .....	18
2.5.2	Agarose Gel Shift Assay.....	18
2.5.3	Serum Stability Assay .....	19
2.6	Biological Characterization <i>in vitro</i> .....	19
2.6.1	Cell Culture.....	19
2.6.2	GFP Knockdown Assay.....	20
2.6.3	Quantitative Real Time Polymerase Chain Reaction .....	21
2.6.4	Western Blot .....	21
2.6.5	Flow Cytometry .....	22
2.6.5.1	Receptor Level Studies .....	22
2.6.5.2	Receptor Binding Studies.....	22
2.6.5.3	Cell Cycle Measurement .....	23

---

2.6.6	Fluorescence Microscopy .....	23
2.6.7	CellTiter Glo Assay .....	24
2.6.8	Dihydrofolatereductase Activity Assay .....	24
<b>2.7</b>	<b>Biological Characterization <i>in vivo</i> .....</b>	<b>25</b>
2.7.1	Mouse Strains .....	25
2.7.2	Histological Studies .....	25
2.7.2.1	Polyplex Distribution .....	25
2.7.2.2	Aster Formation .....	25
2.7.2.3	H&E Staining .....	26
2.7.3	Polyplex Imaging.....	26
2.7.3.1	Polyplex Retention after i.t. Injection .....	26
2.7.3.2	Polyplex Distribution after i.v. Injection.....	27
2.7.3.3	Gel Electrophoresis of Urine Samples .....	27
2.7.4	Therapeutic Assays.....	28
2.7.4.1	Dose Finding .....	28
2.7.4.2	siRNA Comparison .....	28
2.7.4.3	Oligomer Comparison .....	29
<b>2.8</b>	<b>Statistical Analysis.....</b>	<b>29</b>
<b>3</b>	<b>RESULTS.....</b>	<b>30</b>
<b>3.1</b>	<b>Oligoamides for siRNA Delivery .....</b>	<b>30</b>
3.1.1	Design of Precise Carriers for siRNA Delivery .....	30
3.1.2	Identification of Powerful siRNA Carriers.....	31
3.1.2.1	Biophysical Characterization .....	32
3.1.2.2	GFP Knockdown Screen .....	33
3.1.3	Therapeutic Gene Silencing.....	35
3.1.3.1	Eg5 and Ran Silencing on mRNA and Protein Level .....	36
3.1.3.2	Cell Cycle Analysis.....	38
3.1.3.3	Cell Viability Assay .....	42
3.1.4	Distribution of Fluorescence Labeled Polyplexes .....	42
3.1.4.1	Histological Cy3 Analysis .....	43
3.1.4.2	Living Image .....	44
3.1.5	Dose Escalation Study .....	45
3.1.6	Evaluation of Therapeutic siRNAs.....	47

---

3.1.7	Comparison of Different siRNA Carriers.....	49
3.1.8	Oligoamides with Enhanced Stability .....	52
3.1.8.1	Biophysical Characterization .....	52
3.1.8.2	GFP Knockdown Screen .....	54
3.1.8.3	Distribution of Fluorescence Labeled Polyplexes.....	55
3.1.8.4	Oligomer Screen.....	59
<b>3.2</b>	<b>Targeted Oligoamides for siRNA Delivery .....</b>	<b>61</b>
3.2.1	Folic Acid Linked Targeting Oligomers .....	61
3.2.1.1	Biophysical Characterization .....	62
3.2.1.2	Folic Acid Receptor Levels in Different Cell Lines .....	64
3.2.1.3	Uptake Studies in KB and IGROV Cells .....	65
3.2.1.4	GFP and Eg5 Knockdown Studies <i>in vitro</i> .....	66
3.2.1.5	Polyplex Distribution and Polyplex Retention <i>in vivo</i> .....	69
3.2.1.6	Eg5 Knockdown Study <i>in vivo</i> .....	74
3.2.2	Methotrexate linked Targeting Oligomers .....	75
3.2.2.1	Sensitivity of Different Cell Lines to MTX.....	77
3.2.2.2	Cytotoxicity of MTX Oligomers.....	77
3.2.2.3	Uptake Studies .....	79
3.2.2.4	GFP Knockdown in KB Cells .....	80
3.2.2.5	Combined Toxicity of MTX/siEG5 Polyplexes.....	81
<b>4</b>	<b>DISCUSSION.....</b>	<b>83</b>
<b>4.1</b>	<b>Evaluation of Monodisperse, Sequence Defined siRNA Carriers.....</b>	<b>83</b>
4.1.1	Oligomer Evaluation <i>in vitro</i> and <i>in vivo</i> .....	83
4.1.2	Tyrosine Trimer Stabilized T-shape Oligomers .....	86
<b>4.2</b>	<b>Evaluation of Targeted Nanocarriers for siRNA Delivery .....</b>	<b>88</b>
4.2.1	Nanocarriers with Targeting Ligand Folic Acid.....	88
4.2.2	Nanocarriers with Targeting Ligand Methotrexate .....	90
<b>5</b>	<b>SUMMARY .....</b>	<b>93</b>
<b>6</b>	<b>APPENDIX.....</b>	<b>95</b>
<b>6.1</b>	<b>Abbreviations.....</b>	<b>95</b>
<b>6.2</b>	<b>Publications .....</b>	<b>98</b>

---

6.2.1	Original Papers .....	98
6.2.2	Review .....	99
6.2.3	Patent .....	99
6.2.4	Poster Presentations .....	99
<b>7</b>	<b>REFERENCES.....</b>	<b>100</b>
<b>8</b>	<b>ACKNOWLEDGEMENTS.....</b>	<b>110</b>

# 1. INTRODUCTION

## 1.1 Nucleic Acid Therapy

Nucleic acid therapies have been considered as a confident chance for the treatment of life-threatening illnesses like cancer and genetic diseases<sup>1</sup>. The approach is based on technologies which deliver therapeutic nucleic acids into target tissues. Direct uptake into target cells is hindered because of the high molecular weight and the negative charge of nucleic acids. Nucleic acid therapies may occur within the patient's body (*in vivo*) or outside the body (*ex vivo*) using isolated body cells. Therapeutic gene vectors can directly regulate gene expression as viral vectors encapsulating a gene expression vector<sup>2-3</sup>, or nonviral plasmid DNA (pDNA) expression vectors<sup>4</sup>. This strategy is promising for the treatment of inherent deficiencies by replacing either missing or unfunctional genes. In the case of DNA-based vectors, the nucleic acid needs to be introduced into the nucleus where it has to be maintained in accessible, active form to be expressed by the host cell transcription machinery.

With time, other nucleic acid therapeutics have obtained increasing importance where nucleic acids can influence gene expression more indirectly than gene vectors do, most importantly small interfering RNAs (siRNA)<sup>5</sup>, but also single-stranded oligonucleotides<sup>6-8</sup>, or immune system stimulating nucleic acids<sup>9</sup>. RNA interference (RNAi) mediated by 21-23 bp long double stranded siRNA operates in the cytosol<sup>10-12</sup>. Among the two strands the guide strand is designed to be complementary to the target mRNA, whereas the passenger strand normally has no complementarity. After cellular uptake the siRNA duplex is bound to several proteins like Ago2, Dicer and transactivating response RNA binding protein (TRBP), forming the RISC (RNA induced silencing complex) loading complex (RLC)<sup>13-14</sup>. Following 5' phosphorylation by ATP leads to unwinding of the siRNA and the cleavage of the passenger strand by Ago2, resulting in the mature RISC complex<sup>15</sup>. Complementary mRNA is recognized by RISC and consequently cleaved, by PIWI a subunit of Ago2, opposite to nucleotide 10 from the 5' end<sup>16-18</sup>. Active RISC complex can be recycled and repeatedly silence mRNA for several weeks. This demonstrates the high specificity and effectivity of siRNAs ideal for functional studies and therapeutic applications (Figure 1).

Similar effects are mediated by endogenous microRNAs<sup>19-20</sup> (miRNA). Around 1600 miRNAs have been found in humans (miRBase), regulating processes by translational repression. The main difference to siRNAs is the reduced complementarity of miRNAs to their target mRNAs resulting in translational repression without mRNA cleavage. miRNAs are explored as biomarkers<sup>21</sup> for several illnesses and as targets for future therapies<sup>22</sup>.

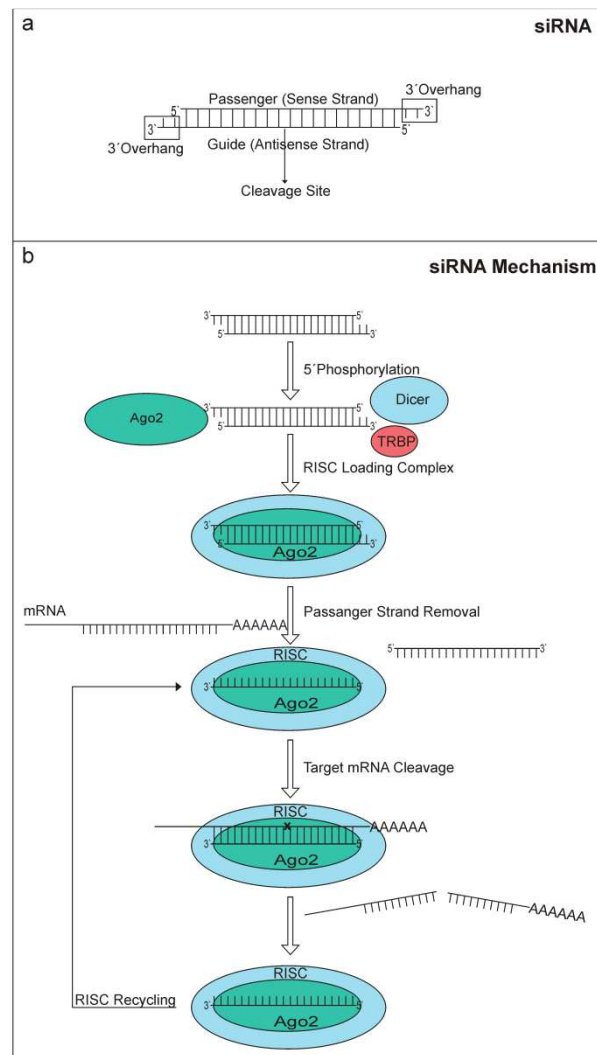


**Figure 1 siRNA structure and mechanism:** a) siRNA double strand consisting of passenger and guide strand with 3' overhangs. b) siRNA is phosphorylated after cellular uptake and loaded into the RISC complex. The guide strand mediates mRNA recognition and binding which leads in case of a perfect match to mRNA cleavage. (Modified from Shukla et al.<sup>23</sup>)

Oligonucleotides (ON) are short single stranded nucleic acids or stabilized nucleic acid analogs with 20 or fewer bases. ONs can be used for several purposes, acting either in the cytosol or the nucleus. As antisense molecules they may bind to complementary mRNA and inhibit their translation or to miRNAs avoiding the inhibition<sup>24</sup>. ONs have also been used as agents in exon-skipping, to repair

defective mRNA by alternative splicing<sup>25</sup>, and as antagomirs, blocking natural micro RNAs<sup>6,26</sup>.

## 1.2 siRNA Design

Computational models have been developed to increase the likelihood of selecting effective and specific siRNAs<sup>27</sup>. Besides the selection of a siRNA sequence the stability of nucleic acids is critical because they are targets of ubiquitous occurring nucleases. Unmodified siRNAs have a serum half life of less than 15 min, so they are impractical for therapeutic applications<sup>28</sup>. Modifications improving nuclease resistance are incorporated into the siRNA sequence either into the backbone, sugar, base or 3' and 5' ends. Common backbone modifications include the replacement of non bridging oxygen by sulfur in the phosphate backbone (phosphorothioate) leading to improved nuclease resistance<sup>29</sup>. This phosphorothioate modification leads to less efficient RISC loading if used heavily in the guide strand. Widely used sugar modifications include 2'-OMe, 2'-fluoro and 2'-MOE<sup>30</sup>. All of these sugar modifications increase the melting temperature and improve nuclease resistance. Another modification with high impact on the melting temperature is the incorporation of locked nucleosides<sup>31</sup>. In this method the position 2' and 4' of the ribose ring are linked through a methylene bridge. Furthermore, the thermodynamic properties of both siRNA ends influence RISC loading. Passenger strand modification increasing the 5' end melting temperature lead to selective incorporation of the guide strand<sup>32</sup>.

In addition to stability reasons, modifications are necessary to combat the immunostimulatory effect of unmodified siRNAs. The effects are mainly mediated due to the activation of toll like receptors TLRs 3, 7 and 8 and cytosolic proteins like RIG-1 (retinoic acid inducible protein), or MDA-5 (melanoma differentiation associated protein)<sup>33</sup>. All these receptors can recognize double stranded RNAs and induce immune response mediated by interferons, cytokines and interleukin-6. For example TLR 3 is activated by double stranded nucleotides longer than 21-23bp, whereas the TLR 7 and 8 are activated by different motifs in the nucleotide sequence. Therefore, several modifications, for example 2'-OMe, are necessary to generate siRNAs without immunostimulatory effects. Great progress in the field of nucleic acid chemistry enabled the synthesis of nucleic acids with high serum stability and low immunostimulatory effects<sup>23,34-35</sup>.

### 1.3 Polymers and Oligomers for siRNA Delivery

Nonviral delivery systems have been proposed as safer alternatives to viral vectors, because polymers and liposomes avoid the inherent immunogenicity of viral proteins and the expensive production in mammalian cell culture systems. Hence, several reasons have supported the use of polymers, including the fact that nucleic acids themselves are polymers which by the nature of their negative charges spontaneously form complexes ('polyplexes') with cationic polymers<sup>36</sup>. Nature utilizes the mechanism in multiple variations, for example in packaging genetic material with basic protein polymers into chromatin, strongly condensing DNA in sperm heads, or compacting DNA into virus core particles. Evolution has optimized such packaging into precise bioresponsive processes, where both assembly and disassembly can occur in a controlled manner. In contrast to nature, the first two to three decades of polymer based gene transfer development have yielded first encouraging, but still very primitive solutions. Low transfer efficiency of polyplexes, significant toxicity, polymer polydispersity and poorly understood delivery mechanisms are road blocks in the way towards therapeutically useful polymer formulations. Fortunately, recent developments present solutions for many of the obstacles<sup>37</sup>. Improved chemistry has resulted in the design of monodisperse polymer structures like dendrimers<sup>38</sup> or other sequence defined oligomers<sup>39-41</sup>. Biodegradable oligomers with reduced cytotoxicity have been designed, allowing the incorporation of targeting ligands and surface shielding polymers. Shielded polyplexes minimize side effects due to unspecific interactions, whereas targeting ligands like small molecules or peptides allow specific interactions with cancer cells. Better understanding of delivery pathways and improved imaging methods<sup>42-45</sup> contributed to the design of improved carriers for siRNA delivery. These bioresponsive carriers can change their properties, for example their conformation, through protonation, or by cleavage of covalent bonds in various biological compartments. This means the biological micro-environment can be used to trigger the oligomer and therefore the polyplex characteristics during the delivery process in a favorable dynamic way. Such dynamic processes are well-known from cellular entry of viruses, bacteria, toxins, and other cellular events. Major delivery tasks (Figure 2) are the transport of a siRNA without undesired interactions in blood and non-target sites.

In contrast, specific interactions with the target cell surface should trigger intracellular uptake followed by endosomal escape.

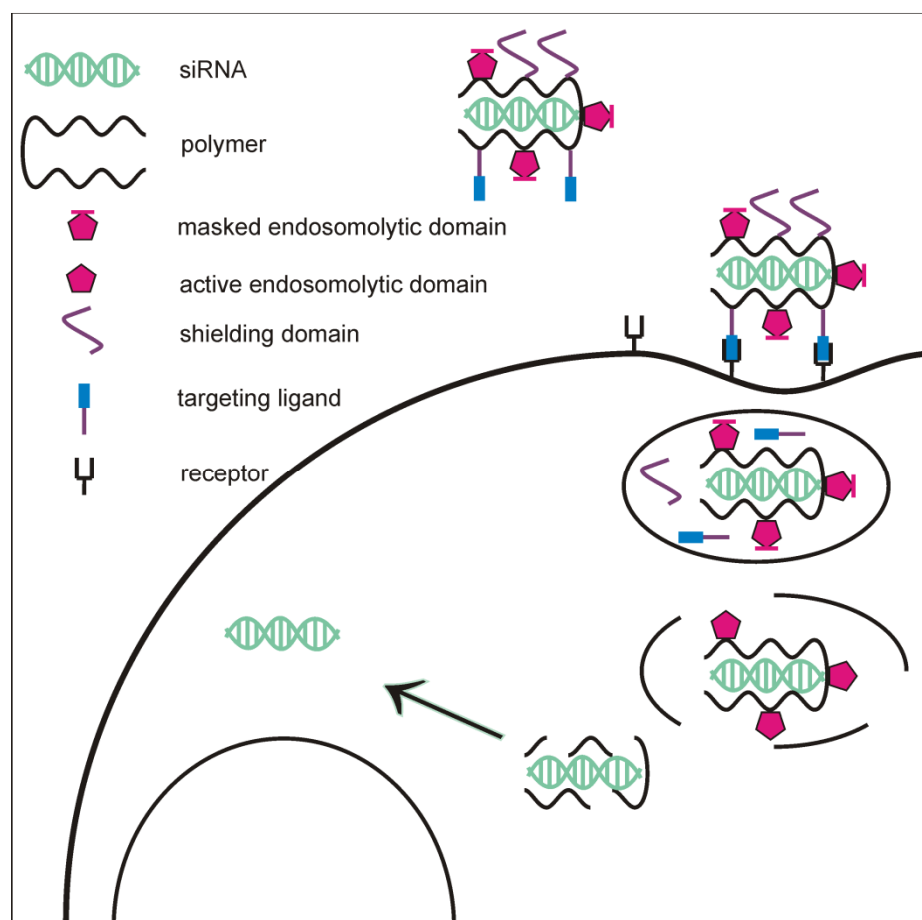


**Figure 2 Uptake process of functionalized polyplexes into the target cell:** Hurdles for the efficient siRNA delivery are the stable binding of the nucleic acid, interactions with the cell surface, endosomal escape and the release of the siRNA into the cytosol (modified from D. Edinger et al.<sup>46</sup>)

### 1.3.1 siRNA Packaging

In the first instance the oligomer has to stably bind the nucleic acid outside the cell, to compact and protect the cargo from nucleases. Inside the cell the polyplex has to disassemble and release the siRNA, so the cargo can be effective. Different chemical characteristics outside the cell, in the endosome, the cytosol, and the nucleus have to manage the “assembly-disassembly” process. Therapeutic nucleic acids can be either noncovalently complexed or covalently conjugated to the carrier (Figure 3). Release of the nucleic acid at the target location from the polymer may proceed for example by exchange processes against polyions such as intracellular RNA<sup>47</sup>, by polymer degradation, or cleavage of the nucleic acid from the polymer attachment sites.

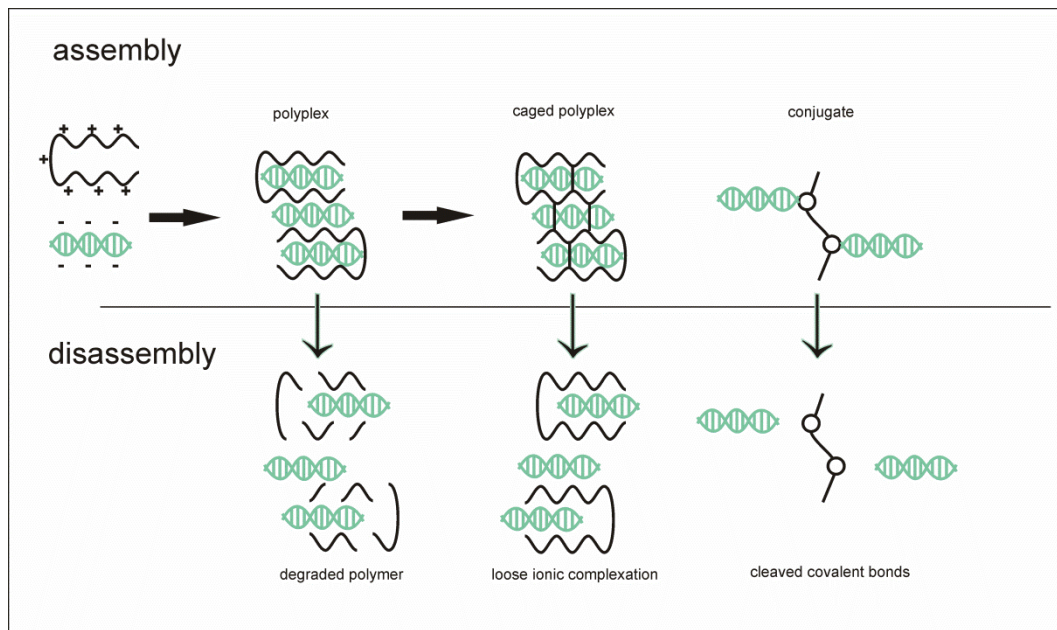


**Figure 3 Assembly-disassembly process:** Nucleic acids can be bound electrostatic or covalent by the polymers. Electrostatic assembled polyplexes can be stabilized by reversible caging. After entering the cell, the nucleic acid is released through exchange reactions or polymer degradation. (from D. Edinger et al.<sup>46</sup>)

Electrostatic binding of siRNA to cationic oligomers is weaker as compared to pDNA, due to the lower number of negative charges in the short phosphate backbones. To overcome this hurdle chemically synthesized siRNAs can be covalently bound to their carriers<sup>48</sup>. This can be performed in a bioresponsive, reversible way, for example, disulfide bonds are stable in the bloodstream, but can be easily cleaved in the cytosol. Rozema et al. applied this strategy for the synthesis of “dynamic polyconjugates” of siRNA with polymers consisting of receptor-targeted, PEG-masked poly-butyl amino vinyl ethers<sup>49</sup>. In a mouse model they could show dose dependent hepatocyte-specific gene knockdown without detectable side effects, monitored by the control of liver enzymes and cytokine levels. Meyer et al. coupled siRNA with a 5′thiol modified sense strand to modified polylysine (PLL) with an endosomolytic peptide via bioreducible disulfide bonds<sup>50</sup>. The covalent character of the conjugates was demonstrated in that the conjugates were only cleavable through a combination of heparin with a reducing reagent. Nucleic acids modified with several functional domains like targeting, shielding and endosomal escape offer a promising approach for future siRNA therapeutics<sup>51</sup>.

In contrast to the covalent binding of siRNA cationic polymers, primarily binding nucleic acids via electrostatic interactions with the negatively charged phosphate backbone have been synthesized. Nucleic acid binding depends on charge density,

size, shape, and flexibility/rigidity of polymers. For example, linear polymers such as poly(L)lysine<sup>52</sup> or linear polyethylenimine (LPEI)<sup>53</sup>, branched structures such as branched PEI (brPEI)<sup>54</sup>, or dendrimers including polyamidoamines (PAMAMs)<sup>55-58</sup> have been used. In addition to electrostatic interaction, hydrogen bonding<sup>59</sup> and hydrophobic polymer interactions<sup>60-61</sup> can increase the stability of polyplexes, but stronger nucleic acid affinity does not necessarily directly correlate with higher transfection efficiency. Apparently an optimum has to be reached. Also the big difference in the size of different types of nucleic acids (pDNA with several thousand negative charges as opposed to siRNA with 42 negative charges) has to be considered in this respect. For example, 22 kDa LPEI and 25 kDa brPEI have been successfully used for pDNA transfection, but do not effectively work for siRNA transfection<sup>62</sup>. Besides the weak silencing activity PEI-siRNA polyplexes are dissociated in full human serum monitored by fluorescence fluctuation spectroscopy<sup>63</sup>. Concatemerization of siRNA into larger structures (“sticky siRNA”)<sup>64</sup> or change to other polymer backbones can partly but not completely overcome the problem.

Bioresponsive carriers are a logical solution for the insufficient stability outside but too high stability inside the cell. Encouraging strategies including the design of biodegradable high-molecular weight polymers or polymer cages intracellularly degrading into low molecular weight nontoxic fragments have been applied. Polymers with cleavable bonds including hydrolysable esters<sup>65-67</sup>, acetal bonds degrading in the acidic environment of endosomes<sup>68-69</sup>, or disulfide bonds which are reduced in the cytosol have been synthesized<sup>70-72</sup>.

Polyplexes can further be stabilized by caging, this means chemical crosslinking of the siRNA bound polymers via cleavable linkers. For example, Russ et al.<sup>73</sup> synthesized pseudodendrimers called HDO consisting of low molecular weight oligoethylenimine (OEI) and diacrylate esters delivering siRNA with moderate gene silencing efficiency *in vitro*. Lateral stabilization by crosslinking surface amines via bifunctional crosslinker (DSP) resulted in improved stability and high knockdown efficiency<sup>74</sup>. The design of pseudo amino acids suitable for solid-phase-supported synthesis in combination with natural amino acids and fatty acids allowed the design of structure defined oligomers for siRNA transfection. From this approach nice structure activity relationships for effective siRNA carriers can be derived<sup>75</sup>. In contrast to the first generation of polydisperse carriers this new

concept also simplifies the GMP production of monodisperse carriers important for future clinical trials.

### 1.3.2 Endosomal Escape

Polyplexes are commonly taken up by a clathrin-, caveolin- dependent or related endocytic pathway, with polyplexes ending up inside endosomes. In time the endosomal pH decreases and endosomes fuse and mature to lysosomes. To deliver the siRNA into the cytosol, polyplexes have to escape this harsh environment. Either the carrier polymer itself or an endosomolytic domain has to mediate this process<sup>76-77</sup>. Because lipid membrane interaction and lysis would be a toxic event if occurring at the cell surface or mitochondrial membrane, the lytic activity has to be limited to the endosomes. Again bioresponsive polymers demonstrating an endosomal dependent lytic activity<sup>78-80</sup> are the solution to this problem (Figure 4). In contrast, small polyplexes can show alternative uptake-mechanisms avoiding the endosomal pathway<sup>81-82</sup>.

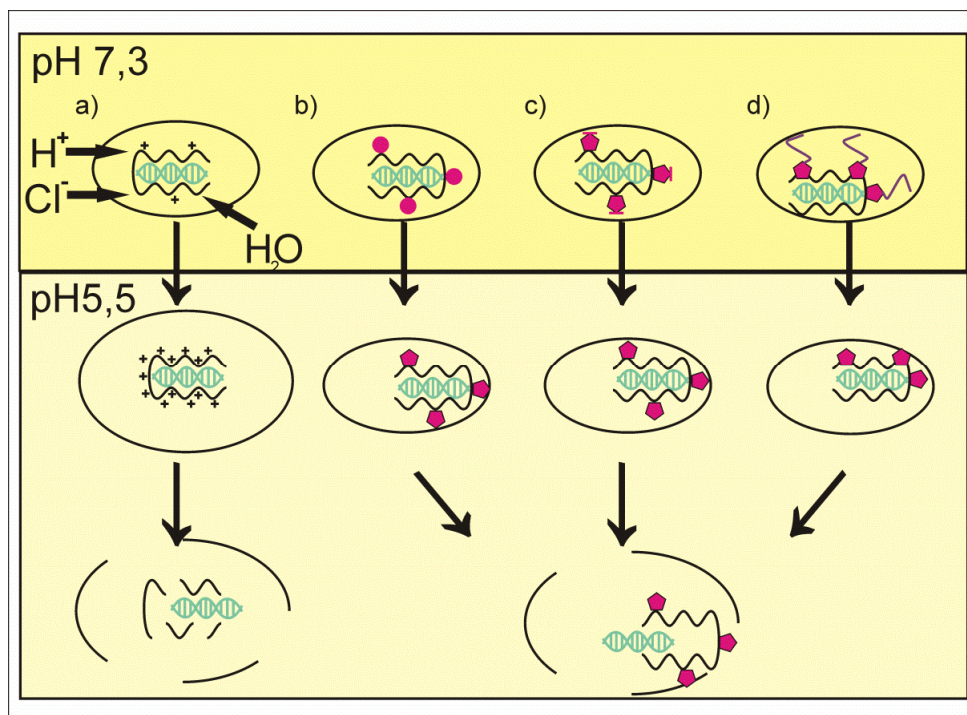


**Figure 4 Endosomal escape:** **a)** mediated by the proton sponge effect, **b)** pH dependent lytic activity, **c)** pH triggered lytic activity, **d)** or by a reductive mechanism (from D. Edinger et al.<sup>46</sup>).

PEI or PAMAM dendrimers are highly active in gene transfer, because these polymers are “proton sponges”, displaying about 20% protonation of nitrogens at neutral pH (important for nucleic acid binding), which increases with endosomal acidification. The increased density of positive charges leads to an influx of

chloride and water into the endosome<sup>83</sup>. Finally, as consequence of the so called “proton sponge effect”, the endosome bursts due to the elevated osmotic pressure and the membrane destabilizing effect of positively charged polymer domains. Efficient endosomal escape however, still presents a bottle neck to be optimized for the delivery process of therapeutic nucleic acids. For PEI the window between effective dose for endosome disruption and cytotoxic dose is very narrow. For efficient siRNA delivery brPEI 25 kDa was modified with succinic acid (PEI-Succ10)<sup>54</sup>. This modification diminishes positive charges at neutral pH, but the polymer still presents a proton sponge, containing both protonable carboxylates and nitrogens. Because of a far lower cytotoxicity it is possible to apply higher doses of the polymer and to improve endosomal escape in this way.

In contrast, polymers like polylysine (PLL) cannot destabilize endosomes themselves. Hence, natural or synthetic lytic domains must be incorporated into such carriers. For example viruses have developed strategies to efficiently overcome the endosomal barrier. In several cases fusion peptides, such as those occurring at the N-terminus of the influenza virus haemagglutinin subunit 2 (HA2), can generate a fusion pore in the membrane, triggering viral and host membrane fusion. Plank et al. suggested the HA2 subunit Inf7 consisting of the 23 amino terminal amino acids as pH specific endosome disruptive peptide<sup>84</sup>. Also lipid-free viruses such as adenovirus or rhinovirus have developed endosomal membrane destabilizing peptides. Therefore, incorporation of synthetic analogs of viral peptides, whole inactivated virus particles<sup>2</sup>, recombinant fusion proteins derived from bacteria<sup>78</sup>, toxins and other natural sources have strongly enhanced endosomal escape<sup>84-87</sup>.

### 1.3.3 Polyplex Shielding

Electrostatic siRNA binding generally results in positively charged polyplexes. This positive charge enhances target cell interaction, but also provokes unintended interactions with biological surfaces including protein surfaces, extracellular matrix and nontarget cells. Shielding the surface charges of polyplexes provides improved solubility, reduced aggregation with serum proteins, better biocompatibility, and prolonged blood circulation. For this reason the addition of Polyethylenglycol (PEG) has been broadly explored. The shielding domain can either be bound through, covalent incorporation of PEG to the polymeric carrier<sup>88-</sup>

<sup>92</sup>, direct PEGylation of the nucleic acid<sup>51,93-95</sup>, or by PEGylation after polyplex formation<sup>96-97</sup>. In addition to PEG, other hydrophilic molecules like polyhydroxypropylmethacrylate (pHPMA)<sup>98-99</sup>, hyaluronan<sup>100</sup> or hydroxyethyl starch (HES)<sup>101</sup> have been applied reducing the positive surface charge of polyplexes. HES is a biodegradable shield, therefore shielded particles are slowly deshielded in the circulation by  $\alpha$ -Amylase. In contrast to the stable, irreversible surface shielding of other shielding agents, this was advantageous for *in vivo* applications enabling the interaction with cell surfaces and lipid membranes<sup>102</sup>.

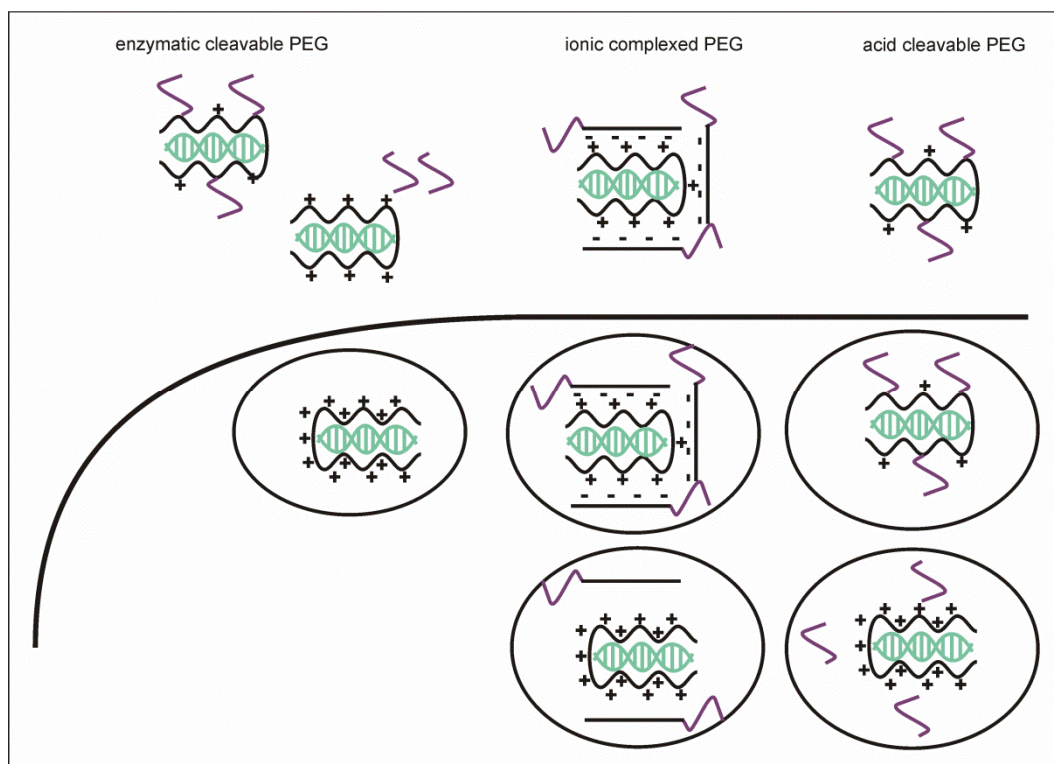


**Figure 5 Different PEGylation methods:** Polymers can be PEGylated through diversely cleavable linkers. The dePEGylation of these cleavable linkers may take place in the microenvironment of the tumor (enzymatic), or inside the endosomes (ionic, acid labile) (from D. Edinger et al.<sup>46</sup>).

For PEGylated polyplexes bioresponsive deshielding strategies have been developed as possible solutions (Figure 5), capitalizing location-specific changes in enzymatic activity<sup>103</sup>, disulfide reducing potential<sup>99</sup> or pH<sup>89,93,96,104</sup>. Another method to regain particle cell interactions is the incorporation of targeting moieties.

### 1.3.4 Receptor Targeting

In many types of cancer certain surface receptor levels are upregulated. Therefore, targeting these cell surface receptors offers the possibility to address defined cells in a tissue. Especially shielded particles used for *in vivo* application profit from

the incorporation of targeting ligands. Several ligands have been shown to be suitable for targeted gene delivery, these are for example vitamins, carbohydrates, peptides, proteins and glycoproteins, antibodies in various modifications, small molecules, or nucleic acid aptamers.

For example the epidermal growth factor receptor (EGFR) is upregulated in many cancers, like lung cancer, colorectal cancer and glioblastomas. For this reason various EGFR binding molecules, including EGF recombinant protein, EGFR binding antibodies, or EGFR binding phage derived peptides<sup>105</sup> have been explored in polyplexes as interesting targeting ligands. Targeting the EGFR also accelerates the cellular uptake of polyplexes. Single particle tracking allowed distinguishing between three phases during the uptake process. In the first phase particle movement is slow, it includes all processes up to the internalization of the polyplexes. The following second phase is characterized by diffusion processes in the cytosol, while in the third phase polyplexes are rapidly transported along microtubules. Cellular uptake of EGFR targeting complexes resulted in a shortening of phase one and so contributed to a faster uptake of the polyplexes.

Another often upregulated receptor is the transferrin receptor (TfR), a glycoprotein responsible for iron ion transport in mammals. After binding to the TfR, the complex consisting of receptor and ligand is absorbed by the cell through a clathrin dependent pathway and then integrated into the endocytic cycle. For this reason Tf has been frequently used as a targeting ligand for siRNA delivering polyplexes<sup>106-109</sup>. Tietze et al used TfR targeted, PEG-shielded crosslinked oligoethylenimines for siRNA delivery into Neuro2A tumor bearing mice<sup>109</sup>. Davis and colleagues<sup>110-112</sup> used Tf targeted cyclodextrin to deliver siRNA, targeting the M2 subunit of ribonucleotide reductase. These targeted polyplexes were evaluated in human clinical trials and they were the first polymeric carriers to show gene knockdown in solid human tumors<sup>113</sup>.

Apart from protein and peptide ligands, also low molecular weight targeting ligands such as the vitamin folic acid have been used for nucleic acid delivery. The related folate receptor (FR) is upregulated in various cancers, mediating cellular uptake of the vitamin folic acid via a caveolin mediated pathway<sup>114</sup>. Thomas et al. could show the impressive targeting efficacy of folic acid using siRNA covalently bound to folate via a short linker. The particles specifically bind to tumor tissues *in vitro* and *in vivo*, but failed to show gene transfer activity

because of lacking carriers<sup>115</sup>. Dohmen et al. combined siRNA linked to folic acid with defined oligomers synthesized by solid-phase-supported macromolecule assembly. This combination showed great and selective uptake and strong marker gene knockdown in folic acid overexpressing KB cells<sup>51,116</sup>. Methotrexate (MTX) has high structure similarity to folic acid and can also be used as a targeting ligand<sup>117</sup> combining the use of a classical chemotherapeutic with the novel approach of RNAi.

## 1.4 Target Genes

Selection of target genes suitable for therapeutic assays is very complex. Clear correlation between target mRNA and illness have to be identified. For example the knockdown of Apolipoprotein B mRNA in the liver led to reduced cholesterol levels in the bloodstream of mice<sup>118</sup>. Reduced mRNA levels were detectable in the liver for several days up to some weeks because target gene knockdown did not affect cell viability<sup>119</sup>. In contrast, the treatment of cancer cells commonly aims at killing the tumor cell. Therefore, target gene knockdown is only detectable for a short period of time.

Eg5 (Kif11, KSP) was suggested as a therapeutic target for cancer therapy by our collaboration partner Axolabs (formerly Roche Kulmbach)<sup>120-121</sup>. Eg5 is involved in the assembly and organization of the mitotic spindle apparatus, a self-assembled and dynamic microtubule based structure which is important for chromosome segregation in dividing cells<sup>122</sup>. During mitosis Eg5 is responsible for centrosome separation thus playing a pivotal role in cell division. In consequence, Eg5 knockdown blocks mitosis and leads to G2 arrest especially harming rapidly dividing cancer cells. The mitotic blockade comparable to the small molecule monastrol leads to the typical “aster formation” of nuclear DNA<sup>123</sup>. In consequence reduced Eg5 protein levels hinder mitosis and lead to cell death. But also high Eg5 levels lead to spindle defects, genetic instability, and tumors, demonstrating the important role of Eg5 during mitosis<sup>124</sup>. Similar to the effects of Eg5 knockdown classical chemotherapeutics like vinca alkaloids and taxanes also influence the microtubule assembly and disassembly.

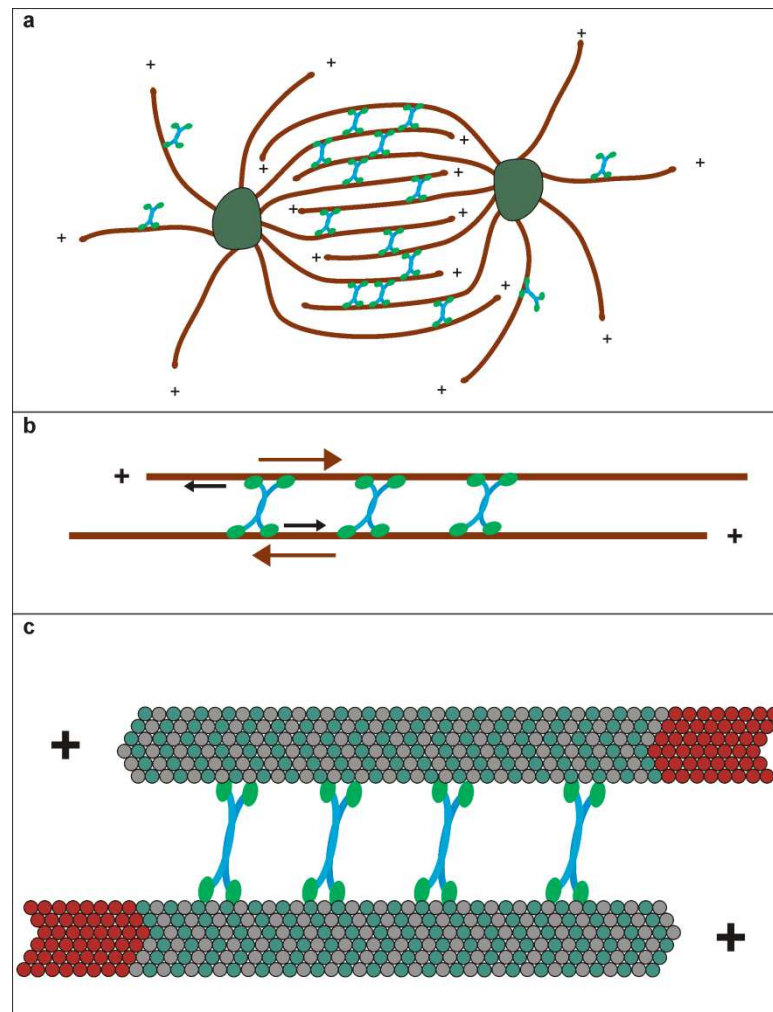


**Figure 6 Role of Eg5 during mitosis:** Tetrameric Eg5 motors help to organize microtubules forming the mitotic spindle. Eg5 moves towards the plus-ends of antiparallel microtubules, leading to the poleward drift of the centrosomes (modified from Valentin et al.<sup>122</sup>).

Another therapeutic relevant target is the RAS related nuclear protein (Ran)<sup>125-126</sup>. As a member of the RAS superfamily, Ran mediates nuclear import and export of proteins and oligonucleotides during interphase. Furthermore Ran is involved in DNA synthesis and in cell cycle progression<sup>127-128</sup>. Ran can exist either in GTP or GDP bound form and has an intrinsic GTPase activity. Activated due to the interaction with Ran GTPase activating protein (Ran-GAP), Ran-GTP is converted into Ran-GDP. Ran-GAP is located in the cytosol reducing Ran-GTP levels in the cytosol. Ran-GEF (RCC1) another protein involved in the Ran cycle is located in the nucleus mediating the exchange of GDP and GTP. Hence, the localisation of the two proteins leads to an imbalance of Ran-GTP in the nucleus and cytosol. This concentration gradient is used for active transport of cargo into or out of the nucleus. High Ran expression levels are associated with cancer<sup>129-130</sup>, therefore Ran is used as a target for siRNA therapy.

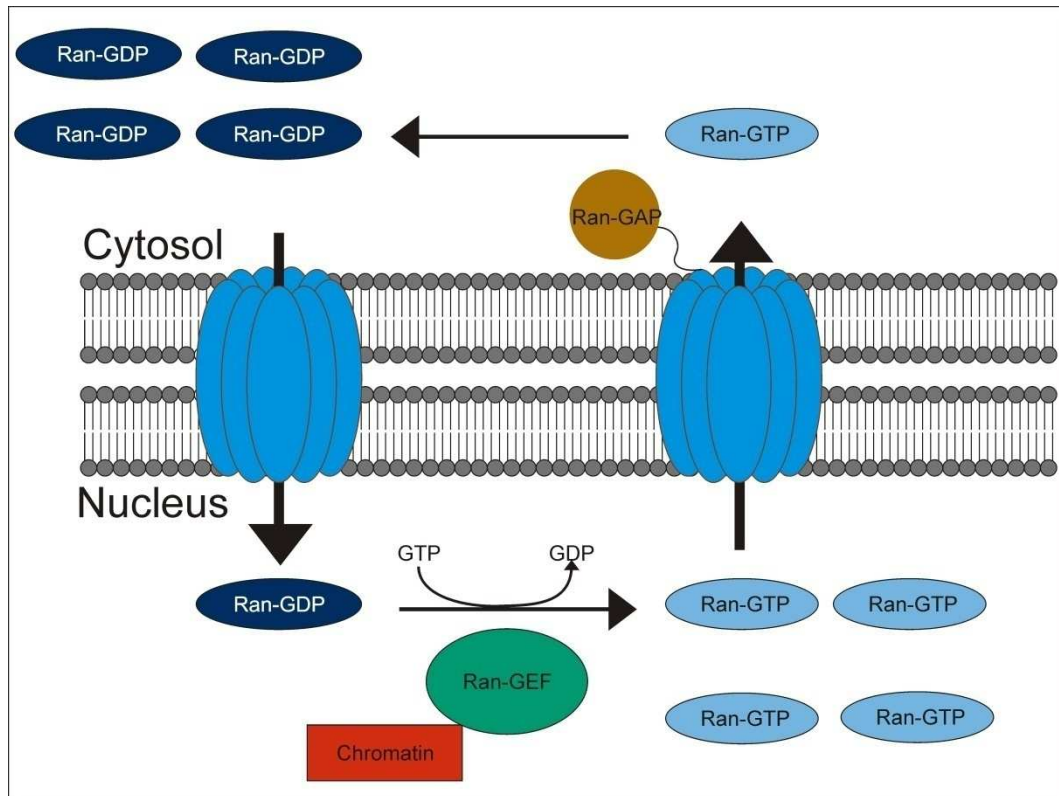


**Figure 7 Role of Ran:** Ran cycle with high Ran-GDP levels in the cytosol mediated by Ran-GAP and high Ran-GTP levels in the nucleus due to Ran-GEF expression. This concentration gradient enables directed transport of cargo into the nucleus or the cytosol.

In contrast, marker genes are usually selected for polymer screening assays, enabling an easy quantification of mRNA knockdown<sup>75,131</sup>. Therefore, the marker genes eGFP or Luciferase are commonly used. After establishing cell lines expressing one or both of this marker genes, mRNA knockdown can be easily detected.

## 1.5 Aims of the Thesis

Discovery of RNAi was a major breakthrough for the research of biological processes and may become an option for the treatment of severe diseases. Especially as siRNAs have the potential to be effective where classical therapeutics, antibodies, and small molecules fail. Target specificity on the one hand and the possible selection of several ten thousand target genes on the other hand are making siRNAs a promising approach for future therapies. However, the broad application of siRNAs is hampered by its size and negative charge. These limitations can either be overcome by minimizing the size and charge of the nucleic acids, by the use of carriers or by a combination of both. The current thesis focusses on the characterization of oligomeric carriers suitable for

successful siRNA transfection *in vitro* and *in vivo*. For this purpose many different biodegradable oligomeric carriers have been synthesized by solid-phase-supported synthesis. This novel strategy allowed the selective incorporation of diverse components like cysteines, tyrosines (stabilization) and histidines (improved endosomal escape) into structures with different topologies. The first aim of the thesis was the *in vitro* evaluation of numerous siRNA carriers to define several requirements for successful *in vitro* gene silencing. Improved understanding of the requirements led to the synthesis of carriers with higher transfection efficiency and greater stability against serum proteins. The second aim of the thesis was the *in vivo* evaluation of different oligomers with successful gene silencing *in vitro*. For this reason, assays for the detection of fluorescence labeled siRNAs in sections or living animals had to be established. Thereby, the distribution and clearance of different polyplexes could be compared in living animals or tumor sections. Furthermore, altered transfection efficiency of *in vitro* active carriers should be compared in an intratumoral assay. Therefore, two therapeutic siRNAs were explored *in vitro* for their target specificity by qPCR and Western blot and their knockdown related cytotoxicity by CellTiter Glo assays. Both therapeutic siRNAs were also evaluated in an intratumoral assay and Ran siRNA was chosen for the comparison of different oligomers. The intratumoral comparison of different polyplexes is an important step towards the *in vivo* use of siRNA therapeutics. The third aim of the thesis was the evaluation of multifunctional siRNA polyplexes *in vitro* and *in vivo*. Folic acid bound to an oligomeric backbone was used as a targeting ligand, whereas siRNA's passenger strand was modified with the endosomolytic peptide Inf7 for improved endosomal escape. At first suitable cell lines overexpressing the folic acid receptor had to be evaluated. Furthermore, *in vitro* transfection experiments were conducted to demonstrate the activity of the different functional domains. The focus was the *in vivo* application of the polyplexes to monitor circulation half-life, targeting and the establishment of histological assays to analyze target gene knockdown. Besides the *in vivo* evaluation of folic acid linked oligomers the *in vitro* classification of novel methotrexate (MTX) containing targeting oligomers was performed. The assays should demonstrate the effectivity and the targeting efficiency of polymer linked MTX.

## 2 MATERIALS AND METHODS

### 2.1 Materials

Consumables (dishes, well plates, flasks) were obtained from NUNC (Germany) or TPP (Switzerland). Cell culture 5 x lysis buffer and D-luciferin sodium salt were obtained from Promega (Germany). Cell culture media, antibiotics, stable glutamine, and fetal calf serum (FCS) were purchased from Invitrogen (Germany) and HEPES was purchased from Biomol GmbH (Germany).

### 2.2 siRNAs

The applied siRNA duplexes were ordered from Dharmacon (ThermoFisher, USA) or Axolabs (Germany, former Roche Kulmbach). They were diluted in RNase free water and the stocks (20 µg/µl) were stored at -80°C. For use in cell culture, stocks were diluted to 0,5 µg/µl, whereas for *in vivo* use stocks were diluted to 2-5 µg/µl. RAN siRNA was ordered in *in vivo* qualities and their sequences is shown in the table below. Small letters represent 2-Methoxy sugar modifications and s represents phosphorothioate backbone modifications. Some siRNAs were further modified with Inf7 peptide by C. Dohmen to demonstrate lytic activity in the endosomes<sup>116</sup>.

siRNA	Target	Supplier	siRNA sequence
siGFP	GFP	Axolabs	AuAucAuGGccGAcAAGcAdTsdT ( <b>Sense</b> ) UGCUUGUCGGCcAUGAuAUdTsdT ( <b>Antisense</b> )
siControl		Axolabs	AuGuAuuGGccuGuAuuAGdTsdT CuAAuAcAGGCcAAuAcAUdTsdT
siAHA1	AHA1	Axolabs	GGAuGAAGuGGAGAuAGudTsdT ACuAAUCUCcACUUC AUCCdTsdT
siEg5	Eg5/KSP	Axolabs	ucGAGAAucuAAAcuAAcudTsdT AGUuAGUuAGAUUCUCGAdTsdT
siRan	Ran	Dharmacon	UAGUACUGAAGAUUCUUCUUU AGAAGAAUCUUCAGUACUAUU
siGlo		Dharmacon	AUGUAUUGGCCUGUAUUAG (Cy3)thiol-AUGUAUUGGCCUGUAUUAG
siAHA1-Cy5		Axolabs	GGAuGAAGuGGAGAuAGudTsdT (Cy5)(NHC6)ACuAAUCUCcACUUC AUCCdTsdT
siAHA1-Cy7		Axolabs	GGAuGAAGuGGAGAuAGudTsdT (Cy7)(NHC6)ACuAAUCUCcACUUC AUCCdTsdT

siGFP-Inf		Axolabs (C. Dohmen)	(Inf-SSC6)AuAucAuGGccGAcAAGcAdTsdT UGCUUGUCGGCcAUGAuAUdTsdT
siControl-Inf		Axolabs (C. Dohmen)	(Inf-SSC6)AuGuAuuGGccuGuAuuAGdTsdT CuAAuAcAGGCcAAuAcAUdTsdT
siEg5-Inf		Axolabs (C. Dohmen)	(Inf-SSC6)ucGAGAAucuAAAcuAAcudTsdT AGUuAGUuAGAUUCUCGAdTsdT

### 2.3 Oligomers

Oligomers were synthesized by solid-phase-supported synthesis as previously described<sup>116,132-133</sup>. The table demonstrates polymer sequences, polymer shapes and polymer IDs. Freeze dried oligomers were diluted in deionized, sterile water for all experiments.

Polymer ID	Polymer shape	Polymer sequence
<b>49</b>	T-Shape	C-Stp <sub>2</sub> -[(OleA) <sub>2</sub> -K]K-Stp <sub>2</sub> -C
<b>229</b>	i-Shape	C-Stp <sub>3</sub> -C-K-(LinA) <sub>2</sub>
<b>386</b>	Branched	[(C-Stp <sub>3</sub> ) <sub>2</sub> ]K-Stp <sub>3</sub> -C
<b>216</b>	T-Shape	A-Stp <sub>2</sub> -[(OleA) <sub>2</sub> -K]K-Stp <sub>2</sub> -A
<b>332</b>	T-Shape	Y <sub>3</sub> -Stp <sub>2</sub> -[(OleA) <sub>2</sub> -K]K-Stp <sub>2</sub> -Y <sub>3</sub>
<b>454</b>	T-Shape	C-Y <sub>3</sub> -Stp <sub>2</sub> -[(OleA) <sub>2</sub> -K]K-Stp <sub>2</sub> -Y <sub>3</sub> -C
<b>468</b>	T-Shape	C-Stp <sub>2</sub> -[(Y <sub>3</sub> ) <sub>2</sub> -K]K-Stp <sub>2</sub> -C
<b>333</b>	T-Shape	Y <sub>3</sub> -Stp <sub>2</sub> -[(Y <sub>3</sub> ) <sub>2</sub> -K]K-Stp <sub>2</sub> -Y <sub>3</sub>
<b>464</b>	T-Shape	C-Y <sub>3</sub> -Stp <sub>2</sub> -[(Y <sub>3</sub> ) <sub>2</sub> -K]K-Stp <sub>2</sub> -Y <sub>3</sub> -C
<b>356</b>	Targeted	Fol-PEG <sub>24</sub> -K(STP <sub>4</sub> C) <sub>2</sub>
<b>188</b>	Targeted	A-PEG <sub>24</sub> -K(STP <sub>4</sub> C) <sub>2</sub>
<b>482</b>	Targeted	Fol-PEG <sub>48</sub> -K(STP <sub>4</sub> C) <sub>2</sub>
<b>483</b>	Targeted	Fol-PEG <sub>72</sub> -K(STP <sub>4</sub> C) <sub>2</sub>
<b>646</b>	Targeted	A-PEG <sub>120</sub> -K(STP <sub>4</sub> C) <sub>2</sub>
<b>647</b>	Targeted	A-PEG <sub>192</sub> -K(STP <sub>4</sub> C) <sub>2</sub>
<b>484</b>	Targeted	Fol-PEG <sub>24</sub> -K(STP <sub>4</sub> Y <sub>3</sub> C) <sub>2</sub>
<b>481</b>	Targeted	Fol-PEG <sub>24</sub> -K(STP <sub>4</sub> K(KCapA) <sub>2</sub> C) <sub>2</sub>
<b>480</b>	Targeted	Fol-PEG <sub>24</sub> -K(STP <sub>4</sub> K(KSteA) <sub>2</sub> C) <sub>2</sub>
<b>638</b>	Targeted	K(PEG <sub>24</sub> -MTX)-K(STP <sub>4</sub> -C) <sub>2</sub>
<b>639</b>	Targeted	K(PEG <sub>24</sub> -E <sub>2</sub> -MTX)-K(STP <sub>4</sub> -C) <sub>2</sub>
<b>640</b>	Targeted	K(PEG <sub>24</sub> -E <sub>4</sub> -MTX)-K(STP <sub>4</sub> -C) <sub>2</sub>
<b>641</b>	Targeted	K(PEG <sub>24</sub> -E <sub>6</sub> -MTX)-K(STP <sub>4</sub> -C) <sub>2</sub>
<b>642</b>	Targeted	K(PEG <sub>24</sub> -αMTX)-K(STP <sub>4</sub> -C) <sub>2</sub>

## 2.4 Polyplex Formation

Polyplex were prepared as follows, unless the use of different solvents is indicated. 500 ng siRNA per well or per slot for untargeted oligomers, 200 ng siRNA per well or per slot for targeted or 50 µg siRNA per animal and the calculated amount of oligomer were diluted in separate Eppendorf tubes each in HBG (20 mM Hepes buffered 5% glucose pH 7.4). The amount of polymer was calculated as follows:

$$m(\text{siRNA}) = \frac{m(\text{siRNA}) * \text{negative charges}(\text{siRNA}) * \frac{N}{P} * M(\text{Oligomer})}{M(\text{siRNA}) * \text{protonable amines}(\text{Oligomer})}$$

For screening experiments several N/P (protonable amines/Phosphates) were tested. The oligomer solution was added to the siRNA, rapidly mixed by gently pipetting up and down (no air bubbles) and incubated for at least 45 min at room temperature in order to allow stable polyplexes formation.

## 2.5 Biophysical Characterization

### 2.5.1 Particle Size and Zeta Potential Measurement

Particle sizes of siRNA formulations were measured by dynamic-laser-light (DLS) scattering using a Zetasizer Nano ZS (Malvern Instruments, U.K.). siRNA polyplexes N/P 12 (10 µg siRNA in 50 µl buffer) were prepared according to the previous mentioned formula and mixed in 20 mM Hepes pH 7.4 buffer. Before DLS measurement polyplexes were diluted 1:20 in Hepes pH 7.4 and measured in a folded capillary cell (DTS1060) with laser light scattering using a Zetasizer Nano ZS with backscatter detection. Samples were measured 3 times each with 10 sub-runs of 10 seconds. Results were displayed as Z-average, whereby the standard deviation shows the difference between the 3 runs. The zeta potentials were also analyzed with the Zetasizer Nano ZS. Samples were measured 3 times, with 10 up to 30 sub-runs of 10 s at 25°C.

### 2.5.2 Agarose Gel Shift Assay

For gel shift assays a 2% agarose gel was prepared by dissolving 2 g ultrapure agarose in 100 ml TBE buffer (trizma base 10.8 g, boric acid 5.5 g, disodium EDTA 0.75 g and 1 l of water). The mixture was heated in a microwave to dissolve the agarose in TBE buffer. After the solution cooled down 80 µl GelRed®

(VWR, USA) were added for the detection of nucleic acids and the clear solution was filled into an electrophoresis chamber. Polyplexes in different N/P ratios, containing 500 ng siRNA in 20  $\mu$ l HBG mixed with 5 x loading buffer (prepared from 6 ml of glycerine, 1.2 ml of 0.5 M EDTA, 2.8 ml of H<sub>2</sub>O, 0.02 g xylene cyanol) were placed into the sample pockets and electrophoresis was performed at 120 V for 40 min.

### **2.5.3 Serum Stability Assay**

A 2% agarose gel was prepared as described above. For the stability assays 500 ng siRNA and the oligomer at N/P 12 were diluted in separate tubes to a total volume of 12.5  $\mu$ l in 20 mM Hepes pH 7.4. The nucleic acid solution was added to the diluted polycation, mixed and incubated for 45 min at room temperature. Afterwards fetal calf serum (FCS) was added to the samples. All samples had a final concentration of 90% FCS. The samples were incubated either at room temperature or 37°C for different time points. After 0, 10, 30, and 90 min, 4  $\mu$ l loading buffer were added and 20  $\mu$ l of the samples were placed into the sample pockets. Electrophoresis was performed at 120 V for 40 min.

## **2.6 Biological Characterization *in vitro***

### **2.6.1 Cell Culture**

Different cell lines were used and cultured in the appropriate medium, except for targeting experiments where cells were cultured in folic acid free medium if possible. All media were supplemented with 10% FCS, 4 mM stable Glutamine, 100 U/ml Penicillin and 100  $\mu$ g/ml Streptomycin (cell lines for animal experiments were cultured without antibiotics). The cells were cultured in ventilated flasks inside incubators at 37°C with 5% CO<sub>2</sub> in a humidified atmosphere. Cell lines were allowed to grow until 80% confluence and splitted when necessary. Cell lines stably expressing the eGFPLuc gene were generated by A. Cengizeroglu through lentiviral transduction and eGFPLuc positive cells were sorted by J. Ellwart.

Cell line	Origin	Media	eGFP/Luc
Neuro2A	Murine; Neuroblastoma	DMEM + 10%FCS + 1%Glutamine + 1% P/S	eGFPLuc
HUH7	Human; Hepatocellular carcinoma	DMEM/HAM's F12 + 10%FCS + 1%Glutamine + 1% P/S	Luc
HEPG2	Human; Hepatocellular carcinoma	DMEM + 10%FCS + 1%Glutamine + 1% P/S	eGFPLuc
KB	Human; Cervical carcinoma	RPMI + 10%FCS + 1%Glutamine + 1% P/S	eGFPLuc
IGROV	Human; Ovarian carcinoma	RPMI + 10%FCS + 1%Glutamine + 1% P/S	eGFPLuc
A431	Human; Epidermoid carcinoma	DMEM + 10%FCS + 1%Glutamine + 1% P/S	
A549	Human; Alveolar Adenocarcinoma	DMEM + 10%FCS + 1%Glutamine + 1% P/S	
MCF7	Human; Breast cancer	DMEM + 20%FCS + 1%Glutamine + 1% P/S	
MDA-MB 231	Human; Breast Cancer	L15 + 10%FCS + 1%Glutamine + 1% P/S	
Az521	Human; Gastric Adenocarcinoma	EMEM + 10%FCS + 1%Glutamine + 1% P/S	eGFPLuc

### 2.6.2 GFP Knockdown Assay

Gene silencing experiments were by default performed in stably transfected Neuro2A-eGFPLuc or KB-eGFPLuc cells using 500 ng (untargeted oligomers) or 200 ng (targeted oligomers) siRNA per well of either GFP siRNA for silencing of the eGFPLuc protein, or control siRNA for the detection of polyplex related cytotoxicity (siRNA sequences are displayed in the previously mentioned table). Experiments were performed in 96-well plates with  $5 \times 10^3$  cells per well. After seeding, the cells were incubated for 24 h to guarantee proper cell adhesion. Before transfection the medium was replaced with 80  $\mu$ l fresh growth medium containing 10% FCS. Transfection complexes for siRNA delivery were formed in 20  $\mu$ l HBG at different N/P and added to the wells in triplicates. Untargeted polyplexes were incubated for 48 h while targeted polyplexes were incubated for 45 min on the cells. After 48 h cells were lysed with 100  $\mu$ l cell lysis buffer. Luciferase activity in the cell lysate was measured using a luciferase assay kit (100  $\mu$ l Luciferase Assay buffer, Promega, Germany) and a Centro LB 960 plate reader luminometer (Berthold Technologies, Germany). The relative light units (RLU) are presented as percentage of the luciferase gene expression obtained with

buffer treated control cells.

### 2.6.3 Quantitative Real Time Polymerase Chain Reaction

$1.5 \times 10^5$  Neuro2A cells per well were seeded in 2000  $\mu$ l medium (DMEM with 10% FCS) using 6-well plates. After 24 h, medium was replaced with 900  $\mu$ l fresh medium (DMEM with 10% FCS). Polyplexes were prepared in a total volume of 100  $\mu$ l as described above and added to the wells after 45 min incubation time. All experiments were performed in triplicates using either Eg5 siRNA, Ran siRNA or control siRNA (sequences see above). Transfected cells were incubated for 24, 48, and 72 h without medium change. After 24, 48, and 72 h cells were lysed and total RNA was isolated using High Pure RNA Tissue Kit<sup>®</sup> (Roche, Germany) and transcribed with the Transcriptor High Fidelity cDNA Synthesis Kit<sup>®</sup> (Roche, Germany) according to the manufacturer's protocol. Quantitative real-time PCR was performed using UPL Probes and Probes Master (both Roche, Germany) on a LightCycler 480<sup>®</sup> system (Roche, Germany) with GAPD as housekeeper. Primers used include murine GAPD (ready to use Universal Probe library assay Roche), Eg5 (UPL Probe #100) forward: TTCCCCTGCATCTTTCAATC, reverse: TTCAGGCTTATTCATTATGTTCTTTG; Ran (UPL Probe #2) forward: ACCCGCTCGTCTTCCATAC, reverse: ATAATGGCACACTGGGCTTG. Results were analysed using the  $\Delta C_T$  method, therefore  $C_T$  values of the housekeeper were subtracted from  $C_T$  values of the gene of interest. The  $\Delta C_T$  values of control transfected cells were set to 100% and compared to Eg5 and Ran siRNA transfected cells.

### 2.6.4 Western Blot

$1.5 \times 10^5$  Neuro2A cells per well were seeded in 2000  $\mu$ l medium (DMEM with 10% FCS) using 6-well plates. After 24 h, medium was replaced with 900  $\mu$ l fresh medium (DMEM with 10% FCS). Transfection complexes were prepared in a total volume of 100  $\mu$ l as described above. After 24, 48, and 72 h cells were lysed and total protein concentration was determined using a BCA (Bicinchonic acid) assay. 50  $\mu$ g of protein per lane were separated by SDS-PAGE under reducing conditions, transferred on a nitrocellulose membrane, and blocked with NET Gelatine or milk powder (5% in TBST) for 1 hour at room temperature. Immunostaining was performed using either primary Ran anti rabbit antibody (Cell Signaling, Germany; 1:500), or Eg5 anti goat antibody (Santa Cruz

Biotechnology Inc., USA; 1:200) or GAPD anti rabbit antibody (Cell Signaling, Germany; 1:5000) overnight at 4°C. After the incubation with primary antibodies membranes were washed 3 times with NET Gelatine or TBST (Tris buffered saline and Tween 20) before incubating with a peroxidase labeled secondary antibody (Vector Laboratories, France) for 1 h. After another 3 washing cycles, proteins were visualized using Lumi-Light Western blotting substrate (Roche, Germany). Blots were quantified using Image J software (NIH, USA).

## **2.6.5 Flow Cytometry**

### **2.6.5.1 Receptor Level Studies**

Cell lines expressing the folic acid receptor were identified by flow cytometry. For this experiment cells were either cultivated in the previously mentioned cell culture medium or in folate free RPMI medium if possible.  $1 \times 10^6$  cells were collected in 150  $\mu$ l FACS buffer and 10  $\mu$ l APC-conjugated anti folic acid receptor 1 mouse IgG<sub>1</sub> (R&D Systems, USA) were added. After 30 min cells were washed twice with FACS buffer, resuspended in 500  $\mu$ l FACS buffer and analyzed using a Cyan<sup>®</sup> ADP flow cytometer (Dako, Germany). Doublets were discriminated by accurately gating forward/sideward scatter and forward scatter/pulse width, while counterstaining with DAPI (4,6-Diamidin-2-phenylindol) allowed distinguishing between dead and living cells. The amount of folic acid receptor positive cells was analyzed through excitation of the dye at 635 nm and detection of emission at 665/20 nm. For each sample  $5 \times 10^4$  events were counted using Summit<sup>®</sup> software (Summit, USA) and evaluated using FlowJo<sup>®</sup> software (FlowJo, USA).

### **2.6.5.2 Receptor Binding Studies**

Polyplex uptake into cells was monitored by flow cytometry. For uptake experiments  $5 \times 10^4$  cells per well were seeded in 1000  $\mu$ l medium using 24-well plates. 24 h later the medium was replaced with 450  $\mu$ l fresh growth medium and polyplexes containing Cy5 labeled siRNA mixed in a total volume of 50  $\mu$ l were added. The 24-well plates were incubated on ice for 45 min to hinder polyplex uptake. After 45 min medium was removed and cells were washed twice with cold PBS (phosphate buffered saline) and trypsinized. Trypsin was inactivated with 1000  $\mu$ l FACS buffer (10% FCS in PBS) and the cells were centrifuged (2000 rpm; 5 min). After two washing cycles with 1000  $\mu$ l PBS the cells were

resuspended in 400  $\mu$ l FACS buffer and analyzed using a Cyan<sup>®</sup> ADP flow cytometer (Dako, Germany). The amount of Cy5 positive cells was analyzed through excitation of the dye at 635 nm and detection of emission at 665/20 nm. Doublets were discriminated by accurately gating forward/sideward scatter and forward scatter/ pulse width, while counterstaining with DAPI (4,6-Diamidin-2-phenylindol) allowed distinguishing between dead and living cells. For each sample  $1 \times 10^4$  events were counted using Summit<sup>®</sup> software (Summit, USA) and evaluated using FlowJo<sup>®</sup> software (FlowJo, USA).

### 2.6.5.3 Cell Cycle Measurement

$2.5 \times 10^4$  Neuro2A cells per well were seeded in 1000  $\mu$ l medium (DMEM with 10% FCS) using 24-well plates. After 24 h, medium was replaced by 450  $\mu$ l fresh medium (DMEM with 10% FCS). Transfection complexes were prepared as described above. After the incubation time (24, 48, 72 h) cells were trypsinized, collected in their culture medium and centrifuged (2000 rpm; 5 min). The supernatant was discarded and the cell pellet was washed with PBS before staining with propidium iodide solution (0.1% sodium citrate; 0.1% Triton-X100; 50  $\mu$ g/ml propidium iodide in millipore water). After 3 h 1000  $\mu$ l PBS were added, cells were centrifuged (2000 rpm; 5 min), resuspended in 500  $\mu$ l PBS and measured with a Cyan<sup>®</sup> ADP flow cytometer (Dako, Germany). Doublets were discriminated by accurately gating forward/sideward scatter and forward scatter/ pulse width. The DNA content was measured through excitation of the dye at 488 nm and detection of emission at 613/20 nm. For each sample  $1 \times 10^4$  events were counted using Summit<sup>®</sup> software (Summit, USA) and evaluated using FlowJo<sup>®</sup> software (FlowJo, USA).

### 2.6.6 Fluorescence Microscopy

$1 \times 10^4$  Neuro2A, KB or IGROV cells per well were seeded in 200  $\mu$ l medium (DMEM or RPMI with 10% FCS) using 8-well Lab-tek<sup>®</sup> chamberslides (Sigma-Aldrich, USA). 24 h after seeding medium was replaced by 180  $\mu$ l fresh medium and 20  $\mu$ l polyplex solution were added (in HBG). Cells transfected with polyplexes containing either Eg5 or control siRNA were incubated for 24 h (untargeted polyplexes) or 45 min (targeted polyplexes). After the incubation time medium was removed and cells were washed with 200  $\mu$ l PBS and fixed with 4% paraformaldehyd (PFA). Fixed cells were stained with DAPI to visualize the DNA

and results were documented using Zeiss Axiovert 200 (fluorescence microscope, Carl Zeiss AG, Germany).

### 2.6.7 CellTiter Glo Assay

$5 \times 10^3$  Neuro2A cells per well were seeded in 100  $\mu$ l medium (DMEM with 10% FCS) using 96-well plates. 24 h later, medium was replaced by 80  $\mu$ l fresh medium (DMEM with 10% FCS) and 20  $\mu$ l polyplex solution were added. After 24, 48, and 72 h 100  $\mu$ l CellTiter Glo solution (Promega, USA) was added and the luminescence was recorded with a Luminometer (Lumat LB9507, Berthold, Germany).

For the detection of methotrexate (MTX) related toxicity cells were also seeded in a 96-well plate as described above. To determine IC<sub>50</sub> values of MTX, MTX targeted oligomers or MTX polyplexes the culture medium was also replaced after 24 h by fresh medium containing different concentrations of the previously mentioned therapeutics. After 48 h 100  $\mu$ l CellTiter Glo<sup>®</sup> solution (Promega, USA) was added and the luminescence was recorded with a Luminometer (Lumat LB9507, Berthold, Germany). IC<sub>50</sub> values were calculated with GraphPad Prism<sup>®</sup> (GraphPad, USA) software.

### 2.6.8 Dihydrofolatereductase Activity Assay

Inhibition of dihydrofolatereductase (DHFR) through MTX or MTX containing oligomers was measured by a spectroscopic assay. All reagents despite the tested oligomers were supplemented in the dihydrofolate reductase assay kit (Sigma-Aldrich, USA). The reduction of absorption is measured by a photospectrometer at 340 nm, as DHFR catalyses the reduction of dihydrofolic acid to tetrahydrofolic acid in a NADPH dependent reaction. MTX blocks the activity of the enzyme DHFR, in consequence the reduction of dihydrofolic acid is hampered leading to higher concentrations of NADPH/H<sup>+</sup> and therefore higher absorption values at 340 nm after 2.5 min. The absorption values without inhibition decreased and the reduction was compared to the reduction with inhibitor.

## 2.7 Biological Characterization *in vivo*

### 2.7.1 Mouse Strains

Female 5 week old A/J mice were purchased from Harlan Winkelmann (Germany) and female 5 week old NMRI-nu (nu/nu) from Janvier (France). After arrival the mice were allowed to acclimatize for one week before starting the experiments. All mice were housed in individually vented cages with food and water provided *ad libitum* and a 12 h day and night cycle. Animal experiments were performed according to guidelines of the German law of protection of animal life and were approved by the local animal experiments ethical committee.

### 2.7.2 Histological Studies

For histological assays  $1 \times 10^6$  Neuro2A cells or  $5 \times 10^6$  KB cells in a volume of 150  $\mu$ l PBS were subcutaneously injected into the left flank of A/J mice (Neuro2A) or NMRI mice (KB). After tumors reached a volume of about 200 mm<sup>3</sup> (10 days) polyplexes were injected.

#### 2.7.2.1 Polyplex Distribution

Polyplexes distribution was measured by incorporation of Cy3 labeled siRNA into the intravenously injected polyplexes (N/P 12). Mice were sacrificed 1 h after tail vein injection of the polyplexes mixed in a total volume of 250  $\mu$ l and organs (tumor, lung, liver, kidneys) were harvested. Organs were immobilized in TissueTek<sup>®</sup> and 5  $\mu$ m fine sections were cut using a cryotom (Leica CM3050 S Leica Microsystems GmbH, Germany). Slices were stained with Hoechst 33342 dye, sealed with FluorSave (Calbiochem, Merck Group, Germany) and analyzed with Zeiss Laser Scanning Microscope LSM510 Meta (Carl Zeiss, Germany).

#### 2.7.2.2 Aster Formation

Mice were intravenously injected twice with Eg5 siRNA (for oligomers **422** and **188** Inf7 modified siRNAs were chosen) containing polyplexes (N/P 12 for oligomers **49** and **229** or N/P 16 for oligomers **472** and **188**) 24 and 48 h before euthanasia. Tumors and livers were harvested, immobilized in TissueTek<sup>®</sup> and cut into 5  $\mu$ m fine sections using a cryotom (Leica CM3050 S Leica Microsystems GmbH, Germany). Slices were fixed with paraformaldehyde (4%), stained with DAPI and aster formations were documented using a fluorescence microscope

(Zeiss Axiovert 200, Carl Zeiss AG, Germany).

### **2.7.2.3 H&E Staining**

Mice were intratumorally injected twice with Eg5-Inf7 siRNA containing polyplexes (N/P 16) 24 and 48 h before euthanasia. Tumors were harvested, fixed in formalin and embedded into paraffin. Tumors were sliced into 4.5  $\mu\text{m}$  fine sections and stained with hematoxylin and eosin (H&E), following standard protocol. Results were documented using an Olympus BX41 microscope (Olympus, Germany).

### **2.7.3 Polyplex Imaging**

For live polyplex imaging  $5 \times 10^6$  Neuro2A or KB cells in a volume of 150  $\mu\text{l}$  PBS were subcutaneously injected into the left flank (Neuro2A) or neck (KB) of NMRI mice. After tumors reached a volume of about 200  $\text{mm}^3$  (10 days) polyplexes were injected.

#### **2.7.3.1 Polyplex Retention after i.t. Injection**

Near infrared (NIR) imaging was performed to display the different retention of intratumorally injected polyplexes (N/P 12) containing 50  $\mu\text{g}$  siRNA including 25  $\mu\text{g}$  Cy7-labeled siRNA mixed in a total volume of 50  $\mu\text{l}$  (HBG). Mice were anaesthetized with 3% isoflurane in oxygen, polyplexes were injected into the tumor and fluorescence was measured after 0, 0.25, 1, 4, 24, and 48 h with a CCD camera. After 48 h mice were sacrificed and tumors, kidneys, lungs, livers, and spleens were excised and fluorescence imaging was performed. All pictures were analyzed utilizing the IVIS Lumina system with Living Image software 3.2 (Caliper Life Sciences, USA). For evaluation of images, efficiency of fluorescence signals was analyzed, after color bar scales were equalized.

Targeted and untargeted polyplexes, containing 50  $\mu\text{g}$  Cy7-labeled siRNA, or pure Cy7-labeled siRNA, were injected intratumorally in 50  $\mu\text{l}$  HBG. NIR imaging was performed with a CCD camera 0, 4, 24, 48, 72, 96, and 120 h after polyplex injection. For evaluation of images, efficiency of fluorescence signals was analyzed, after color bar scales were equalized. For quantification of the tumor retention of the polyplexes, regions of interest (ROIs) were defined and total signals per ROI were calculated as total efficiency/area with Living Image software 3.2. The average signal intensities per group were compared over time

(mean  $\pm$  S.E.M. of five mice per group). Pictures were taken with an exposure time of 5 s and medium binning.

### **2.7.3.2 Polyplex Distribution after i.v. Injection**

Different untargeted polyplexes (N/P 12) containing 50  $\mu$ g siRNA including 25  $\mu$ g Cy7-labeled siRNA were mixed in a total volume of 250  $\mu$ l (HBG) and injected into the tail vein of tumor free NMRI mice. Fluorescence imaging was performed utilizing the IVIS Lumina system with Living Image software 3.2 (Caliper Life Sciences, Hopkinton, MA, USA). After anesthetizing the mice with 3% isoflurane in oxygen, polyplexes were injected into the tail vein and the distribution was measured after 0, 0.25, 0.5, 1, 4, and 24 h with a CCD camera. Experiments were performed in triplicates and pictures were analyzed using the Living Image software. Pictures were taken with an exposure time of 5 s and medium binning.

Folate-oligomer containing targeted polyplexes with different PEG spacers (1 x, 2 x, 3 x PEG24) or with hydrophobic modifications (tyrosine, caprylic acid, stearic acid) containing 50  $\mu$ g Cy7-labeled siRNA, were mixed in 250  $\mu$ l HBG and injected into the tail vein of KB tumors bearing NMRI mice. Untargeted polyplexes with 5 x or 8 x PEG24 chains were injected into tumor free NMRI mice. Each polymer was injected intravenously into three animals, with only one exception. The stearic acid containing polyplexes were injected once, as this mouse died after the application. NIR fluorescence measurement was started immediately after polyplex injection and repeated after 0.25, 1, 4, and 24 h (polyplexes with 1 x, 2 x, 3 x PEG24, tyrosine, caprylic acid or stearic acid) or after 0.25, 0.5, and 1 h (polyplexes with 5 x PEG24 and 8 x PEG24). For evaluation, the efficiency of the fluorescence signals was presented, using equalized color bar scales for each group. Pictures were taken with an exposure time of 5 s and medium binning.

### **2.7.3.3 Gel Electrophoresis of Urine Samples**

Folate receptor targeted polyplexes with different PEG spacers (1 x, 3 x PEG24) containing 50  $\mu$ g Cy7-labeled siRNA, were mixed in 250  $\mu$ l HBG and injected intravenously into tumor free NMRI mice. The mice were injected with oligomer **472** (n=2), **478** (n=2) polyplexes or pure siRNA (n=1). After 4 h, mice were anesthetized with 3% isoflurane in oxygen and placed in dorsal position. Bladders

were blindly punctured with an insulin syringe. Urine samples were analyzed in a 2% (w/v) agarose gel in TBE buffer (800 mM Tris, 3.8 M boric acid, 2 mM EDTA) without further dilution. For staining, GelRed<sup>®</sup> was added to the liquid gel. Where indicated, 2  $\mu$ l of a 0.5 M TCEP solution and 2  $\mu$ l of a heparin solution were added. Gel electrophoresis was performed at 80 V for 60 min.

#### **2.7.4 Therapeutic Assays**

For therapeutic assays  $5 \times 10^6$  Neuro2A cells in a volume of 150  $\mu$ l PBS were subcutaneously injected into the left flank of NMRI mice.

##### **2.7.4.1 Dose Finding**

Two days after tumor inoculation, intratumoral treatment with polyplexes, containing 12.5, 25, or 50  $\mu$ g Eg5 or control siRNA and oligomer **49** (N/P 12) mixed in a total volume of 50  $\mu$ l was started. Treatment was repeated on day 4, 7, 9, and 11. Bioluminescence signal was measured before each treatment and at day 14 by a CCD camera (IVIS Lumina<sup>®</sup>) 15 min after peritoneal injection of 100  $\mu$ l luciferin solution ( $c = 60$  mg/ml). After the final measurement animals were sacrificed.

##### **2.7.4.2 siRNA Comparison**

Two days after tumor inoculation mice were separated into 4 groups ( $n=9$ ) based on their bioluminescence signal (Caliper Life Sciences, USA). For this reason, bioluminescence imaging was performed using a CCD camera (IVIS Lumina<sup>®</sup>) and Living Image software 3.2, 15 min after intra peritoneal injection of 100  $\mu$ l luciferin solution ( $c=60$  mg/ml). Polyplexes consisting of oligomer **49** (N/P 12) either complexing Ran siRNA, Eg5 siRNA or control siRNA (50  $\mu$ g/mouse) were mixed in a total volume of 50  $\mu$ l (HBG), incubated for 60 min and injected intratumorally. Treatment was started at day 2 and repeated at day 4, 7, 9, 11, and 14 (3 times per week). Tumor growth was recorded through bioluminescence imaging at day 4, 7, 9, 11, 14 and caliper measurement thrice a week. Mice were sacrificed after their tumors reached a size of 1500 mm<sup>3</sup> ( $\text{length} \times \text{width}^2/2$ ). Bioluminescence signals and tumor volumes were analyzed with GrapPad Prism<sup>®</sup> software. The dates when tumors reached the endpoint criteria were recorded and Kaplan-Maier Survival analysis was performed.

### 2.7.4.3 Oligomer Comparison

Mice were injected with  $5 \times 10^6$  Neuro2A-eGFPLuc cells subcutaneously into their left flank at day 0. 2 Days later the mice were separated into 6 groups (n=5) based on their bioluminescence signal (Caliper Life Sciences, USA). Polyplexes consisting of oligomers **49** (chloride salt), **386** (TFA salt in the first experiment, chloride salt in the second experiment), and **229** (TFA salt) (N/P 12) complexing either Ran or control siRNA (50  $\mu\text{g}/\text{mouse}$ ) in a total volume of 50  $\mu\text{l}$  (HBG) were intratumorally injected. Treatment started at day 2 and was repeated at day 4, 8, 11, 15 or at day 4, 8, 11, 14. Tumor growth was recorded through bioluminescence imaging at day 4, 8, 11, 15 or at days 4, 8, 11, 14, 16, 18. In the first experiment mice were sacrificed 2 days after the last treatment. In the second experiment mice were sacrificed when the tumor of the first mouse in the polymer group, Ran or control siRNA treated reached a volume of 1500  $\text{mm}^3$  ( $\text{length} \times \text{width}^2/2$ ). Bioluminescence signals and tumor weights were analyzed with GrapPad Prism<sup>®</sup> software.

## 2.8 Statistical Analysis

Statistical analysis of all results (mean  $\pm$  standard error of the mean) was performed using GraphPad Prism<sup>®</sup>. Statistical significance of the results was evaluated by one way t-test; ns = not; \*  $p < 0.05$ ; \*\*  $p < 0.01$ ; \*\*\*  $p < 0.001$ .

## 3 RESULTS

### 3.1 Oligoamides for siRNA Delivery

#### 3.1.1 Design of Precise Carriers for siRNA Delivery

Solid-phase-supported macromolecule assembly offered the possibility to synthesize a large library of diverse, sequence defined, synthetic oligomers<sup>133-134</sup> (Figure 8). Therefore, artificial Fmoc/Boc-protected amino acids with defined 1,2-diaminoethane units were designed by D. Schaffert and N. Badgular<sup>132</sup>. The diaminoethane motif in contrast to diaminopropane has unique properties as it is not completely protonated at physiological pH<sup>135</sup>. Diaminoethane motifs are protonated in the endosomes (pH 5.5) and mediate the so called “proton sponge effect”, responsible for the high transfection activity of polyethylenimine (PEI). Four artificial amino acids (Stp = Succinyl-tetraethyl-pentamine, Gtp = Glutaryl-tetraethyl-pentamine, Ptp = Phthalyl-tetraethyl-pentamine and Gtt = Glutaryl-triethyl-tetramine) were applied together with lysines (branching), cysteines (bioreversible disulfide-forming), tyrosines (stability), histidines (endosomal escape) and various fatty acids (stability and lysis) to generate a library of more than 600 defined structures by N. Badgular, C. Dohmen, U. Lächelt, I. Martin, E. Salcher, D. Schaffert, C. Scholz, and C. Troiber<sup>75,133,136-137</sup>. Polycations with different topologies (T-shapes, i-shapes, U-shapes and branched structures) were synthesized to discover novel biodegradable, sequence defined siRNA carriers. The first two oligomer classes contain two terminal cysteines and a hydrophobic domain either in the middle (T-shape) or at the N terminus (i-shape). The third oligomer class is modified at the C and N terminus with hydrophobic domains (U-shape) either with or without terminal cysteines. The last oligomer class contains three terminal cysteines for cross-linking (branched) and has no hydrophobic modifications. This novel approach also allowed the incorporation of shielding agents (for example Polyethylenglycol) and targeting ligands (for example folic acid, methotrexate).

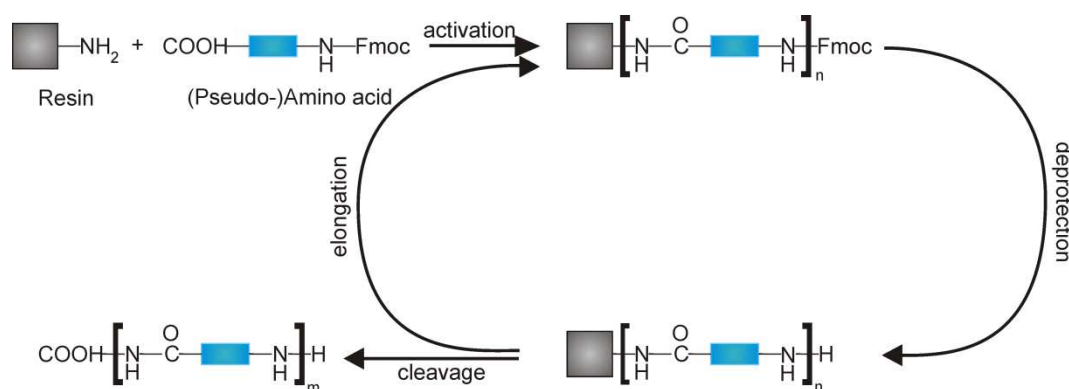


**Figure 8 Scheme of solid-phase-supported oligomer synthesis:** Demonstrates the different steps during oligomer assembly like coupling, basic deprotection and acidic cleavage.

### 3.1.2 Identification of Powerful siRNA Carriers

To identify the requirements for successful siRNA delivery, oligomers consisting of different building blocks and with different topologies have been synthesized. Screening of these structures in a marker gene silencing screen *in vitro* revealed several structure-activity-relations<sup>75</sup>.

Polymers containing Stp and Gtp building blocks showed the best transfection efficiencies in i-shape and branched structures. In contrast, the shorter Gtt building block was inactive in both topologies whereas the Ptp building block was only active in i-shaped oligomers. EtBr assays revealed Stp as the building block with the best binding capacity for siRNA. For branched structures and T-shapes at least two Stp units per arm were necessary to efficiently bind siRNA and mediate effective target gene knockdown. In contrast, U-shape oligomers with only one Stp unit were suitable for siRNA binding and mediated target gene knockdown.

For better siRNA complexation and because of their lytic activity different fatty acids were incorporated into the lipo-oligomers (T-shape, i-shape and U-shape). Oligomers with linolic and oleic acid showed pH dependent lytic activity and performed best in transfection experiments compared to other fatty acids (for example myristic acid, stearic acid).

Especially for branched structures, but also for T- and i-shaped oligomers stabilization by terminal cysteines was essential for successful siRNA transfection. On the contrary, U-shaped oligomers mediated efficient siRNA delivery without cysteines, because of the high amount of fatty acids. Serum challenge revealed that U-shaped oligomers with terminal cysteines form the most stable polyplexes, followed by U-shaped oligomers without cysteines, i-shaped

oligomers and branched structures.

The different oligomer topologies mediated similar target gene knockdown in a murine neuroblastoma cell line (Neuro2A). On the other hand, different cell lines did react diversely to oligomers with different topologies. For further experiments three diversely shaped oligomers (**49** = T-shape, **229** = i-shape, **386** = branched) have been chosen to demonstrate biophysical properties (siRNA binding, particle size) and *in vitro* gene silencing activity (Figure 9). U-shaped oligomers were excluded because they showed toxicity in a DNA transfection experiment *in vivo*.

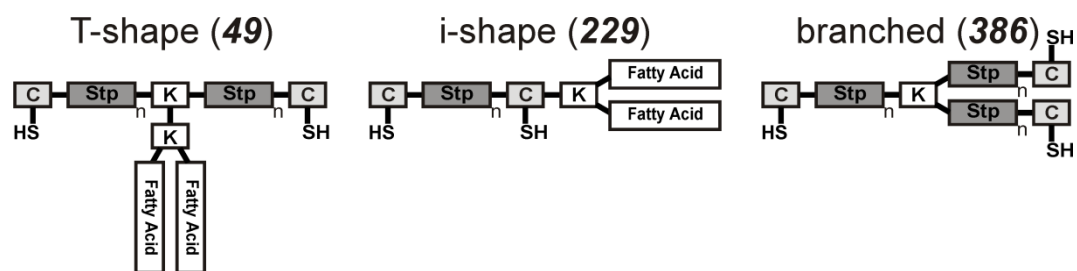


**Figure 9 Oligomer classes:** Sketches of T-shape oligomer **49** ( $n=2$ ) containing 4 STP units and oleic acid, i-shape oligomer **229** ( $n=3$ ) containing 3 STP units and linolic acid and branched oligomer **386** ( $n=3$ ) containing 9 STP units.

### 3.1.2.1 Biophysical Characterization

As described previously, effective binding of nucleic acids was a major hurdle for successful siRNA delivery. Different siRNA binding capacities of the three oligomers (**49**, **229**, **386**) were demonstrated (Figure 10). All 3 oligomers were able to complex the nucleic acid already at low N/P ratios. Oligomer **386** completely bound siRNA at an N/P ratio of 3, whereas the other two carriers needed slightly higher oligomer amounts to completely bind siRNA.

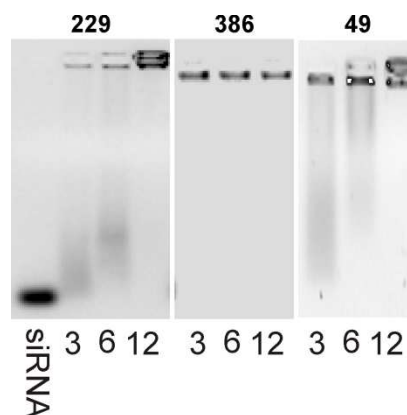


**Figure 10 Gel shift assay:** siRNA binding capacity of oligomers **49**, **229** and **386** at different N/P ratios (experiment performed by C. Troiber and T. Fröhlich).

In conclusion, the gel shift assay demonstrated the absence of free siRNA at an

N/P ratio of 12 for oligomers **49**, **229** and **386**. Therefore, this N/P was chosen for further characterization, like particle size and zeta potential. DLS (dynamic light scattering) measurement revealed very small polyplexes size for the lipooligomers **49** and **229** in a range of 20-50 nm. In contrast, oligomer **386** formed big particles with a size of approximately 600 nm (Table 1). Zeta potential of oligomers **49** and **386** were medium high, whereas oligomer **229** showed only low zeta potential.

Oligomer ID	Oligomer sequence	Z-Average (nm)	Zeta potential (mV)
<b>49</b>	C-Stp <sub>2</sub> -[(OleA) <sub>2</sub> -K]K-Stp <sub>2</sub> -C	23 ± 4	24.9 ± 1.0
<b>229</b>	C-Stp <sub>3</sub> -C-K-(LinA) <sub>2</sub>	48	6.12
<b>386</b>	[(C-Stp <sub>3</sub> ) <sub>2</sub> ]K-Stp <sub>3</sub> -C	597 ± 3	20.8 ± 1.3

**Table 1 Size and zeta potential measurement:** Polyplex size and zeta potential at N/P 12 of oligomer **49**, **229** and **386** (experiment performed by C. Troiber and T. Fröhlich).

The biophysical characterization demonstrated successful siRNA binding for the three oligomers and the formation of polyplexes with different sizes and zeta potentials.

### 3.1.2.2 GFP Knockdown Screen

Target gene silencing was examined in an eGFPLuc silencing assay, enabling the comparison of different oligomers at several N/P ratios. For this reason, cell lines stably expressing the marker gene eGFPLuc have been generated by lentiviral transduction. These cell lines were transfected with polyplexes containing either GFP siRNA targeting the eGFPLuc or a scrambled control siRNA. Reduced luciferase signals in the GFP siRNA group, two days after siRNA transfection, demonstrated successful target gene silencing. In contrast, reduced luciferase signals in both groups indicated unspecific toxicity. First knockdown experiments were always carried out in the Neuro2A-eGFPLuc cell line. For comparison reasons Neuro2A cells were transfected with “gold standard” Lipofectamine 2000 (LF2000, standard protocol), a modified Polyethylenimine<sup>54</sup> (PEI Succ10, w/w = 4/1), or the novel T-shape oligomer **49** (Figure 11).

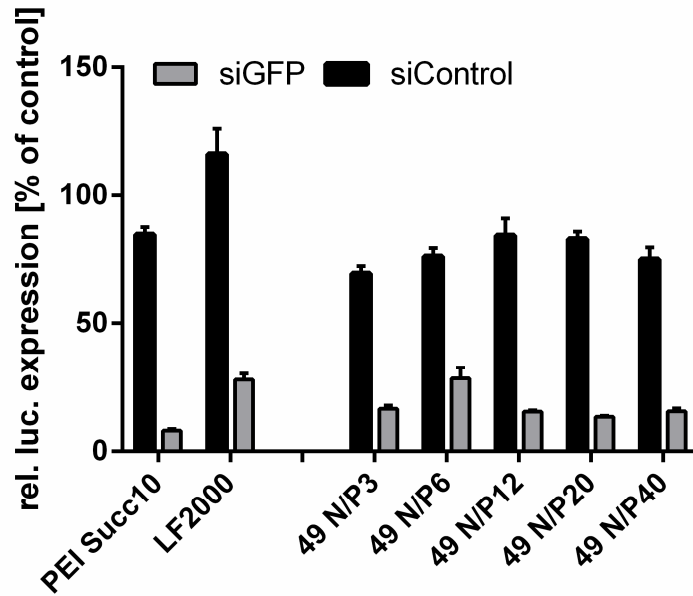


**Figure 11 eGFPLuc silencing assay:** Target gene silencing of standard polymer PEI-Succ10 and standard liposome LF2000 was compared to sequence defined oligomer **49** at different N/P ratios.

Both standards and oligomer **49** were able to mediate specific target gene knockdown, in the GFP siRNA group, without unspecific toxicity. Oligomer **49** showed effective target gene knockdown beginning with N/P 3 and displayed no toxicity even in the high N/P of 40.

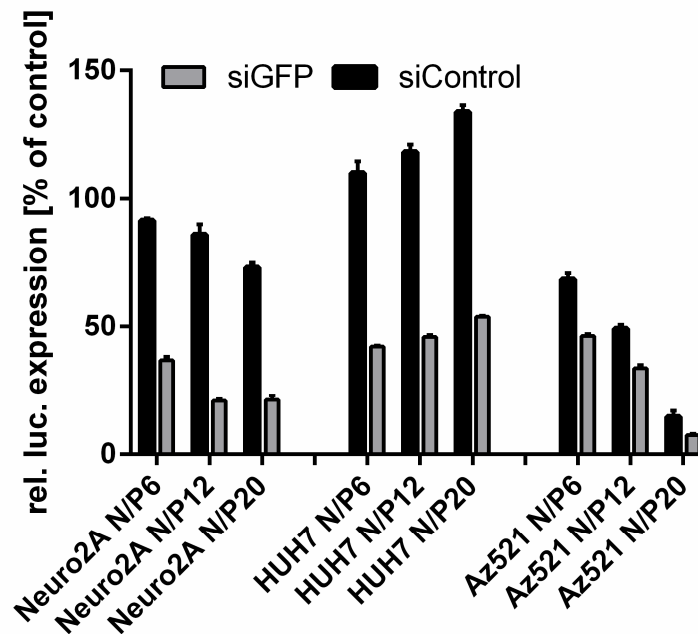


**Figure 12 eGFPLuc silencing assay:** Target gene silencing of oligomer **49** polyplexes in standard cell line Neuro2A was compared to HUH7 and Az521 cell lines.

For further evaluation eGFPLuc knockdown in Neuro2A cells was compared to

the knockdown in human hepatocellular carcinoma cells (HUH7) and a gastric cancer cell line (Az521) (Figure 12). The results demonstrated the diverse transfection efficiency of this oligomer in different cell lines. Oligomer **49** was a highly effective oligomer for the transfection of Neuro2A and HUH7 cells, whereas the gastric cancer cell line Az521 showed unspecific toxicity after transfection. Thereafter, the transfection efficiencies of oligomers **49**, **229** and **386** were compared in the Neuro2A cell line (Figure 13). The results demonstrated similar eGFPLuc silencing mediated by the lipo-oligomers **49** and **229** and the branched oligomer **386**.

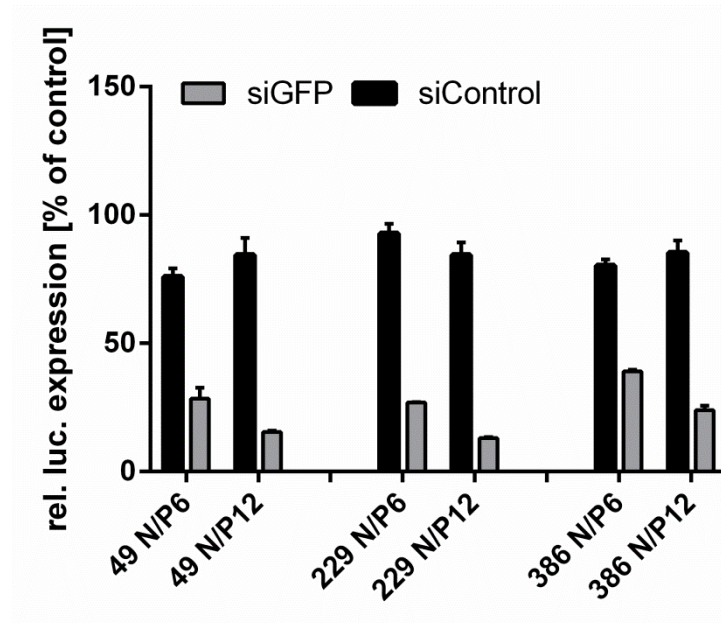


**Figure 13 eGFPLuc silencing assay:** Target gene silencing of oligomer **49** polyplexes was compared to oligomer **229** and **386** polyplexes at N/P 6 and 12.

In conclusion, all oligomers mediated marker gene knockdown comparable to the standards LF2000 and PEI Succ10. The successful marker gene knockdown and the low toxicity of the oligomers indicated their applicability for *in vivo* testing.

### 3.1.3 Therapeutic Gene Silencing

Knockdown of genes involved in cell division, metabolic processes or angiogenesis can affect tumor progression<sup>138-140</sup>. Hence, siRNA polyplexes targeting genes essential for cancer cells reduce tumor cell viability and in consequence lead to reduced tumor growth. The previous described target genes Eg5 and Ran were evaluated *in vitro* and in an intratumoral assay *in vivo* for this purpose. Knockdown of both therapeutic targets should lead to reduced tumor cell

viability and tumor growth.

### 3.1.3.1 Eg5 and Ran Silencing on mRNA and Protein Level

The knockdown of therapeutic targets, Eg5 and Ran, was determined by qPCR (Figure 14) and Western blot analysis (Figure 15), demonstrating delivery efficiency and knockdown kinetics of the applied oligomers **49**, **229**, and **386**. Also, the target specificity of utilized siRNA sequences was assured by these assays. For this purpose, Neuro2A cells were transfected with either Eg5, Ran or control siRNA, and cells were lysed for mRNA or protein isolation after 24, 48, and 72 h. Results showed effective silencing of Eg5 mRNA after 24 h for all Eg5 siRNA containing polyplexes (Figure 14a), however with a recovery after 48 h (Figure 14b) and nearly no difference of Eg5 and control siRNA transfected cells after 72 h (Figure 14c).

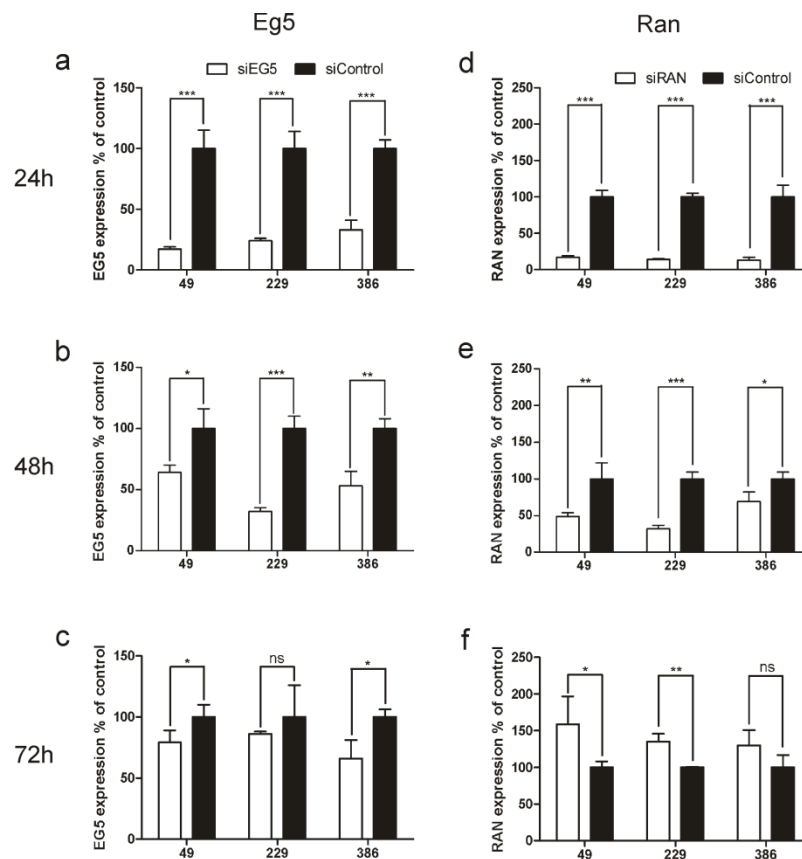


**Figure 14 Gene silencing on mRNA level:** qPCR data of control, Eg5 and Ran siRNA (370 nM) transfected cells delivered by oligomers **49**, **229** and **386**. GAPDH was used as housekeeper for all experiments.  $\Delta$ Ct values of control siRNA transfected cells were set to 100% and compared to the  $\Delta$ Ct values of either Eg5 or Ran siRNA transfected cells. Graphs (a-c) demonstrate Eg5 knockdown and (d-f) Ran knockdown after 24, 48, and 72h

Western blot results indicated a similar but shifted time course with a delay of one

day for Eg5 protein reduction. Protein knockdown at day 1 and 2 was followed by a recovery at day 3 (Figure 15). Efficiencies and kinetics of Ran knockdown on mRNA and protein level were similar to Eg5 knockdown. The main difference was an observed counter regulation of Ran mRNA expression (up to 150%) at 72 h after Ran siRNA transfection (Figure 14f).

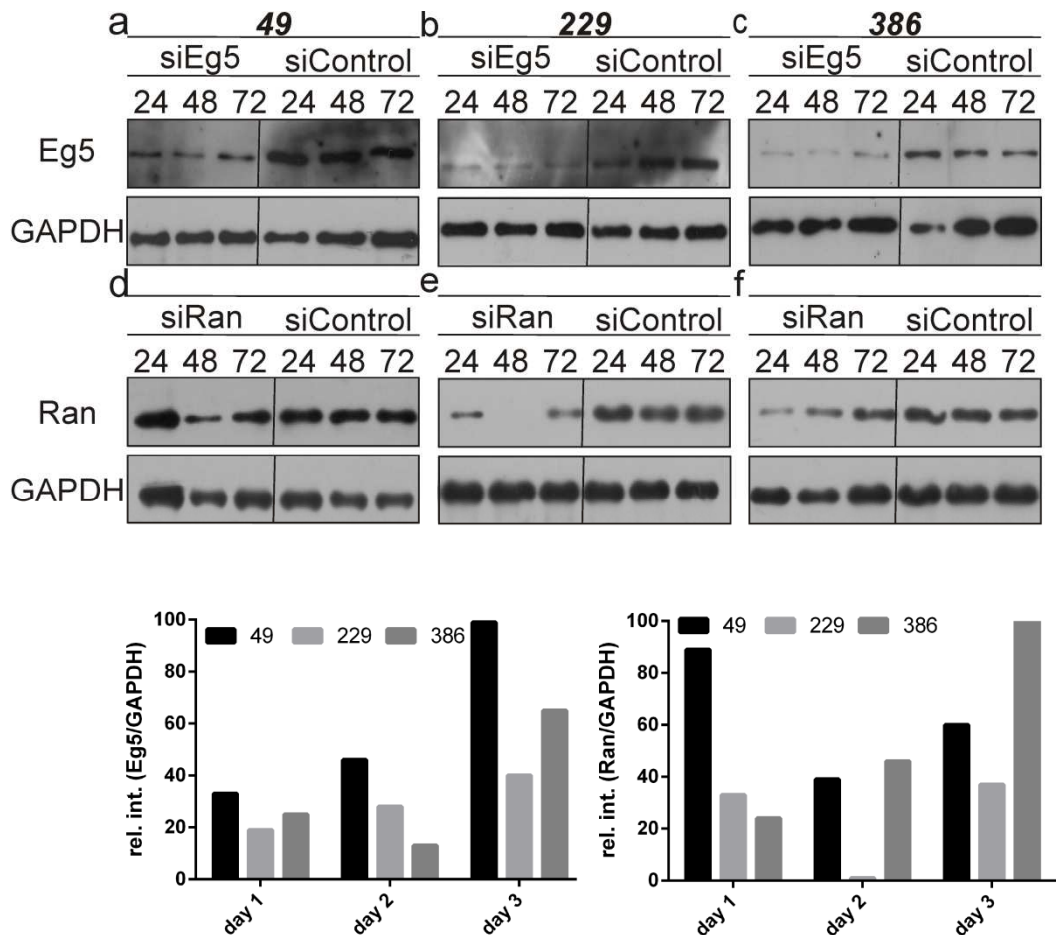


**Figure 15 Gene silencing on protein level:** Western blot analysis of control, Eg5 and Ran siRNA (370 nM) transfected cells using oligomers **49**, **229** and **386**. GAPDH was used as loading control for all experiments. Western blots (a-c) demonstrate Eg5 knockdown and (d-f) demonstrate Ran knockdown after 24, 48, and 72 h. Blots were further quantified with ImageJ software and control siRNA transfected relative intensities were set to 100%.

These transfection results demonstrated the effective knockdown of Eg5 and Ran mRNA with minor differences in the time course, but no differences in the knockdown efficiency triggered by the different carriers. The branched oligomer **386** showed the fastest kinetic, with strong protein and mRNA knockdown at day 1 and the most persistent knockdown with significant Eg5 mRNA reduction at day 3. Both lipo-oligomers, **49** and **229**, showed comparable time courses, with oligomer **229** mediating slightly stronger target mRNA knockdown. These results demonstrated similar and efficient Eg5 and Ran knockdown on mRNA and

protein level. Thus they were, in accordance with our previous studies, showing effective eGFPLuc marker gene knockdown for the three oligomers. Further *in vitro* assays were carried out to gain a better understanding of the transfection efficiencies and the related biological effects.

### 3.1.3.2 Cell Cycle Analysis

Eg5 is responsible for the formation of bipolar mitotic spindles during mitosis, in consequence Eg5 knockdown caused cell-cycle arrest and induced apoptosis. Successful application of Eg5 siRNA was demonstrated by the detection of the typical monoastral spindles of cell nuclei in cell culture. Only dividing cells are affected by Eg5 knockdown, hence typical aster formation can be visualized in mitotic cells after DAPI (DNA) and tubulin (spindle apparatus) staining (Figure 16).

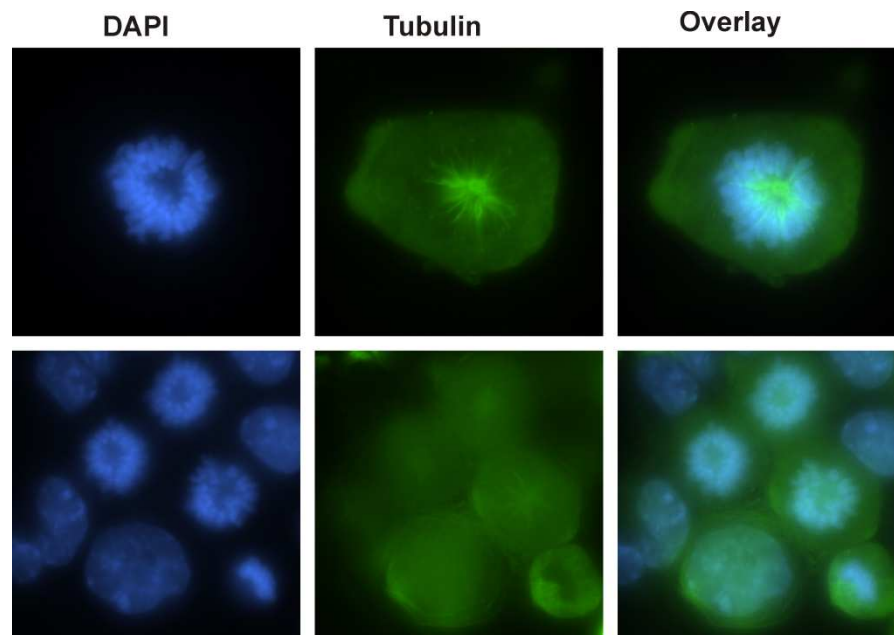


**Figure 16 Aster formation assay:** Eg5 knockdown by oligomer **49** polyplexes caused Aster formation in Neuro2A cells visualized by staining of nuclei (DAPI = blue) and tubulin (green).

The previously successful oligomers **49** and **229** were compared in terms of their transfection efficiency in Neuro2A cells demonstrating successful Eg5 knockdown for both oligomers (Figure 17). Aster formation is a positive readout system, therefore no mitotic figures could be observed after application of control siRNA.

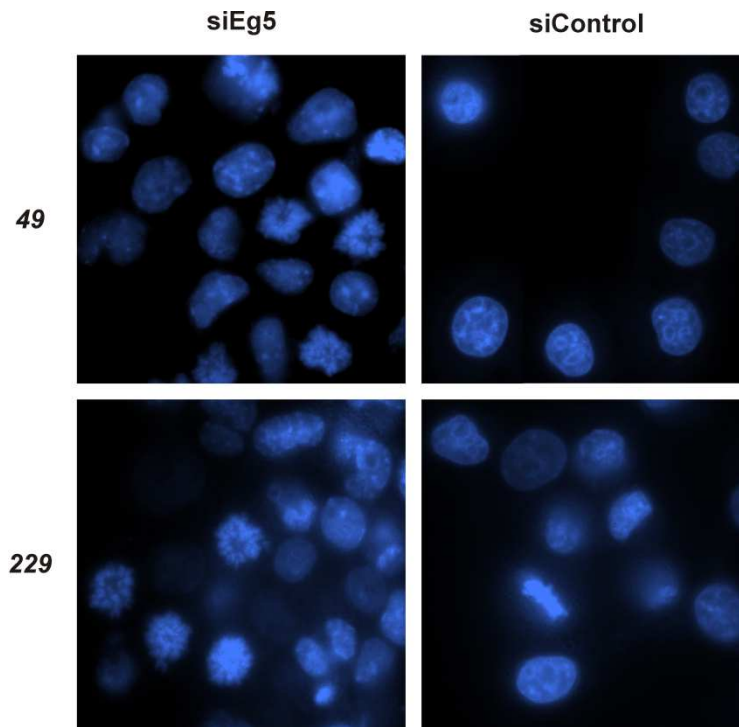


**Figure 17 Aster formation assay:** Eg5 knockdown visualized by staining of nuclei (DAPI = blue) demonstrates aster formation in Neuro2A cells after transfection with polyplexes of oligomers **49** or **229**. Control siRNA did not cause aster formation.

Aster formation is equivalent to a mitotic block, because cells are unable to divide into daughter cells after Eg5 knockdown. This mitotic block led to accumulation of cells in G2 phase which were detectable through a flow cytometric assay. For this assay nuclear DNA of Eg5 and control siRNA transfected cells was stained with propidium iodide (PI). Untransfected and control siRNA transfected cells showed typical histograms with a prominent G1-0 peak and a much smaller G2 peak, while Eg5 transfected cells showed a diminished G1-0 peak and a much greater G2 peak (Figure 18). Cells between G1/G0 and G2 phase are in synthesis phase and were not affected by the transfection.

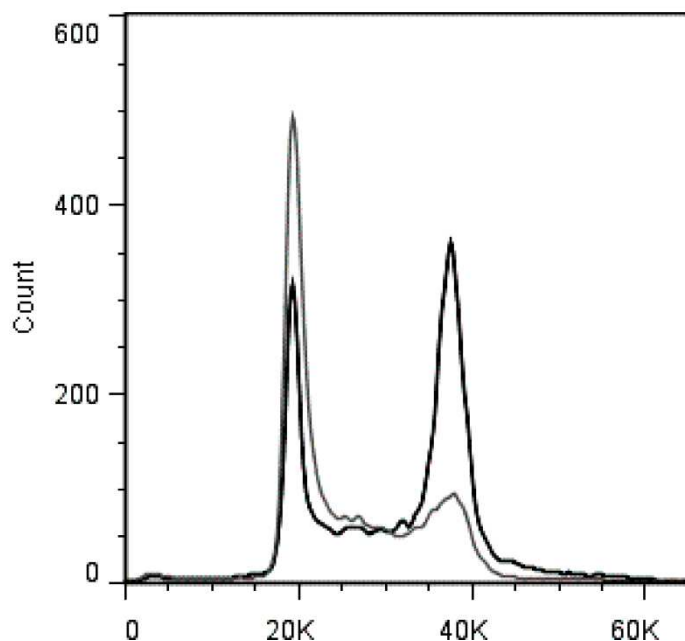


**Figure 18 Cell cycle analysis by flow cytometry:** Representative histograms of PI stained Neuro2A cells 24 h after Eg5 (black) or control (light grey) siRNA transfection. The Peak at 20K demonstrates cells with haploid set of chromosomes (G1/G0) whereas the peak at 40K demonstrates cells with diploid set of chromosomes (G2).

Again the two oligomers **49** and **229** were tested for their transfection efficiency in the flow cytometric assay. Significant difference between Eg5 siRNA treated and control siRNA treated samples was detected for both polymer formulations (Table 2). Although, both assays allowed the detection of successful Eg5 knockdown *in vitro*, particularly the histological assay offered an interesting possibility for the detection of functional *in vivo* gene silencing.

Polymer	siRNA	% of cells in sub G1-G0	% of cells in G1-G0	% of cells in S	% of cells in sub G2-M
49	Eg5	2.4 ± 0.7	20.1 ± 2.9	11.7 ± 0.2	65.8 ± 2.4
	Control	3.9 ± 0.4	57.1 ± 2.5	15.1 ± 1.1	23.6 ± 1.2
229	Eg5	4.4 ± 1.3	23.6 ± 8.5	14.5 ± 2.5	55.0 ± 7.8
	Control	3.3 ± 1.2	59.6 ± 0.6	14.3 ± 0.8	21.2 ± 3.3

**Table 2 Comparison of Eg5 knockdown by flow cytometry:** Cell cycle stages of Neuro2A cells 24 h after transfection with oligomer **49** and **229** polyplexes. Cells in G1/G0, G2 and S phase were quantified after Eg5 and control siRNA transfection.

In a further flow cytometric assay the effects of Eg5, Ran and control siRNA, mediated by oligomers **49**, **229** and **386** were compared to buffer treatment after 24, 48, and 72 h (Figure 19). Altered cell cycle distribution for Eg5 and Ran

siRNA transfected cells was observed, while transfection with control siRNA showed no effect. This indicated the absence of notable unspecific oligomer effects.

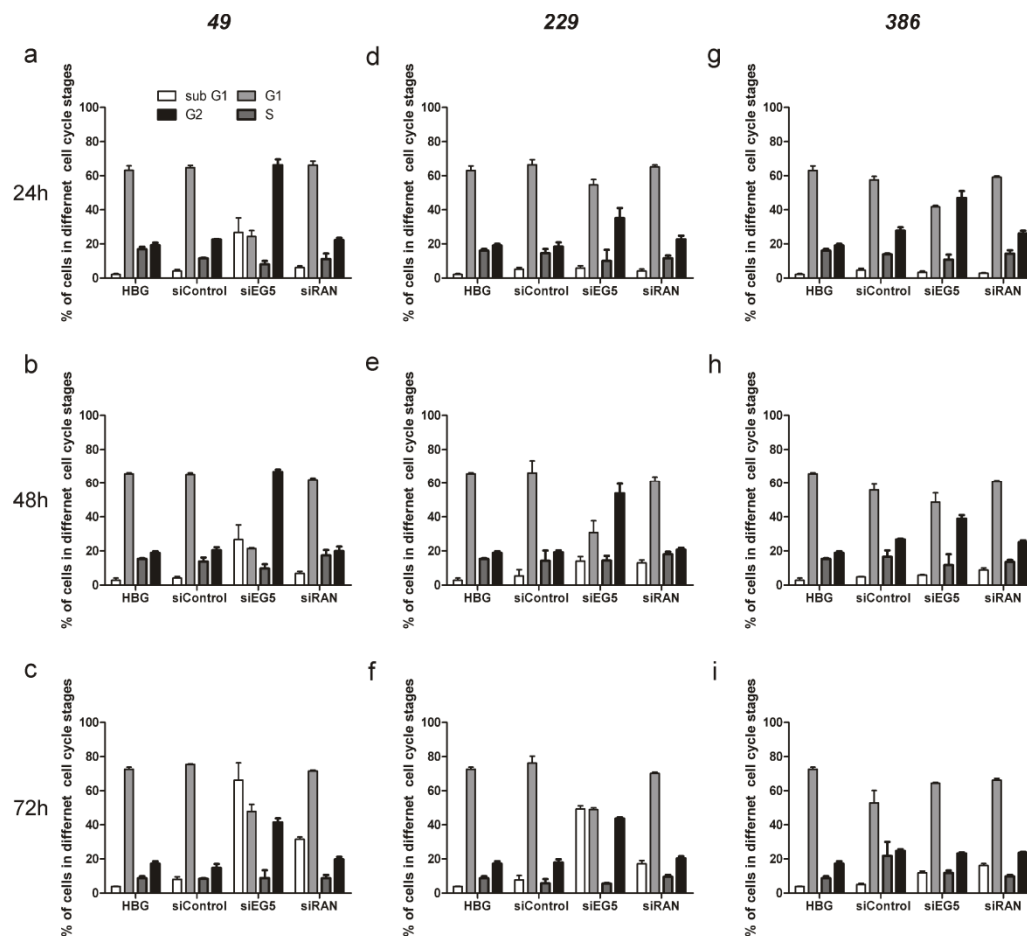


**Figure 19 Effect of siRNA delivery on tumor cell cycle:** Flow cytometric analysis of cell cycle distributions of control, Eg5 and Ran siRNA (370 nM) transfected Neuro2A cells using oligomers (a-c) **49**, (d-f) **229** and (g-i) **386**. Transfected cells were stained with propidium iodide after 24, 48, and 72 h. Eg5 and Ran siRNA transfected cells were compared to control siRNA and buffer (HBG) transfected cells.

Ran knockdown caused cell death detectable through the increased sub G1/G0 peak after 72 h (Figure 19a,d,g compared to Figure 19c,f,i), whereas Eg5 knockdown principally led to cell cycle arrest in G2 phase (Figure 19a,d,g and Figure 19b,e,h) and consequently to cell death (Figure 19c,f,i). Therefore, Eg5 knockdown could be detected by an increased G2 peak and a sub G1/G0 population appearing 24 h after transfection (Figure 19a,d,g). The sub G1/G0 peak increased after 48 h (Figure 19b,e,h) and 72 h (Figure 19c,f,i), while the G2 peak decreased. This result indicated that transfected cells undergo cell death. In contrast, Ran siRNA transfected cells only showed a moderate increase of dead cells (sub G1/G0) after 48 and 72 h compared to control and buffer treated cells. The greatest effects on cell cycle were mediated by oligomer **49** (Figure 19a-c),

while oligomers **229** (Figure 19d-f) and **386** (Figure 19g-i) mediated the same but considerably reduced effects on cell cycle. This assay demonstrated that especially Eg5 knockdown had influence on the G2 peak, while both therapeutic siRNAs led to increased sub G1/G0 peaks.

### 3.1.3.3 Cell Viability Assay

A cell viability assay (by ATP measurement, CellTiter Glo) demonstrated reduced viability of tumor cells after Eg5 and Ran siRNA transfection. In accordance with previous assays, control siRNA transfected cells did not show reduced viability compared to buffer treated cells. Polyplexes containing either Eg5 or Ran siRNA decreased cell viability for the three tested oligomers.

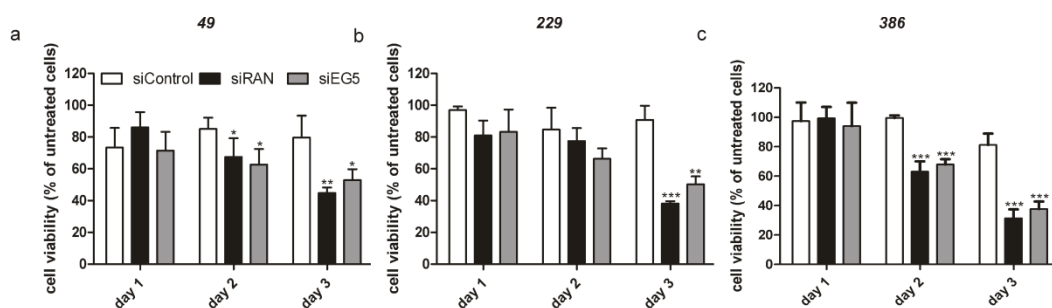


**Figure 20 siRNA dependent tumor cell killing:** Cell viability of Eg5, Ran and control siRNA (370 nM) transfected Neuro2A cells was measured 24, 48, and 72 h after transfection with oligomers (a) **49**, (b) **229** and (c) **386**. Viability of buffer treated cells was set to 100% cell viability and compared to Eg5, Ran and control siRNA transfected cells.

However, differences between oligomers concerning kinetics and cell killing efficiency were observed (Figure 20). Oligomer **386** (Figure 20c) led to the fastest and strongest reduction of cell viability whereas oligomers **49** (Figure 20a) and **229** (Figure 20b) showed slower kinetics and reduced effects on cell viability. In accordance with the Western blot experiments, the CellTiter Glo measurements confirmed the fast kinetic of oligomer **386**. In summary, the *in vitro* assays demonstrated efficient siRNA delivery for all tested oligomers, as indicated by mRNA silencing. Furthermore, the target knockdown on mRNA and protein levels consequently leading to reduced tumor cell viability made the tested oligomers and siRNAs interesting for following *in vivo* experiments.

### 3.1.4 Distribution of Fluorescence Labeled Polyplexes

To determine polyplex retention after intratumoral injection or passive tumor targeting after intravenous injection siRNAs conjugated to fluorescent dyes were

incorporated into the polyplexes. Fluorescent polyplexes allowed the detection either in organ sections or in living animals. For imaging experiments near infrared dyes like Cy7 had to be applied because of the auto fluorescence of red blood cells and food ingredients.

### 3.1.4.1 Histological Cy3 Analysis

For the detection of successful siRNA delivery *in vivo*, Cy3 labeled siRNA was integrated into the polyplexes and injected intravenously into the tail vein of tumor bearing mice.

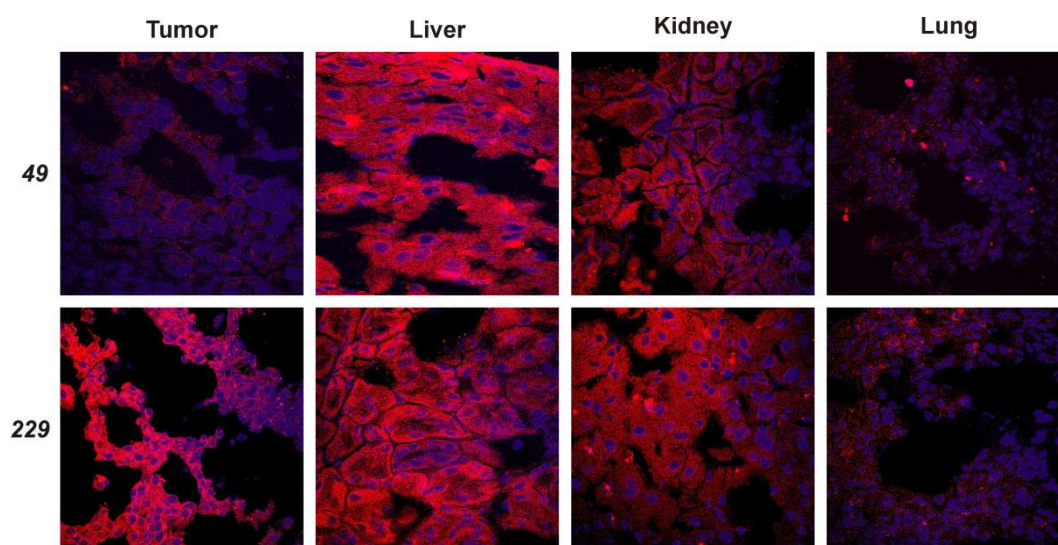


**Figure 21 LSM images of tumor, liver, kidney and lung cryo sections:** Fluorescence images of organ slices after intravenous polyplex injection were analyzed by laser-scanning-microscopy. Nuclei were stained with Hoechst dye (blue) and the slices were analyzed for Cy3 labeled siRNAs (red). Experiment performed together with Raphaela Kläger (veterinary MD thesis, LMU 2013).

One hour after polyplex injection mice were sacrificed and tumors, livers, kidneys, and lungs were harvested. The tumor images confirmed that both polymers were able to compact siRNA, protect it from degradation in the blood stream and deliver siRNA into the tumors (Figure 21). LSM (laser-scanning-microscopy) images revealed superior accumulation of Cy3 siRNA in tumors of oligomer **229** injected mice compared to tumors of oligomer **49** injected mice. Great accumulation in the liver and kidneys could be observed for both lipopolyplexes, whereas the Cy3 signal in the lungs was very weak. Accumulation in the liver can be explained by the lipophilic character of the oligomers while the strong kidney signals are influenced by the clearance of pure siRNA or small particles.

### 3.1.4.2 Living Image

For the comparison of oligomers **49**, **229** and **386** after intratumoral injection, at first polyplex retention was assayed, because this is a crucial requirement for siRNA activity *in vivo*. Therefore, mice were injected intratumorally with polyplexes containing Cy7 labelled siRNA.

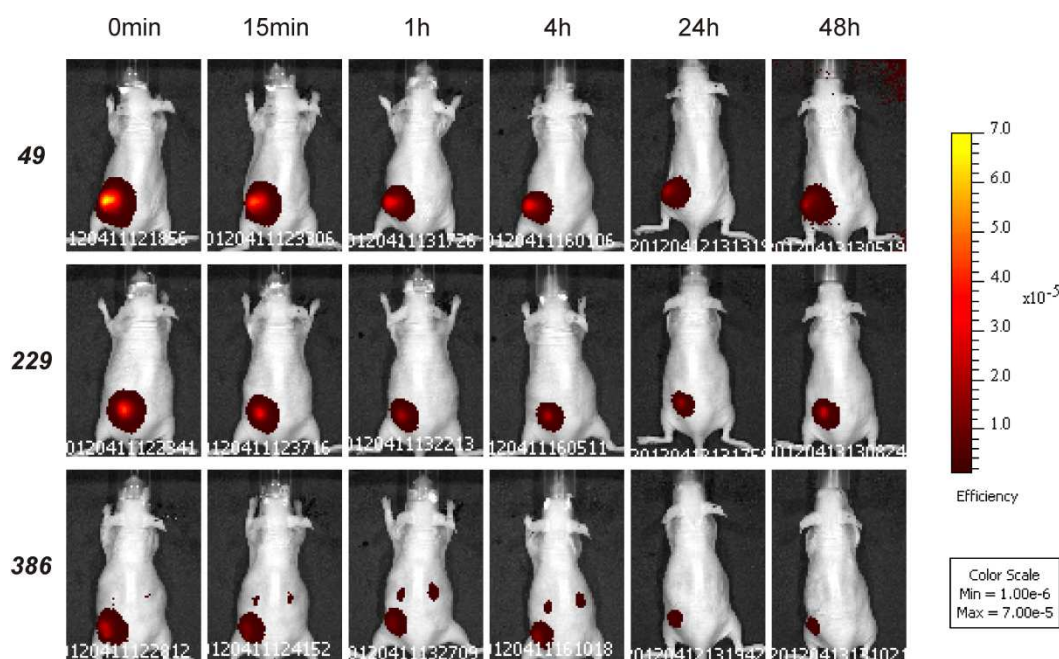


**Figure 22: Retention of siRNA in tumors.** Fluorescence imaging of intratumoral injected polyplexes showed Cy7-siRNA signals in tumors over 48 h for all oligomers. Oligomer **386** showed increasing kidney signals already detectable right after injection. Experiment performed together with Raphaela Kläger (veterinary MD thesis, LMU 2013).

Fluorescence signals were measured directly after polyplex injection and after 0.25, 1, 4, 24, and 48 h (Figure 22). The images showed that all oligomers were able to retain siRNA in the tumors for 48 h. Oligomers **49** and **229** showed the best retention of siRNA with extensive Cy7 signals detectable in the tumor for 48 h. In contrast to lipo-oligomers **49** and **229**, polyplexes of oligomer **386** showed additional early Cy7 siRNA signals in the kidneys of intratumoral injected mice. Cy7 signals in the tumors decreased but were still detectable after 48 h, whereas kidney signals increased within the first 4 h and were not detectable after 24 and 48 h. This is consistent with renal clearance of free Cy7 siRNA after polyplex dissociation, analogously to the previous observation<sup>116,136</sup>. Hence, the Cy7 siRNA experiment demonstrated the higher stability and improved retention of polyplexes with the lipid-modified oligomers **49**, **229** in contrast to oligomer **386** without fatty acid modification.

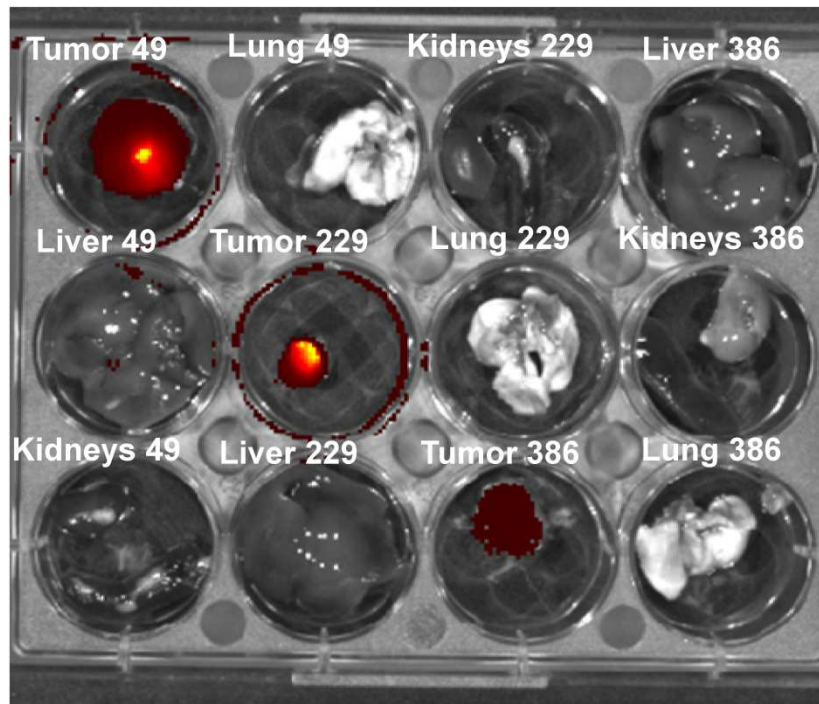


**Figure 23 Cy7 signals in mouse organs:** Fluorescence imaging of i.t. injected polyplexes showed Cy7-siRNA signals in tumors after 48 h for all oligomers. Oligomer **49** showed Cy7 signals detectable in the liver. Experiment performed together with Raphaela Kläger (veterinary MD thesis, LMU 2013).

The results were confirmed by measuring the harvested organs after euthanasia of the mice (Figure 23). Only tumors showed measurable Cy7 signals and the lipooligomer **49** and **229** showed stronger tumor signals than the branched oligomer **386**.

### 3.1.5 Dose Escalation Study

A dose response experiment was performed to determine the siRNA dose necessary for successful tumor growth reduction after intratumoral polyplex injection. For this experiment oligomer **49** was chosen and injected in an N/P of 12 for all siRNA concentrations. Hence, 12.5, 25, or 50  $\mu\text{g}$  Eg5 siRNA or control siRNA containing polyplexes were injected into subcutaneous Neuro2A-eGFPLuc tumors. Successful delivery of Eg5 siRNA has been previously demonstrated to result in cell cycle arrest and apoptosis of tumor cells. Therefore, successful Eg5 knockdown slowed down tumor progression. The subcutaneous tumors were treated five times starting with day 2 (2, 4, 7, 9, 11) after tumor cell inoculation and the bioluminescent tumor signals were measured at indicated time points (Figure 24).

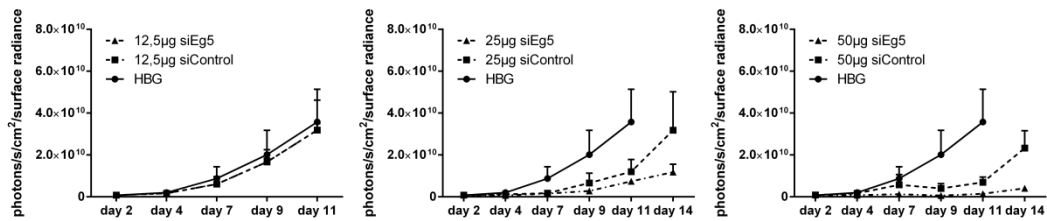


**Figure 24 Dose escalation experiment:** Tumor growth of subcutaneous Neuro2A-eGFPLuc tumors in mice after repeated intratumoral treatment (3 mice per group) with oligomer **49** and Eg5 or control siRNA (N/P 12) polyplexes. Animals were treated with 50  $\mu\text{g}$ , 25  $\mu\text{g}$ , or 12.5  $\mu\text{g}$  siRNA per mouse at day 2, 4, 7, 9 and 11 after tumor cell inoculation. The treatment group with 12.5  $\mu\text{g}$  siRNA was terminated on day 11 due to excessive tumor size. Experiment performed together with Raphaela Kläger (veterinary MD thesis, LMU 2013).

Experiments had to be terminated on day 11 and 14, respectively, because of excessive tumor growth in the control groups. With a concentration of 12.5  $\mu\text{g}$  siRNA, no positive effect of the Eg5 siRNA on tumor growth could be observed after 11 days. In contrast, 25  $\mu\text{g}$  Eg5 siRNA per treatment slightly reduced tumor growth, but a relatively large variation within the treatment group was observed. Best results were achieved with 50  $\mu\text{g}$  Eg5 siRNA per treatment resulting in significantly reduced tumor growth compared to control siRNA.

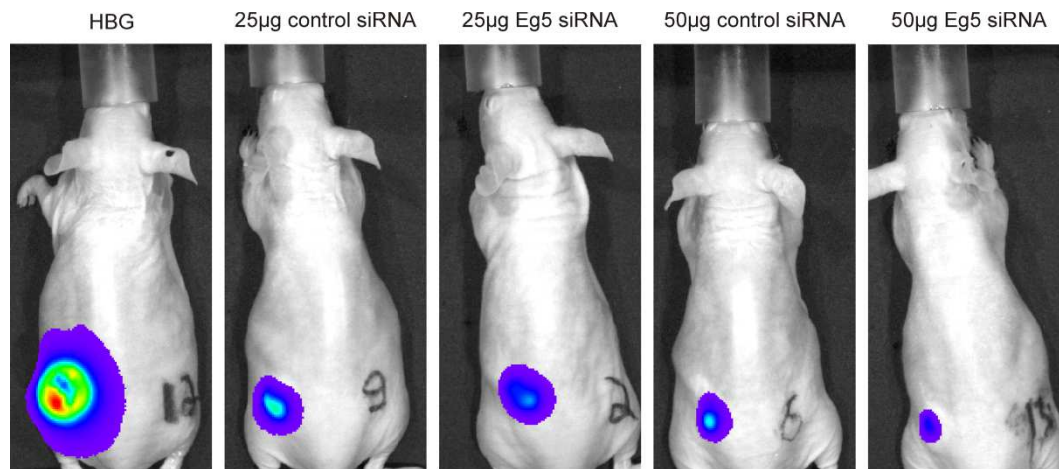


**Figure 25 Bioluminescence images of Neuro2A-eGFPLuc tumors:** Polyplex treatment resulted in reduced tumor growth compared to buffer treatment. The Eg5 polyplexes mediated siRNA specific tumor growth reduction in contrast to control siRNA polyplexes. Experiment performed together with Raphaela Kläger (veterinary MD thesis, LMU 2013).

The bioluminescence images demonstrated the dose dependency of tumor growth reduction mediated by Eg5 polyplexes (Figure 25). This experiment helped to determine the minimal siRNA doses per injection and demonstrated the ability of this new class of oligomers to deliver siRNA *in vivo* upon intratumoral injection.

### 3.1.6 Evaluation of Therapeutic siRNAs

After the required dose for an intratumoral treatment had been defined, the effects of Eg5 and Ran siRNA on tumor growth were compared. Two days after implantation of Neuro2A-eGFPLuc cells, mice were imaged detecting the bioluminescence signals of implanted tumor cells. According to this, mice were divided into four groups receiving either buffer or siRNA polyplexes. Polyplexes consisting of oligomer **49** complexing either Eg5-, Ran- or control siRNA were injected directly into the tumor. The treatment was started at day 2 and repeated at days 4, 7, 9, 11, and 14.

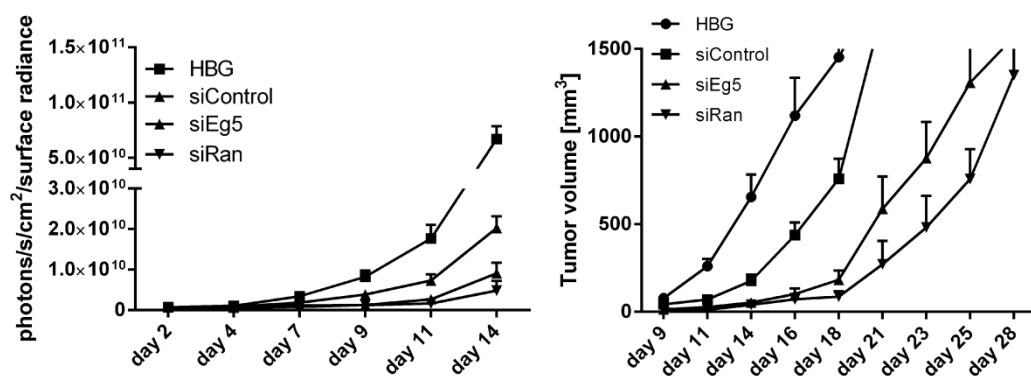


**Figure 26 siRNA comparison after intratumoral treatment:** Intratumoral injection of oligomer **49** polyplexes for the treatment of subcutaneous Neuro2A-eGFPLuc tumors. Polyplexes were injected thrice weekly and in total 6 times. Left figure shows bioluminescence imaging of the subcutaneous tumors. Eg5 and Ran siRNA treated tumors showed significantly reduced bioluminescence starting with day 9 compared to control siRNA transfected tumors (Eg5: day 9\*, day 11\*\*, day 14\*\*; Ran day 9\*, day 11\*\*, day 14\*\*\*). Right figure shows the reduced tumor volumes of Eg5 and Ran siRNA transfected tumors compared to control siRNA transfection (Eg5: day 11\*, day 14\*\*, day 16\*\*\*, day 18\*\*\*; Ran day 11\*\*, day 14\*\*, day 16\*\*\*, day 18\*\*\*). Experiment performed together with Raphaela Kläger (veterinary MD thesis, LMU 2013).

During the treatment period, tumor growth was detected by bioluminescence imaging (Figure 26). Altered bioluminescence signals concerning the different treatments could be detected starting with day 9. All polyplex treated mice showed reduced luciferase signals compared to buffer treated mice. However, Eg5 and Ran siRNA treatment resulted in far more reduced bioluminescence signals than control siRNA treatment. From day 9 on, tumor growth was also determined by calliper measurement controlling the experimental endpoint criteria of 1500 mm<sup>3</sup> tumor volume (Figure 26). Mice were sacrificed, when tumors exceeded a volume of 1500 mm<sup>3</sup> and dates were recorded enabling Kaplan-Maier survival analysis (Figure 27). The most significant reduction of tumor volume was mediated by Ran siRNA followed by Eg5 siRNA, whereas control siRNA and buffer treatment were far less effective (Figure 26a,b). Consequently, survival of

Ran and Eg5 siRNA treated groups was significantly prolonged compared to control siRNA and buffer treated groups.

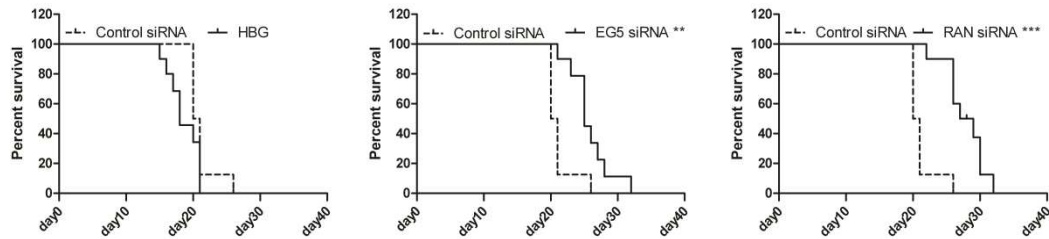


**Figure 27 Kaplan Maier survival analysis:** After the treatment interval tumors were allowed to grow until they reached a volume of  $1500 \text{ mm}^3$ , then mice were sacrificed and Kaplan-Maier survival analysis was performed (Mean survival: HBG 18 d; control siRNA 20,5 d; Eg5 siRNA 25 d; Ran siRNA 28 d). Experiment performed together with Raphaela Kläger (veterinary MD thesis, LMU 2013).

Mean survival after 6 intratumoral treatments with Ran siRNA was 28 days compared to Eg5 siRNA with 25 days, control siRNA with 20.5 days and buffer with 18 days (Figure 27). To exclude unspecific effects of oligomer **49**, tumor growth reduction of Ran and Eg5 siRNA treated mice was always compared to control siRNA treatment. The reduced bioluminescence signals and tumor sizes, as well as a prolonged survival of Ran and Eg5 treated mice provided significant evidence of the positive *in vivo* effect of both therapeutic siRNAs.

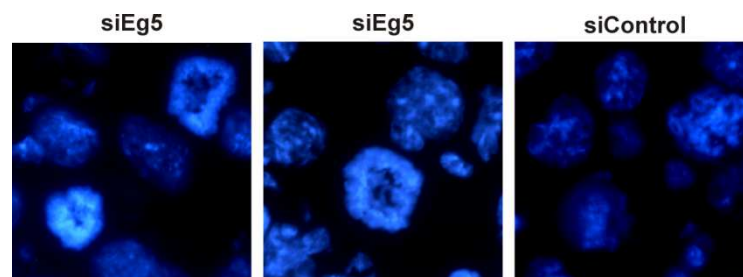


**Figure 28 Aster formation assay *in vivo*:** Intratumoral injection of oligomer **49** Eg5 siRNA polyplexes showed aster formation and confirmed Eg5 knockdown in Neuro2A tumor cells. Cryo sections were stained with Hoechst dye (blue) and analyzed with a fluorescence microscope. Experiment performed together with Raphaela Kläger (veterinary MD thesis, LMU 2013).

Additionally, mitotic arrest by Eg5 siRNA indicated successful *in vivo* target gene silencing (Figure 28). Tumors were excised 24 h after polyplex injection and  $5 \mu\text{m}$  fine sections were cut. After Hoechst staining aster formation was only detected in Eg5 siRNA treated tumors, in accordance with the previous *in vitro* results. Ran knockdown was demonstrated with a TUNEL assay, for the detection of apoptotic cells (Figure 29). This assay allowed the binding of fluorescent labelled nucleotides to the free 3' ends of DNA fragmented during apoptosis. Tumors treated with Ran siRNA polyplexes showed positive TUNEL staining in contrast

to control siRNA treated tumors.

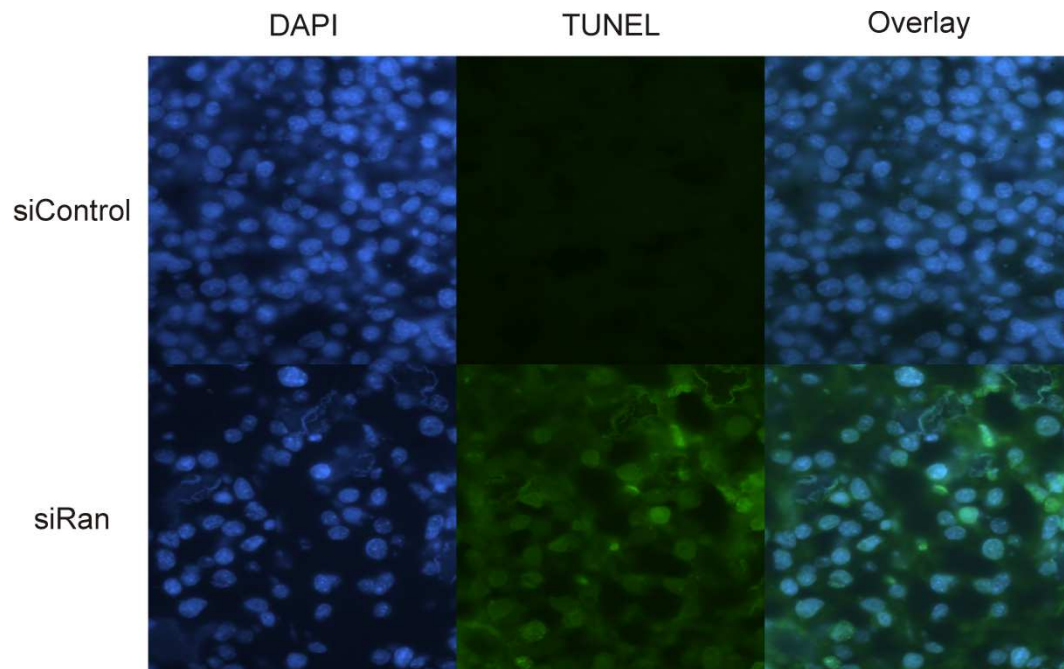


**Figure 29 TUNEL assay for the detection of apoptotic cells:** Intratumoral injection of oligomer **49** Ran siRNA polyplexes showed positive tunnel staining and confirmed that Ran knockdown led to apoptosis of Neuro2A tumor cells. Experiment performed together with Raphaela Kläger (veterinary MD thesis, LMU 2013).

Ran siRNA was chosen for subsequent experiments, as treated tumors showed the lowest bioluminescence signals, the smallest tumor volumes and the most extended survival.

### 3.1.7 Comparison of Different siRNA Carriers

Next, the three oligomers were evaluated using Ran siRNA polyplexes for intratumoral treatment as described before. Accordingly, mice were grouped based on their bioluminescence signal 2 days after the implantation of Neuro2A-eGFP<sub>Luc</sub> cells and the intratumoral treatment with Ran or control siRNA was started. siRNA polyplexes consisting of oligomers **49**, **229** and **386** were injected directly into the tumors. The injection interval was changed to only two injections per week compared to three injections per week in the previous study. Tumor progression was measured by bioluminescence imaging. Bioluminescence signals were detected at day 4, 8, 11, and 15 enabling the comparison of Ran and control siRNA treated groups. All animals were sacrificed two days after the last treatment and tumors were excised to compare tumor weights of the different groups. Despite the less frequent treatment regime, the previously tested oligomer **49** still mediated a measurable antitumoral effect in the Ran siRNA treated group

(Figure 30b), which was confirmed comparing the tumor weights of Ran and control siRNA treated groups (Figure 30a). The i-shape oligomer **229** failed to mediate any positive effect on tumor growth for Ran siRNA treated animals (Figure 30c). In contrast, the branched oligomer **386** showed a great reduction of the bioluminescence signal and also a significant effect on tumor weight for the Ran siRNA treated mice (Figure 30d).

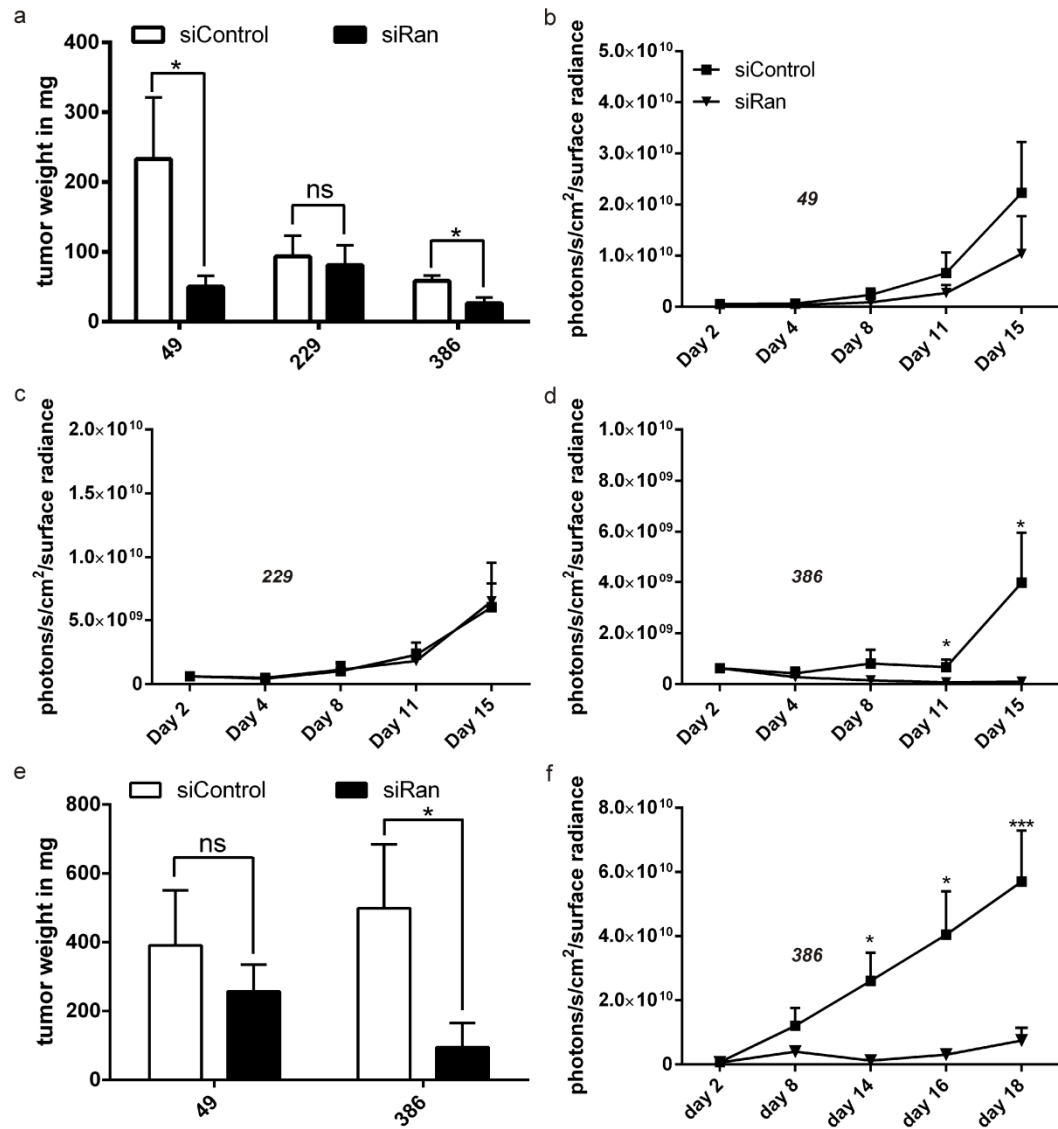


**Figure 30 Comparison of different oligomer polyplexes in antitumoral efficacy:** Intratumoral injection of oligomer **49**, **229** and **386** containing polyplexes (50  $\mu$ g siRNA per animal; N/P 12) for the treatment of Neuro2A-eGFPLuc tumors. Polyplexes containing either Ran or control siRNA were injected twice weekly in total 5 times. (a) At 2 days after the last treatment mice were sacrificed and tumor weights were analyzed to compare the tumors of control and RAN siRNA treated mice. (b-d) show tumor bioluminescence counts of Ran and control siRNA treated mice with the (b) **49**, (c) **229** and (d) **386** oligomer formulations. (e) Intratumoral injection of oligomer **49** and **386** containing polyplexes for the treatment of Neuro2A-eGFPLuc tumors as described above. After the treatment period tumors were allowed to grow until one tumor in the oligomer groups reached a volume of 1500 mm<sup>3</sup> (day 18 for **49**, day 18 for **386**). Mice were sacrificed and tumor weights were analyzed to compare the tumors of control and Ran siRNA treated mice. (f) Shows bioluminescence tumor counts of siRNA/**386** polyplex treated mice. Experiment performed together with Raphaela Klager (veterinary MD thesis, LMU 2013).

This experiment allowed the separation of the oligomers which were all effective *in vitro*, into a clear *in vivo* efficiency order. In this first *in vivo* oligomer comparison all mice were sacrificed 2 days after the last treatment. Oligomers **229** and **386** were used as trifluoroacetic acid (TFA) salts instead of chloride salt. Apparently TFA mediated some unspecific antitumoral toxicity, therefore in a second experiment only chloride salts of the previously active oligomers **49** and

**386** were applied to allow better comparability between the oligomers. Mice were sacrificed at day 18 when the first mouse in the oligomer group reached a tumor volume of 1500 mm<sup>3</sup>. Tumors were excised to compare tumor weights of Ran siRNA and control siRNA treated mice. In conclusion, tumor weights and bioluminescence signals revealed significant tumor growth reduction in the Ran siRNA group of oligomer **386** (Figure 30e,f) in both experiments. In contrast, oligomer **49** showed borderline efficiency when injected twice a week, with significant effects on tumor weights in the first but without significant effects in the second experiment (Figure 30e, bioluminescence data not shown).

### 3.1.8 Oligoamides with Enhanced Stability

High stability is an important requirement for the *in vivo* administration of polyplexes. Particularly after intravenous injections, polyplexes interact with serum proteins and blood cells leading to dissociation of the particles<sup>141</sup>. Therefore, precise changes in the oligomer structure affecting size, charge and stability of the polyplexes can positively influence *in vivo* gene silencing. For this reason C. Troiber included tyrosine-trimers into the T-shaped structures replacing terminal cysteines, central fatty acids or in addition to terminal cysteines to enhance polyplex stability<sup>142</sup>. The new polyplexes were investigated according to biophysical properties, transfection efficiency, *in vivo* distribution upon intravenous injection and *in vivo* transfection efficiency after intratumoral injection.

#### 3.1.8.1 Biophysical Characterization

Agarose gel shift assays were performed to demonstrate siRNA binding capacity of oligotyrosine containing polyplexes. Control oligomers **216** with only central fatty acids for stabilization and **468** with central oligotyrosines and terminal cysteines showed reduced siRNA binding capacity compared to standard oligomer **49**. In contrast, replacement of terminal cysteines by oligotyrosines (**332**) or the substitution of terminal cysteines and central fatty acids by oligotyrosines (**333**) displayed siRNA binding properties analogous to oligomer **49**. This demonstrated that terminal oligotyrosines can substitute the stabilizing activity of either terminal cysteines or central fatty acids. Combination of terminal oligotyrosines and cysteines (**454**, **464**) independent of their central modification improved siRNA binding compared to oligomer **49**. Gel shift assays demonstrated the increased

stability of oligomers with compared to oligomers without additional oligotyrosines (Figure 31).

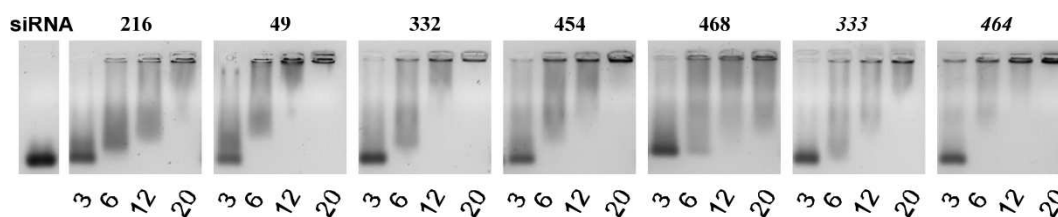


**Figure 31 Gelshift assay:** siRNA binding capacity of oligomers at different N/P ratios was tested in 2% agarose gels (experiment performed by C. Troiber).

For further characterization, particle size and zeta potential of the polyplexes were analyzed by DLS measurement (Table 3). Oligomer **468** polyplexes with solely central oligotyrosines could not be analyzed as no signal was measurable, whereas the sizes of all other siRNA polyplexes at N/P 12 was in a range applicable for further *in vivo* evaluations.

Oligomer ID	Oligomer sequence	Z-average (nm)	Zeta potential (mV)
<b>216</b>	A-Stp <sub>2</sub> -[(OleA) <sub>2</sub> -K]-Stp <sub>2</sub> -A	32 ± 2	5.1 ± 0.3
<b>49</b>	C-Stp <sub>2</sub> -[(OleA) <sub>2</sub> -K]-Stp <sub>2</sub> -C	23 ± 4	24.9 ± 1.0
<b>332</b>	Y <sub>3</sub> -Stp <sub>2</sub> -[(OleA) <sub>2</sub> -K]-Stp <sub>2</sub> -Y <sub>3</sub>	150 ± 2	38.1 ± 0.8
<b>454</b>	C-Y <sub>3</sub> -Stp <sub>2</sub> -[(OleA) <sub>2</sub> -K]-Stp <sub>2</sub> -Y <sub>3</sub> -C	99 ± 2	50.7 ± 0.8
<b>468</b>	C-Stp <sub>2</sub> -[(Y <sub>3</sub> ) <sub>2</sub> -K]-Stp <sub>2</sub> -C	n.d.*	n.d.*
<b>333</b>	Y <sub>3</sub> -Stp <sub>2</sub> -[(Y <sub>3</sub> ) <sub>2</sub> -K]-Stp <sub>2</sub> -Y <sub>3</sub>	334 ± 46	16.7 ± 0.3
<b>464</b>	C-Y <sub>3</sub> -Stp <sub>2</sub> -[(Y <sub>3</sub> ) <sub>2</sub> -K]-Stp <sub>2</sub> -Y <sub>3</sub> -C	243 ± 12	13.3 ± 0.4

**Table 3 Size and zeta potential measurement:** Polyplex size and zeta potential of different oligomer at N/P 12 was determined by DLS measurement (experiment performed by C. Troiber).

Simulating *in vivo* conditions, the polyplexes were analyzed for their stability in fetal calf serum (FCS). Therefore, polyplexes were formed in Hepes buffer, followed by the addition of FCS. The samples were incubated at 37°C for 0, 10, 30, and 90 min. Afterwards, gel electrophoresis was performed to investigate whether the polyplexes were stable, partially stable, or instable. Moreover, polyplexes were treated with 50 I.U. of heparin per sample after 90 min in order to dissociate polyplexes, and to investigate if the siRNA was degraded by serum proteins.

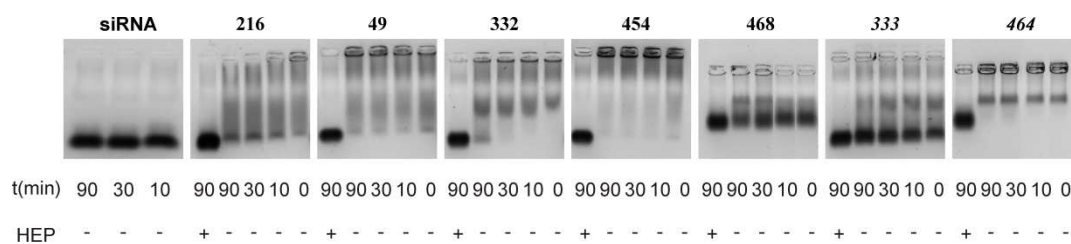


**Figure 32 Polyplex stability:** Agarose gel shift assay demonstrate siRNA binding and release after addition of 90% FCS for several tyrosine modified oligomers at N/P 12. Polyplexes were incubated for 0, 10, 30, or 90 min with FCS and afterwards analyzed by gel electrophoresis. For control reasons samples incubated for 90 min in FCS were treated with heparin to dissociate the polyplex and visualize free siRNA (experiment performed by C. Troiber).

The siRNA band of heparin treated samples was comparable to free siRNA at all points in time. Hence, no degradation of the complexed or free siRNA occurred during the incubation time. This is not unexpected as 2'-methoxy stabilized siRNA was applied in the experiments. After gel electrophoresis, no siRNA migration was observable for **454** and **464** polyplexes, confirming the serum stability of these polyplexes (Figure 32). In contrast, **332** and **49** polyplexes dissociated partially at 37°C after 90 min, as a band at the free siRNA level appeared. The remaining oligomer polyplexes were instable in serum and free siRNA was detected immediately after addition of serum. This data showed that a combination of oligotyrosines and cysteines at the ends of our oligomers led to a favorable stabilization and improved resistance to serum protein mediated disassembly. The different polyplex stability was confirmed by C. Troiber through fluorescence correlation spectroscopy measurements<sup>136</sup>.

### 3.1.8.2 GFP Knockdown Screen

Target gene silencing of the stabilized polyplexes was examined in the previously described eGFPLuc marker gene assay. Oligomers **216** and **333** demonstrating low stability against FCS were also ineffective mediating eGFPLuc knockdown. In contrast, all other oligomers successfully mediated target gene silencing (Figure 33). The addition of terminal oligotyrosines was a favorable modification (oligomers **454** and **464**) leading to stronger target gene knockdown compared to oligomer **49**. In contrast, the alteration of the central domain (fatty acid **454**, oligotyrosine **464**) showed only moderate influence on the transfection efficiency. This experiment demonstrated that polyplex stability directly correlated with eGFPLuc knockdown *in vitro*.

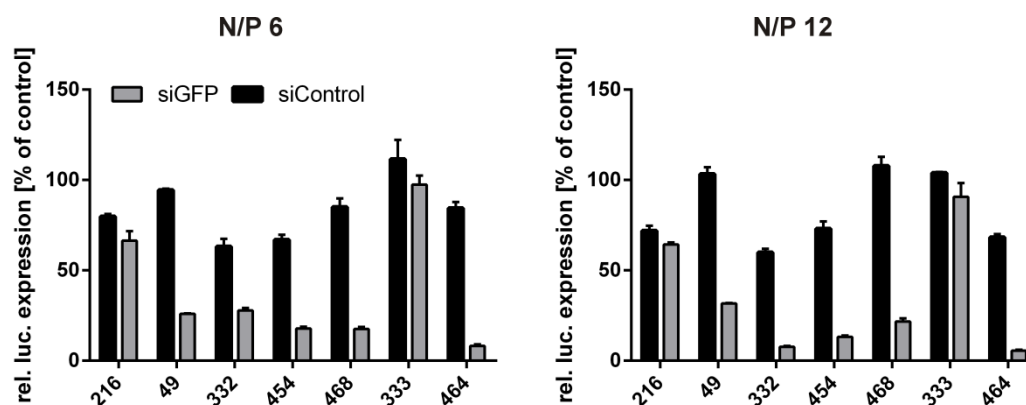


**Figure 33 eGFPLuc silencing assay:** Target gene silencing of different unmodified and tyrosine modified polyplexes at N/P 6 and 12. Gene silencing of the novel oligomers was compared to standard oligomer **49**.

In summary, the class of oligotyrosine containing oligomers was efficient in siRNA transfection. Replacement of terminal cysteines by tyrosines generated oligomers with equal transfection efficiency to standard oligomer **49**, whereas the addition of terminal oligotyrosines created carriers superior to standard oligomer **49**.

### 3.1.8.3 Distribution of Fluorescence Labeled Polyplexes

Polyplex distribution after systemic administration was evaluated through NIR fluorescence imaging. Pure Cy7 labeled siRNA revealed a short circulation time followed by fast renal clearance comparable to oligomer **216** polyplexes (Figure 34). Renal clearance was possible for pure siRNA but not for polyplexes with a size above 30 nm. Therefore, Cy7 signals detectable in the kidneys and bladder of oligomer **216** polyplexes are caused by free siRNA after polyplex degradation in the blood stream.

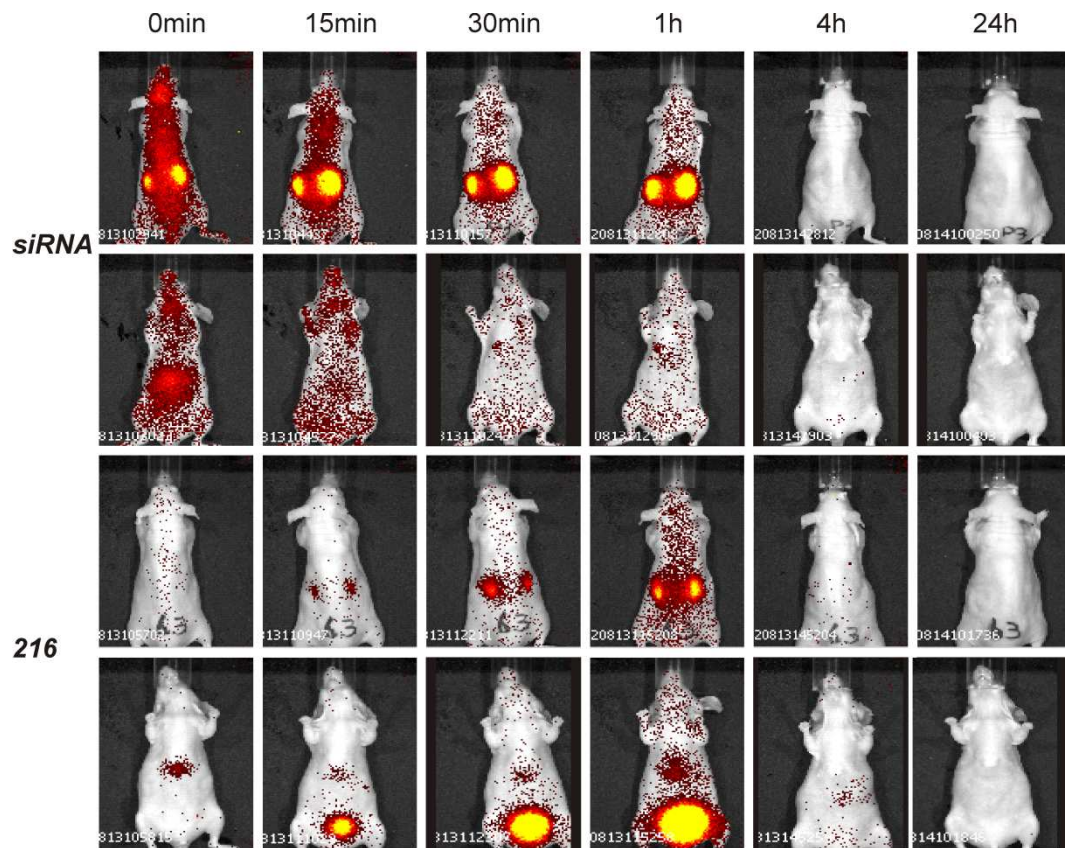


**Figure 34 Fluorescence imaging:** Images of a representative mouse (n=3) demonstrating distribution of Cy7 labeled siRNA or Cy7 labeled siRNA complexed with oligomer **216** in ventral (upper row) and dorsal (lower row) position. The efficiencies were recorded and all images were adjusted to same maxima and minima. Experiment performed together with Annika Hermann (veterinary MD thesis, LMU).

In contrast, to oligomer **216** all other oligomers are able to complex siRNA more stably leading to longer circulation times for the polyplexes. The lipophilic character of the oligomers caused liver accumulation for oligomer **49** and **332** polyplexes after intravenous injection. Replacing the terminal cysteines (**49**) by tyrosines (**332**) increased circulation times and liver accumulation (Figure 35).

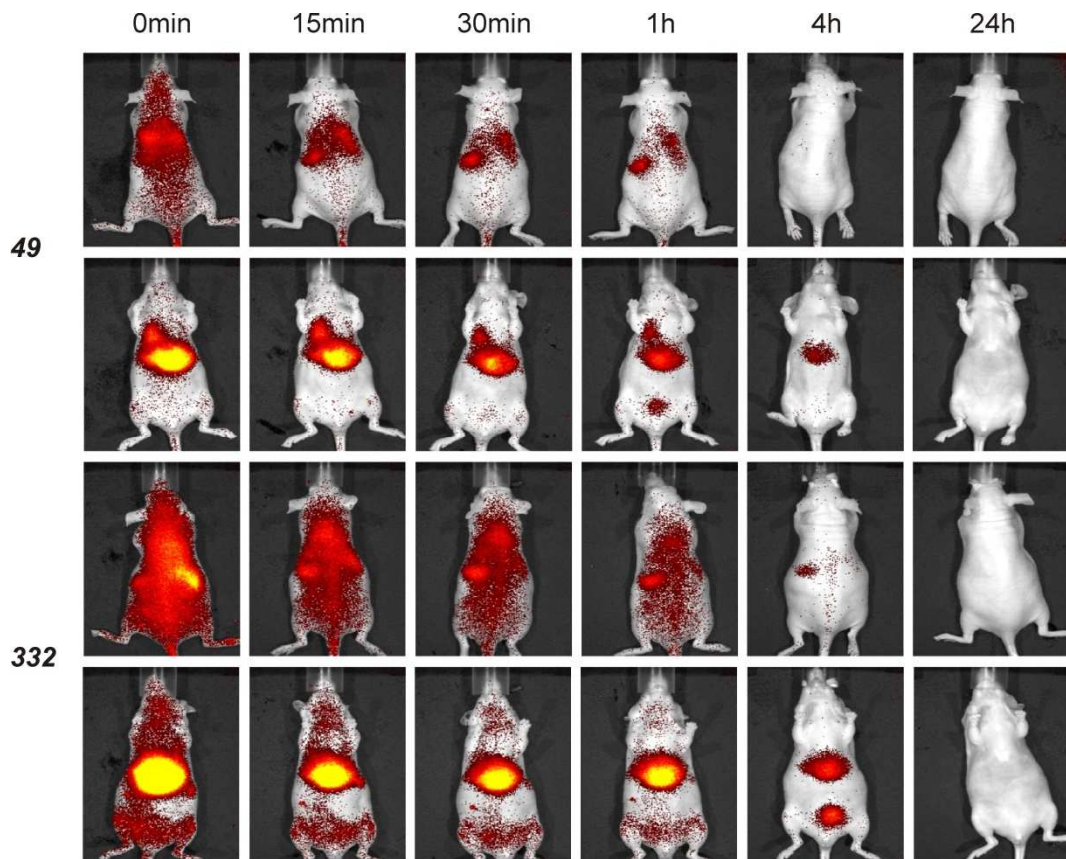


**Figure 35 Fluorescence imaging:** Images of a representative mouse (n=3) demonstrating distribution of Cy7 labeled siRNA complexed with oligomer **49** and **332** in ventral (upper row) and dorsal (lower row) position. The efficiencies were recorded and all images were adjusted to same maxima and minima. Experiment performed together with Annika Hermann (veterinary MD thesis, LMU).

Oligomer **454** confirmed the previously described high stability and showed long circulation times (Figure 36). Cy7 signals were still detectable in the bloodstream 4 h after polyplex injection demonstrating the presence of stable circulating polyplexes. Oligomer **468** polyplexes were not detectable in the circulation, because the fluorescence signal was quenched due to the strong compaction of the labeled siRNA.

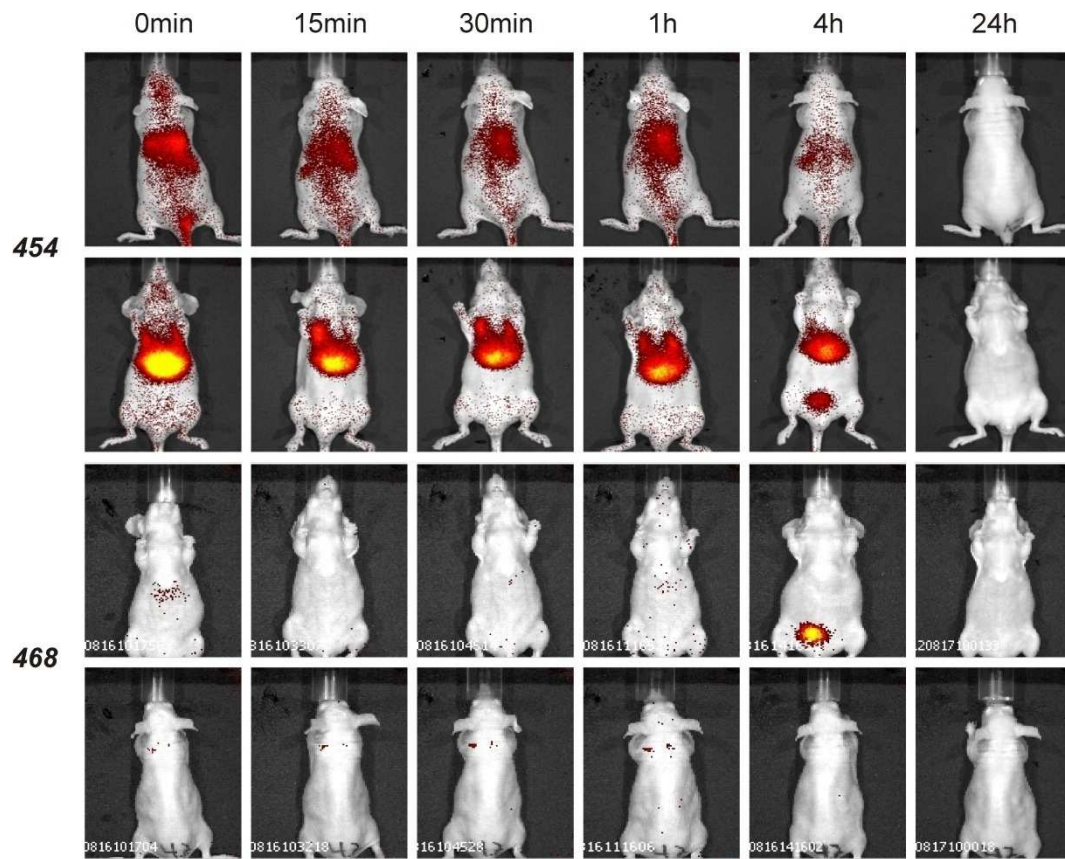


**Figure 36 Fluorescence imaging:** Images of a representative mouse (n=3) demonstrating distribution of Cy7 labeled siRNA complexed with oligomer **454** and **468** in ventral (upper row) and dorsal (lower row) position. The efficiencies were recorded and all images were adjusted to same maxima and minima. Experiment performed together with Annika Hermann (veterinary MD thesis, LMU).

Oligomer **333** initially displayed good systemic tissue distribution, whereas after 4 h only a high signal in the kidneys and the bladder was detected (Figure 37). Polyplexes of oligomers **464** also showed a strong quenching of the fluorescent Cy7 signal upon polyplex formation and hampered monitoring of polyplex distribution by NIR imaging.

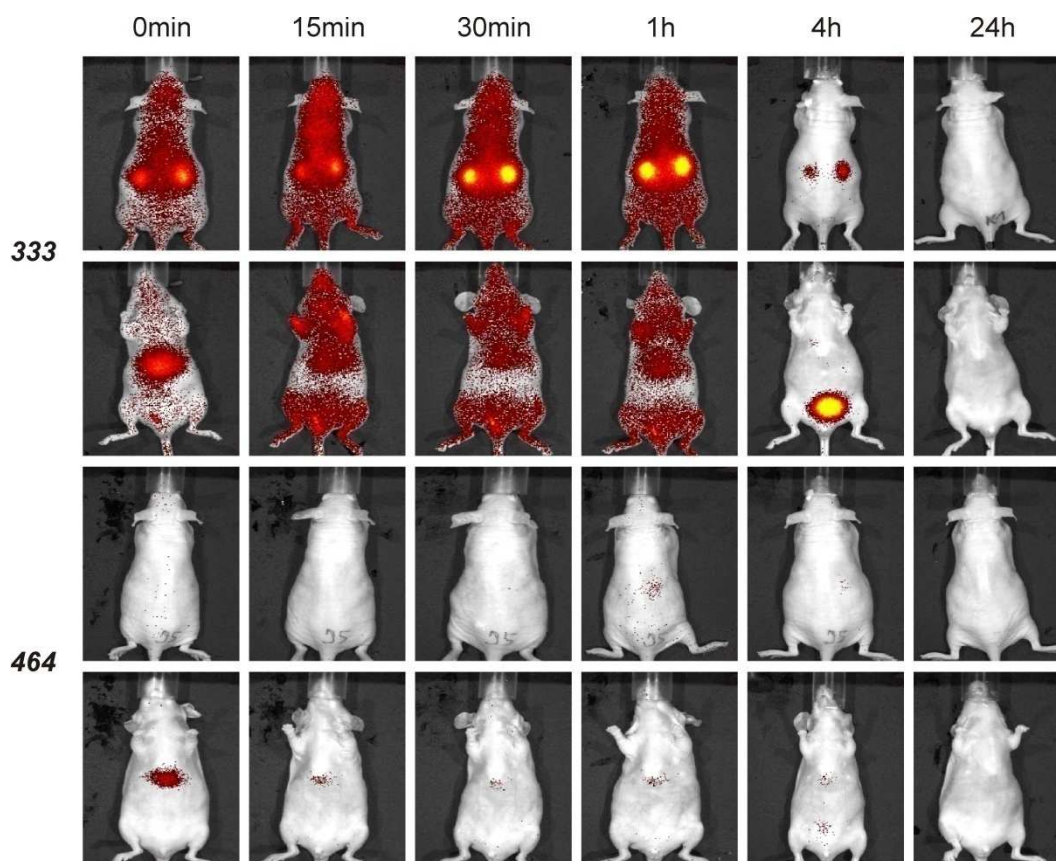


**Figure 37 Fluorescence imaging:** Images of a representative mouse (n=3) demonstrating distribution of Cy7 labeled siRNA complexed with oligomer **333** and **464** in ventral (upper row) and dorsal (lower row) position. The efficiencies were recorded and all images were adjusted to same maxima and minima. Experiment performed together with Annika Hermann (veterinary MD thesis, LMU).

Excluding the non detectable oligomers, polyplexes of oligomers **49**, **332**, and **454** initially displayed good systemic distribution. Shortly after polyplex injection, a liver signal was observed in dorsal position due to the lipophilic character of the oligomers. The **454** and **332** polyplexes showed the most beneficial distribution, followed by **49** polyplexes. This experiment proved the favorable characteristic of oligotyrosine modified polyplexes.

#### 3.1.8.4 Oligomer Screen

Consequently, the polyplexes of oligomers **49** (control), **332**, **454**, **464** and **468** were investigated for their therapeutic potential after intratumoral injection. According to the previous described intratumoral treatment, polyplexes containing either Ran or control siRNA were injected. Tumor growth of subcutaneously implanted Neuro2A-eGFPLuc tumors was again monitored by bioluminescence imaging (Figure 38). This time control oligomer **49** failed to reduce tumor growth in the Ran siRNA treated group compared to the control siRNA group. In contrast, mice treated with oligomers **332** and **468** Ran siRNA polyplexes showed

reduced tumor growth compared to control siRNA treated mice. Only these two polyplexes were able to selectively reduce tumor volume and tumor weight in the Ran siRNA group, whereas mice treated with other polyplexes formulations could not reduce tumor growth.

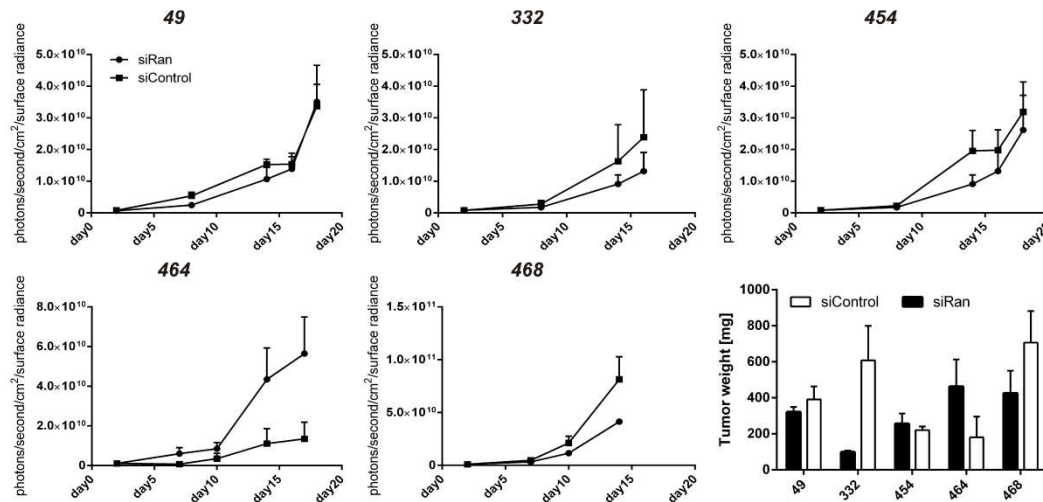


**Figure 38 Bioluminescence signals and tumor weights of polyplex treated tumors:** Bioluminescence imaging of subcutaneously implanted Neuro2A tumors after treatment with several T-shaped oligomer polyplexes either containing Ran siRNA or control siRNA. Mice were sacrificed when one mouse in the polymer group reached a tumor volume 1500 mm<sup>3</sup> and tumor weights of the two groups were recorded. Experiment performed together with Raphaela Kläger (veterinary MD thesis, LMU 2013) and Annika Hermann (veterinary MD thesis, LMU).

Contrary effects in the groups treated with oligomer **464** can be explained due to the strong necrotic effects caused by these polyplexes. Hence, the antitumoral effects in this group were mediated by the toxicity of the polyplexes and not by target gene knockdown. Oligomer **454** showed some effects on tumor growth in the Ran siRNA group between day 10 and day 15, but in conclusion bioluminescence signals and tumor weights were on the same level in both siRNA groups. In summary, oligomers **332** and **468** and in the previous study oligomer **386** and **49** mediated tumor growth reduction in the Ran siRNA group. These results indicated that highly stable polyplexes were not suitable for intratumoral applications, in particular the less stable polyplexes showed good tumor reduction in the Ran siRNA group. After the evaluation of 7 oligomers and the exclusion of oligomer **464** because of necrotic effects this intratumoral assay allowed the classification of 6 *in vitro* effective oligomers into an *in vivo* effectivity order: **229**<**454**<**49**<**468**<**332**<**386**. Again polyplex stability was not the most important factor for successful gene silencing after intratumoral injection.

## 3.2 Targeted Oligoamides for siRNA Delivery

### 3.2.1 Folic Acid Linked Targeting Oligomers

Targeted structures were synthesized by solid-phase-supported peptide synthesis as afore described. C. Dohmen generated a cationic backbone consisting of two arms each with 4 STP units, terminal cysteines, and one central lysine (Figure 39). Monodisperse polyethylene glycol (PEG) was coupled to the central lysine, followed by region-selective coupling of folic acid as ligand for specific cell targeting. For control experiments alanine instead of folic acid was coupled to the monodisperse PEG. For the generation of a structure library different fatty acids (caprylic acid, stearic acid) and tyrosine-trimers were incorporated into the structures to increase polyplex size and stability. Also, extended PEG chains (2 x-, 3 x-, 5 x-, 8 x 24 monomers) were introduced to increase polyplex size.

To increase the low endosomal escape ability particularly of carriers without fatty acid modification, the endosomolytic peptide Inf7 was coupled to the 5'-end of the siRNA sense strand by C. Dohmen (LMU, PhD thesis 2012). On the contrary to conventional delivery systems, the current design enabled the separation of requirements for successful siRNA delivery between carrier and siRNA. In the novel delivery system the oligomeric carrier was responsible for the binding of nucleic acids and specific transport to the target cell, whereas the siRNA provided the endosomal escape domain. C. Dohmen showed the efficient synthesis and purification of these molecules, including a qualitative and quantitative analysis of the products.

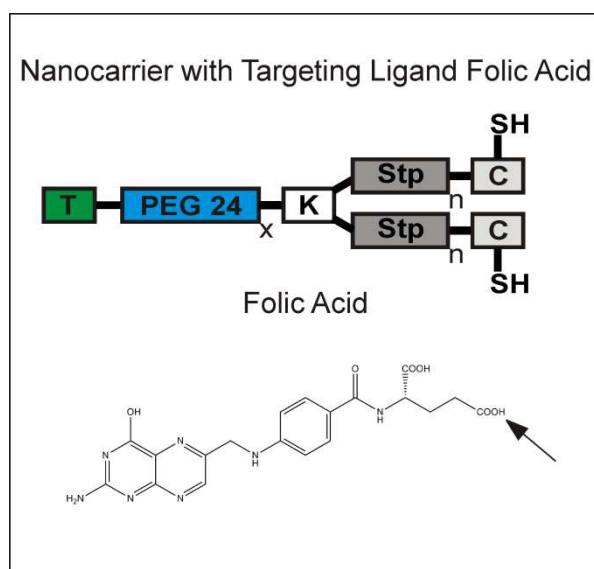


**Figure 39 Chemical structures of the oligomer backbone and folic acid:** Upper structure shows the backbone of standard oligomer **356** with  $n = 4$  and  $x = 1$ . Folic acid is coupled *via* the  $\gamma$ -carboxy group indicated by the arrow.

### 3.2.1.1 Biophysical Characterization

Successful siRNA binding by the carrier was demonstrated through gel shift assays. The assays demonstrated siRNA binding of the standard structure (**356**) starting with N/P 3 and nearly complete siRNA binding at N/P 20 (Figure 40). This siRNA binding capacity was lower than for the previously described oligomers. Therefore, N/P 16 was chosen for further characterizations. Incorporation of longer PEG chains (maximum 8 x more than oligomer **356**) reduced nucleic acid complexation detectable by reduced siRNA retardation in the gel shift assay.

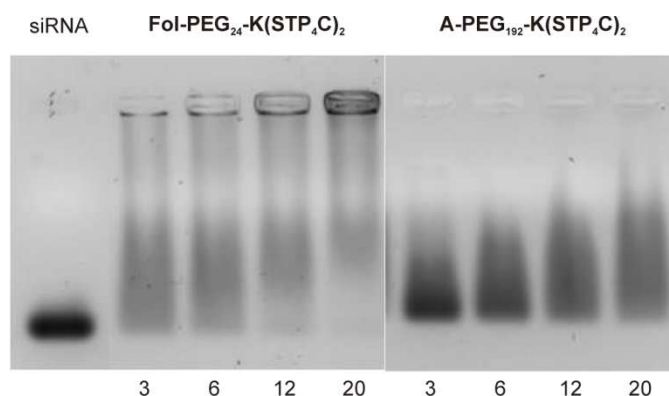


**Figure 40 Gel shift assay:** Targeted oligomer **356** demonstrating efficient siRNA binding at high N/P ratios. Oligomer **647** with maximal prolonged PEG chain showed low binding efficiency (experiment performed by C. Dohmen)

The necessity of terminal cysteines for successful siRNA binding was previously demonstrated by T. Fröhlich (PhD thesis 2012) comparing oligomer **356** with and

oligomer **420** without terminal cysteines.

Size of the nanoparticles and pure siRNA was measured by fluorescence correlation spectroscopy (C. Troiber, C. Dohmen and D. Edinger). Standard oligomer **356** formed nanoparticles with a hydrodynamic diameter of only 5.8 nm, only 1.4-fold larger than free siRNA with 4.2 nm hydrodynamic diameter (Table 4). Prolonged PEG spacer resulted in nanoparticles with a maximal size of 50.8 nm hydrodynamic diameter. Increasing sizes of oligomers **482** < **483** < **646** can be explained due to the prolonged PEG spacers. In contrast, the strongly increased size of oligomer **647** was caused by the looser particle formation also demonstrated in the gel shift experiment. Modification with tyrosines did not influence particle size whereas the incorporation of fatty acids led to structures with highly increased hydrodynamic diameters.

Oligomer ID	Oligomer sequence	$r_h$ (nm)
	siRNA	$2.1 \pm 0.1$
<b>356</b>	Fol-PEG <sub>24</sub> -K(Stp <sub>4</sub> -C) <sub>2</sub>	$3.0 \pm 0.1$
<b>482</b>	Fol-PEG <sub>48</sub> -K(Stp <sub>4</sub> -C) <sub>2</sub>	$3.2 \pm 0.1$
<b>483</b>	Fol-PEG <sub>72</sub> -K(Stp <sub>4</sub> -C) <sub>2</sub>	$4.4 \pm 0.1$
<b>646</b>	Fol-PEG <sub>120</sub> -K(Stp <sub>4</sub> -C) <sub>2</sub>	$5.8 \pm 0.2$
<b>647</b>	Fol-PEG <sub>192</sub> -K(Stp <sub>4</sub> -C) <sub>2</sub>	$25.4 \pm 0.9$
<b>484</b>	Fol-PEG <sub>24</sub> -K(Stp <sub>4</sub> -Y <sub>3</sub> -C) <sub>2</sub>	$2.8 \pm 0.2$
<b>481</b>	Fol-PEG <sub>24</sub> -K[Stp <sub>4</sub> -K(K-CapA <sub>2</sub> )C] <sub>2</sub>	$16.9 \pm 0.2$
<b>480</b>	Fol-PEG <sub>24</sub> -K[Stp <sub>4</sub> -K(K-SteA <sub>2</sub> )C] <sub>2</sub>	$160.3 \pm 0.6$

**Table 4 Particle size measurement by FCS:** Fluorescence correlation spectroscopy revealed the hydrodynamic radius for folic acid targeted oligomers. (Experiments performed by C. Troiber)

DLS measurements demonstrated an overall zeta potential of 0 mV ( $\pm 3$  mV) for PEGylated siRNA nanoparticles whereas the same polyplexes lacking the PEG shielding showed significantly higher zeta potential between 10 and 15 mV (experiments performed by C. Dohmen). Low zeta potential is favorable for *in vivo* application because it inhibits interactions with cell surfaces and blood proteins (22, 23) through electrostatic interactions. To enable efficient cellular uptake, folic acid was covalently attached to the PEG shield. As this ligand has a very high binding affinity to its receptor, (24-25) it should selectively mediate cell attachment and endocytosis into its target cell.

### 3.2.1.2 Folic Acid Receptor Levels in Different Cell Lines

Before transfection experiments could be conducted cell lines expressing the folic acid receptor had to be determined. For this reason several cell lines were screened for their receptor status (Figure 41). In this screen only the ovarian carcinoma (IGROV) and the cervical carcinoma (KB derived from HeLa cells) cell lines showed high folic acid receptor status.

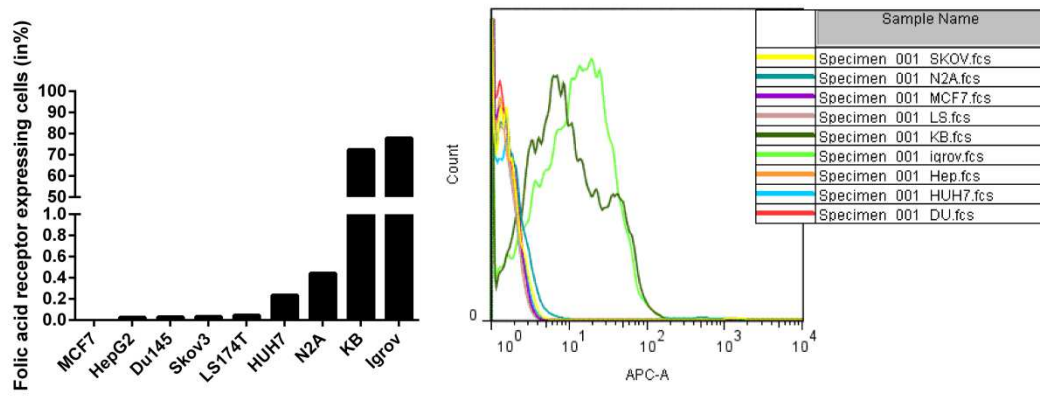


**Figure 41 Folic acid receptor status of several cell lines:** Flow cytometry experiments were performed to quantify the membrane bound folic acid receptor status after antibody staining.

For this reason KB cells stably expressing the eGFPLuc plasmid were generated and used as standard cell line for transfection experiments with folic acid targeted nanocarriers.

### 3.2.1.3 Uptake Studies in KB and IGROV Cells

To verify the receptor mediated uptake, polyplexes were formed with Cy5 label siRNA. Transfection of KB cells, with folic acid targeted and untargeted nanoparticles, revealed increased uptake solely for targeted nanocarriers by flow cytometric analysis. Competition with an excess of free folic acid or the use of Neuro2A cells with a low folic acid receptor level, led to a strongly reduced cellular association. In summary, the requirement of targeting ligands for successful siRNA uptake and the receptor selective uptake was demonstrated by T. Fröhlich. Further experiments using folic acid receptor expressing KB and IGROV cells confirmed polyplex uptake with Cy3 containing siRNA polyplexes. Histological analysis of these pictures revealed high numbers of Cy3 positive cells in both cell lines after 45 min incubation time (Figure 42).

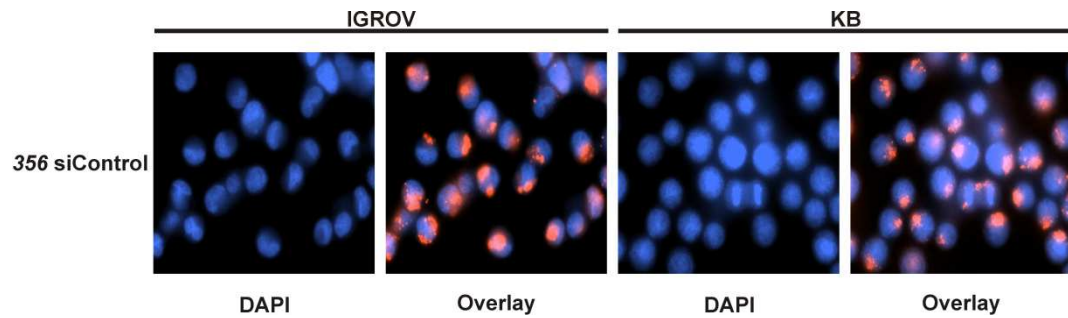


**Figure 42 Histological analysis of polyplex uptake:** KB and IGROV cells were transfected with Cy3 siRNA containing polyplexes. Nuclei were stained with Hoechst (blue) to analyze Cy3 (red) positive cells by fluorescence microscopy.

The results confirmed the flow cytometry studies performed by T. Fröhlich and showed efficient polyplex uptake after short incubation time.

#### 3.2.1.4 GFP and Eg5 Knockdown Studies *in vitro*

KB cells stably expressing the eGFPLuc plasmid were used as a reporter system for marker gene silencing studies. To demonstrate the importance of every single component controls lacking the folic acid ligand, the endosomolytic peptide or incorporating control siRNA sequences were used.

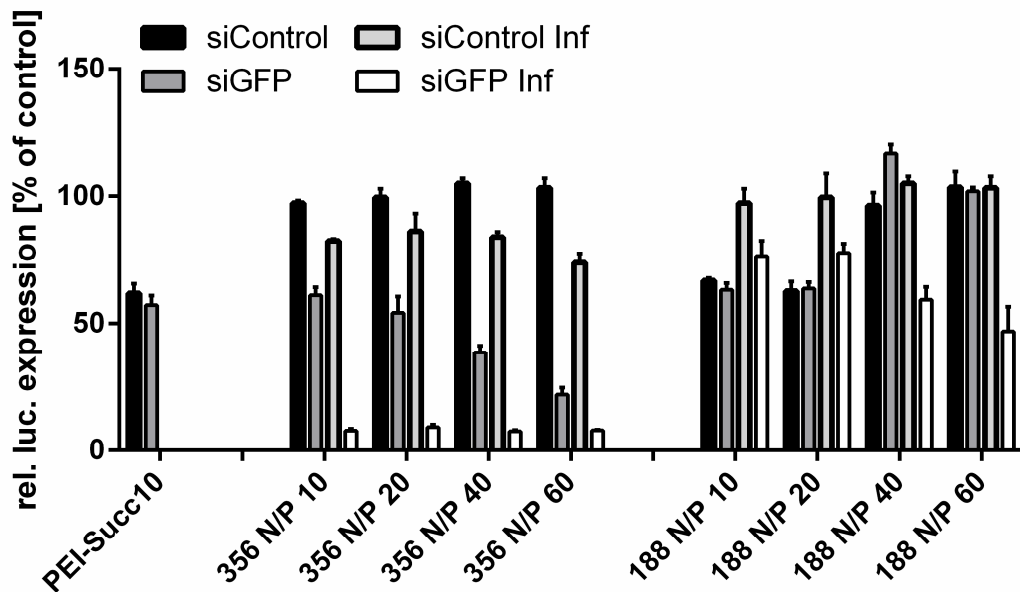


**Figure 43 eGFPLuc silencing experiments:** KB eGFPLuc cells were transfected with folic acid targeted (356) and untargeted (188) oligomers. GFP and control siRNAs modified with the lytic peptide Inf7 or without Inf7 modification were used to demonstrate siRNA specific silencing and the necessity of the lytic peptide Inf7.

Standard polymer PEI-Succ10 demonstrated poor transfection efficiency on KB cells with unspecific eGFPLuc silencing in the control siRNA group (Figure 43). In contrast, the targeting oligomers demonstrated efficient target gene knockdown

with Inf7 modified siRNA in all tested ratios. Unmodified siRNAs required higher N/P ratios, for successful endosomal escape and efficient target gene knockdown. This finding was consistent with the postulated poor endosomal escape efficiency of the nanocarriers. Polyplexes incorporating control siRNA with and without Inf7 modification could not show any knockdown effect, demonstrating the absence of unwanted side effects. Untargeted oligomers only showed moderate target gene knockdown at high N/P ratios with Inf7 modified GFP siRNA, whereas all other untargeted groups did not show silencing effects. The results clearly showed the high transfection efficiency of the novel delivery system while all mentioned controls showed reduced or no silencing efficiency under the transfection conditions employed.

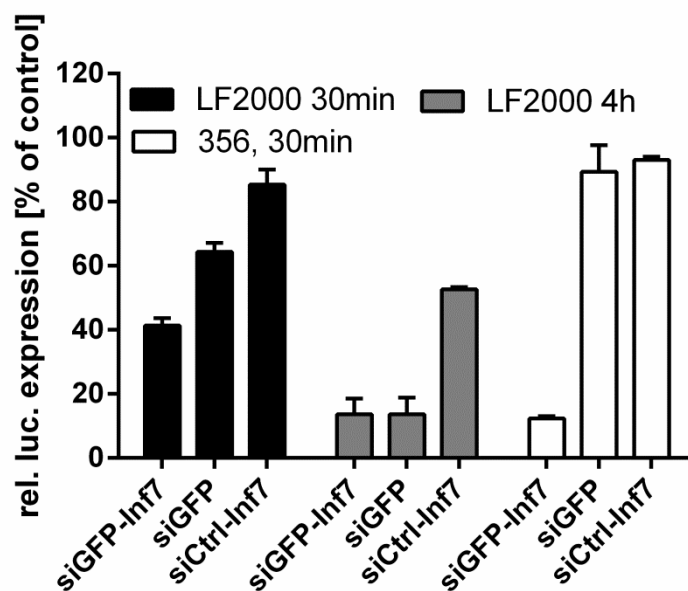


**Figure 44 Comparison of eGFP-Luc knockdown:** Shows the transfection results of KB-eGFP<sub>Luc</sub> cells with targeted (356) oligomers compared to the gold standard LF2000 using GFP and control siRNAs modified with the lytic peptide Inf7 or without Inf7 modification.

Furthermore, transfection efficiency of the novel delivery system was compared to the efficiency of the gold standard (LF2000). Again the KB cells showed high sensitivity towards transfection reagents demonstrated by the unspecific reduction in the control siRNA group transfected with LF2000. GFP silencing was reduced compared to the novel carrier system because of the high toxicity of LF2000 lipoplexes after 4 h incubation time (Figure 44). Reducing the incubation time to 30 min reduced the cytotoxicity but also the knockdown efficiency of LF2000 lipoplexes. In summary, the novel nanocarrier mediated improved silencing with reduced cytotoxicity compared to the gold standard for transfection experiments.

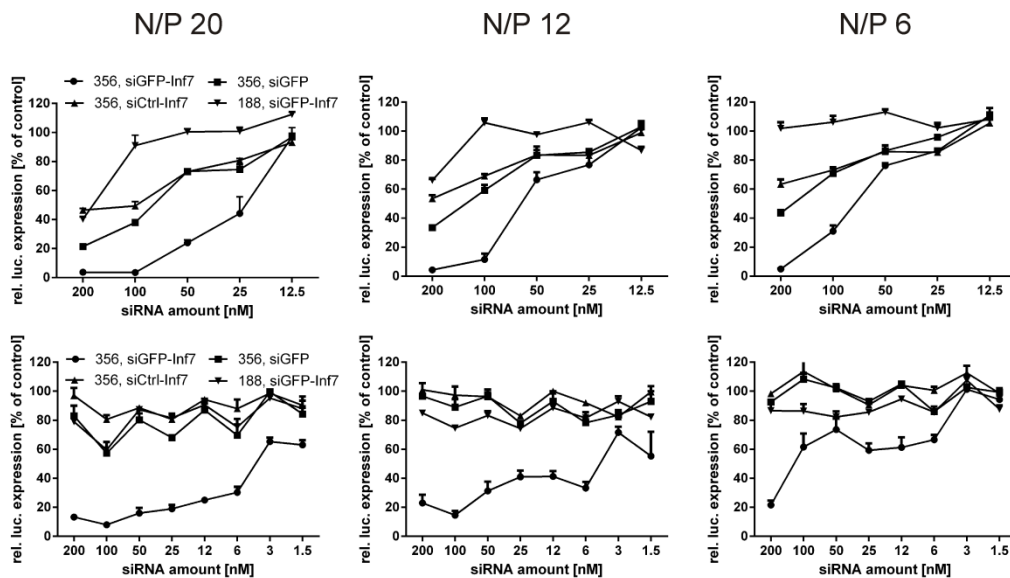


**Figure 45 Titration of siRNA concentrations:** In the upper row the amounts of oligomer and siRNA were reduced accordingly, whereas in the lower row only the amounts of siRNA were reduced.

For previous transfection experiments relatively high amounts of siRNA (200 nM) were used. Hence, titration experiments were performed to examine the critical oligomer and siRNA concentrations for successful gene silencing (Figure 45). In a first experiment N/P ratios were kept constant for all siRNA ratios and the diverse polyplexes were incubated for 48 h on the cells. Targeted oligomer in combination with lytic GFP siRNA mediated about 50% target gene knockdown down to a siRNA concentration of 25 nM for N/P 20. Decreasing knockdown efficiencies for N/P 12 and 6 demonstrate the importance of critical oligomer amounts. Subsequently knockdown experiments were performed with constant amounts of oligomer for all siRNA ratios (increasing N/P ratios) and the diverse polyplexes were incubated for 45 min on the cells. The highest oligomer concentration with N/P 20 for siRNA concentrations of 200 nM demonstrated good GFP silencing down to siRNA concentrations of 6 nM. Medium oligomer concentrations were also effective down to siRNA concentrations of 6 nM, whereas the lowest oligomer concentration was only effective for the highest siRNA concentration. These experiments demonstrated the importance of critical oligomer concentration, whereas only very low siRNA concentrations are required for successful target gene knockdown.

For further characterization a second target was selected. Again Eg5 silencing was chosen enabling the analysis of mitotic cell arrest and characteristic aster formation. In accordance with the eGFP<sub>Luc</sub> silencing experiments, only KB cells

transfected with folic acid targeted carrier **356** demonstrated aster formations. Untargeted nanocarriers could not mediate target gene silencing because of the short incubation time of 45 min. After DAPI staining the microscopic pictures showed the characteristic aster formation only in the Eg5 siRNA group, demonstrating the effectiveness of this positive read out system (Figure 46).

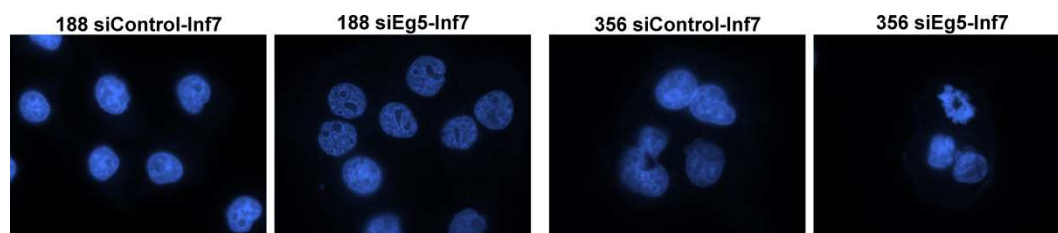


**Figure 46 Aster formation assay:** KB cells after transfection with Eg5-Inf7 and control-Inf7 siRNA. Polyplexes of targeted (**356**) and untargeted oligomer (**188**) were compared.

Positive aster formation results were also important for further *in vivo* assays, providing a positive read out system for functional siRNA studies.

### 3.2.1.5 Polyplex Distribution and Polyplex Retention *in vivo*

After the novel multifunctional nanocarrier proved its efficiency *in vitro*, *in vivo* experiments were carried out to further evaluate the applicability. Initially a suitable *in vivo* testing system for the targeting efficiency had to be evaluated. Therefore, both folic acid overexpressing cell lines were injected into the left flank or the nape of NMRI mice. Tumor growth was recorded for several days, with tumors being palpable one day after subcutaneous injection of tumor cells. In contrast to Igrov cells, KB cells continued growing after implantation and reached a volume of about 200 mm<sup>3</sup> after 10 days (Figure 47).

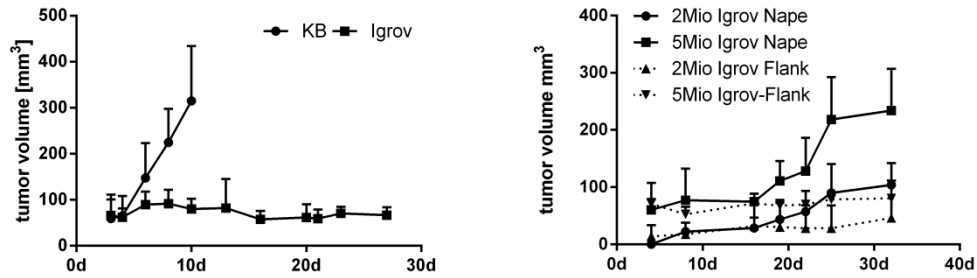


**Figure 47 Comparison of tumor growth after subcutaneous injection of KB and Igrov cells:**  $5 \times 10^6$  KB and Igrov cells were injected into the left flank or the nape of NMRI mice and tumor volumes were measured with a caliper (length x width<sup>2</sup>/2). In the left graph tumor growth of KB and Igrov cells injected into the flank of NMRI mice were compared, whereas in the right graph tumor growth of Igrov cells injected into the flank or the nape were compared. Experiments were performed with Katarina Farkasova (veterinary MD thesis, LMU 2011).

In a second experiment the injection site of the tumor cells was evaluated, but again Igrov cells failed to demonstrate appropriate tumor growth. Hence, KB cells were used for all *in vivo* experiments.

For the first experiments polyplexes were injected intratumorally into subcutaneous KB tumors of NMRI nude mice to determine the targeting efficiency *in vivo*. NIR fluorescence imaging experiments using Cy7 labeled siRNA proved the significantly increased retention of folic acid targeted nanoparticles in tumor tissue compared to untargeted particles. Fluorescence signals decreased rapidly after intratumoral injection, but Cy7 signals were detectable in the tumors of mice injected with the folic acid targeted oligomer for 120 h (Figure 48). In contrast, free siRNA and untargeted polyplexes were only detectable for 24 h. This experiment proved the receptor binding of folic acid targeted siRNA carriers in contrast to untargeted carriers after intratumoral injection. The small size of the multifunctional nanocarrier system was responsible for the fast elution and renal clearance of unbound polyplexes.

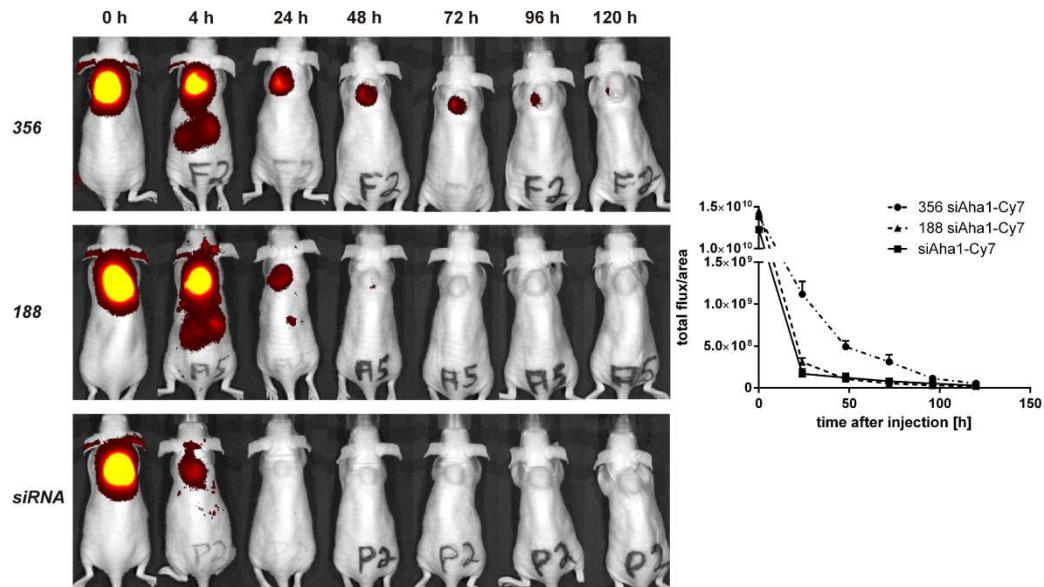


**Figure 48 Fluorescence imaging after intratumoral polyplex injection:** Different retention effect of pure Cy7 siRNA or Cy7 siRNA complexed by oligomers **356** or **188** after intratumoral injection into KB tumors of NMRI mice ( $n = 3$ ). The diagram shows the calculated amount of Cy7 siRNA in the tumors after ROIs were placed on the tumors. Experiments were performed with Laura Schreiner (veterinary MD thesis, LMU 2013).

As the intratumoral retention was shown to work efficiently the behavior of these nanosized particles after systemic application was evaluated. In accordance with the intratumoral experiment NIR fluorescence imaging revealed a short circulation time of oligomer **356** polyplexes followed by fast renal clearance with strong fluorescence signals detectable in the kidney and bladder. This can be explained by the small particle size. Significantly, due to the excellent shielding of the polyplexes unspecific affinity to tissues like lung, liver or spleen often observed with nanoparticles was not detected (Figure 49).

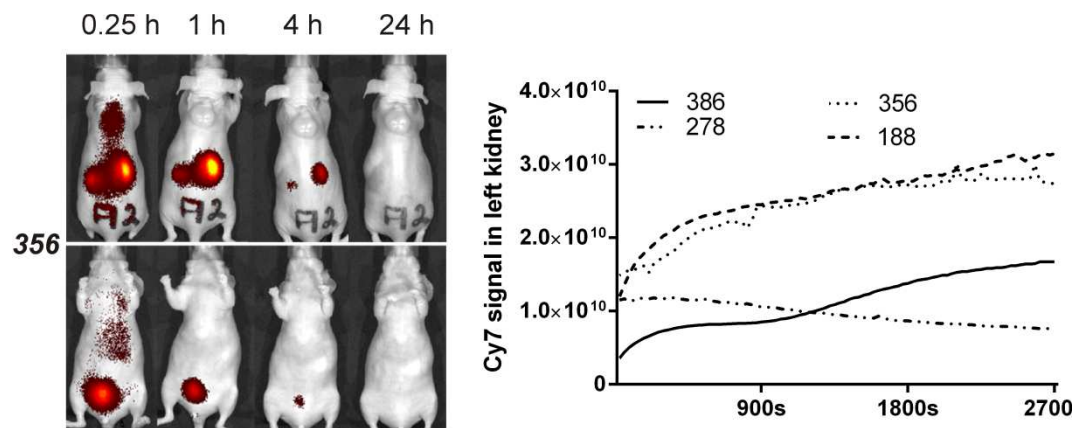


**Figure 49 Distribution of nanocarriers after intravenous injection:** Fluorescence imaging of oligomer **356** polyplexes after intravenous injection revealed short circulation times followed by renal clearance. Circulation time was compared to different untargeted polyplexes by placing ROIs over the left kidney and Cy7 signals were compared after several timepoints. Experiments were performed with Laura Schreiner (veterinary MD thesis, LMU 2013).

Renal clearance was not influenced by the presence/absence of the folate targeting

ligand. Compared to other carriers, kidney signals of untargeted and targeted nanocarriers increased shortly after polyplex injection and reached a maximum after 10 min. Previously mentioned oligomer **386** without fatty acids showed longer circulation times with increasing kidney signals after 20 min, whereas the very lipophilic U-shape oligomer **278** is cleared through the liver (Figure 49).

To investigate if bladder signals were caused by pure siRNA or by polyplexes L. Schreiner (veterinary MD thesis, LMU 2013) collected urine samples of living mice 4 h after polyplexes injection. In a gel shift assay, performed by C. Dohmen, free siRNA was only detectable after preincubation of the urine samples with TCEP and heparin, demonstrating the stability of the nanocarrier. In summary, the particles were very stable in the circulation as no free siRNA could be detected after 4 h but the circulation time was short and the polyplexes did not show tumor targeting.

To prolong circulation half life and improve tumor targeting carriers with longer precise PEG spacers, increasing the size of nanoparticles from 5.8nm (**356**) up to 8.8nm (**483**) hydrodynamic diameter were injected. These polyplexes have very comparable gene silencing efficiency in an eGFPLuc silencing assay (reported by T. Fröhlich). However, the nanocarriers with slightly increased sizes behaved very similar to oligomer **356** polyplexes after intravenous injection. Strong kidney and bladder signals were detected shortly after polyplex injection proving the fast clearance through the kidneys (Figure 50). As polyplex size increased with integration of a greater amount of monodisperse PEG spacers, this concept was used to further increase polyplex size.

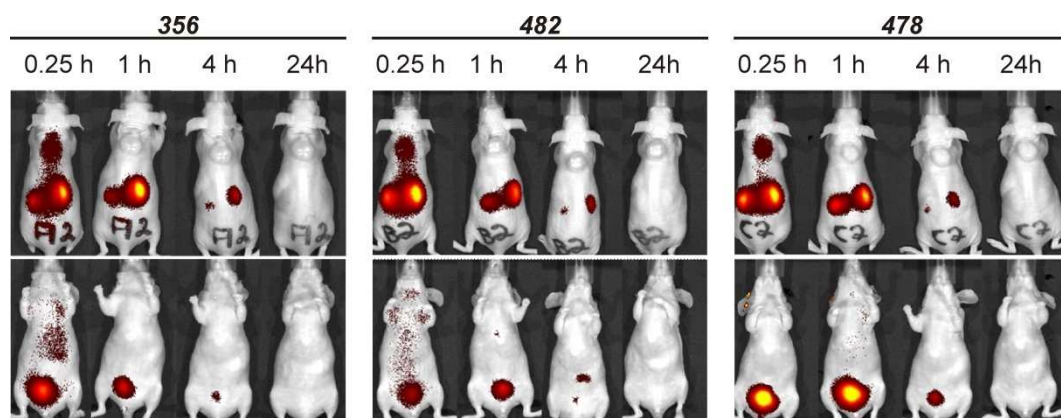


**Figure 50** Circulation time of nanocarriers with increasing amount of PEG after intravenous injection: Oligomer **356** (1 x PEG24), oligomer **482** (2 x PEG24) and oligomer **478** (3 x PEG24) were compared after intravenous injection in NMRI mice (n = 3). Experiments were performed with Laura Schreiner (veterinary MD thesis, LMU 2013).

Polyplexes with 5 PEG spacers and a size of 11.6 nm (**646**) showed the longest circulation time, while oligomers with 8 PEG spacers and a size of 50.8 nm (**647**) showed circulation times comparable to the standard carrier **356**. The short circulation time of oligomer **647** with 8 PEG spacer must be influenced by the low stability of these polyplexes demonstrated in the gel shift assay. However, the circulation time was only slightly prolonged by the incorporation of longer PEG chains with limitations due to particle stability (Figure 51). Further backbone modifications had to be tested aiming on an increased circulation time.

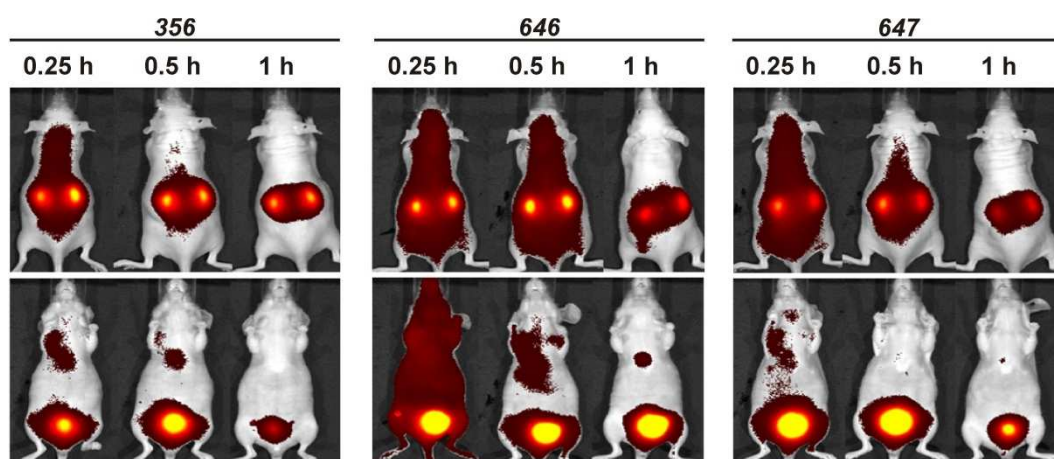


**Figure 51** Circulation time of nanocarriers with increasing amount of PEG after intravenous injection: Oligomer **356** (1 x PEG24), oligomer **646** (5 x PEG24) and oligomer **647** (8 x PEG24) were compared after intravenous injection in NMRI mice (n = 3). Oligomers were synthesized by U. Lächelt (PhD thesis, LMU). Experiments were performed with Laura Schreiner (veterinary MD thesis, LMU 2013).

The backbone of the oligomeric carrier was modified with fatty acids or tyrosines which already showed their positive influence on particle stability and size for untargeted oligomers. Therefore, C. Dohmen synthesized oligomers containing tyrosine, caprylic acid and stearic acid modifications.

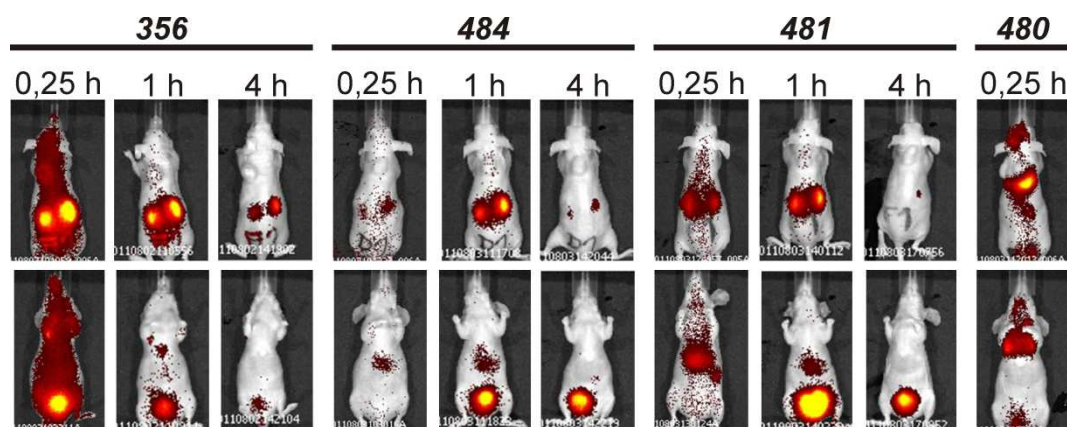


**Figure 52** Circulation time of nanocarriers with different backbone modifications after intravenous injection: Oligomer **356**, oligomer **484** (tyrosines), oligomer **481** (caprylic acid) and oligomer **480** (stearic acid) were compared after intravenous injection in NMRI mice (n = 3). Experiments were performed with Laura Schreiner (veterinary MD thesis, LMU 2013).

Modifications with tyrosines did not increase particle size and therefore could not prolong circulation half-life. Only the liver signals slightly increased for these modified nanocarriers. Integration of fatty acids into the backbone led to increased liver signals for both nanocarriers **480** and **481** and fatal neuronal toxicity for stearic acid modified polyplexes. In conclusion, the modifications could not significantly increase circulation half life and improve tumor targeting compared to the standard oligomer **356**.

### 3.2.1.6 Eg5 Knockdown Study *in vivo*

For the evaluation of functional gene silencing after intravenous and intratumoral application the previously described aster formation assay was used. Although no significant detectable amounts of labeled siRNA were found in the tumor tissue after intravenous injection, still moderate aster formation was observed using Eg5-Inf7 siRNA. On the contrary, mice treated with control-Inf7 siRNA did not show any aster formation. The quantification of aster formation is very complicated and did not allow a reliable quantitative comparison of targeted and untargeted structures. However, the tumor sections displayed in Figure 53 showed superior aster formation for mice treated with folic acid targeted nanocarriers compared to untargeted carriers.

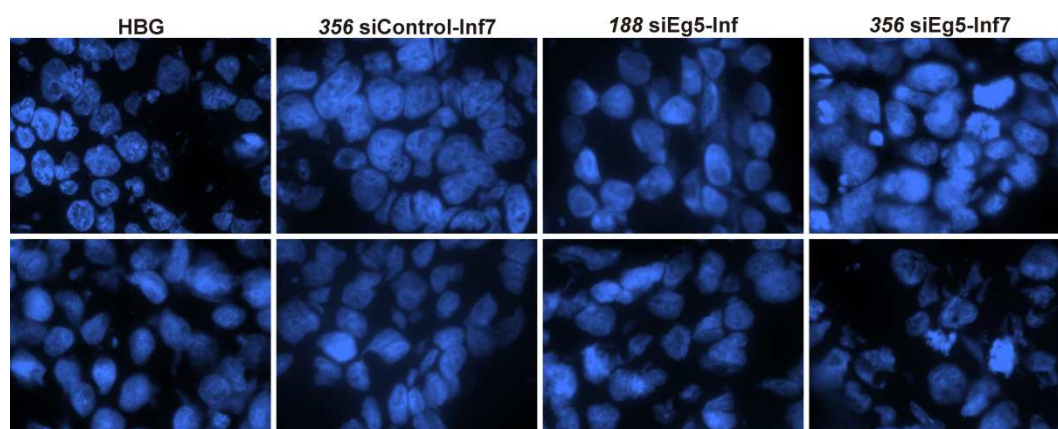


**Figure 53 Aster formation after intravenous polyplex injection:** 10 days after subcutaneous injection of  $5 \times 10^6$  KB cells into NMRI mice ( $n = 5$ ) polyplexes were injected intravenously. After mice were sacrificed DAPI staining in cryo sections displayed aster formation only for Eg5-Inf7 siRNA containing polyplexes. Untargeted and targeted polyplexes containing Eg5-Inf7 siRNA showed moderate aster formation. Experiments were performed with Laura Schreiner (veterinary MD thesis, LMU 2013).

For the detection of mitotic figures after intratumoral polyplex injection an H&E staining was established according to the assay published by Judge et al.<sup>120</sup>. After H&E staining, mitotic figures were analyzed and Eg5-Inf7 and control-Inf7 tumors were compared. Mitotic figures also included dividing cells, whereas aster formation only detected cells after mitotic block. Therefore, control siRNA treated tumors also displayed mitotic figures to some extent. However, higher amounts of mitotic figures were detectable because of the mitotic block in the Eg5-Inf7 siRNA treated tumors. These results proved the successful target gene silencing with the multifunctional nanocarrier system.

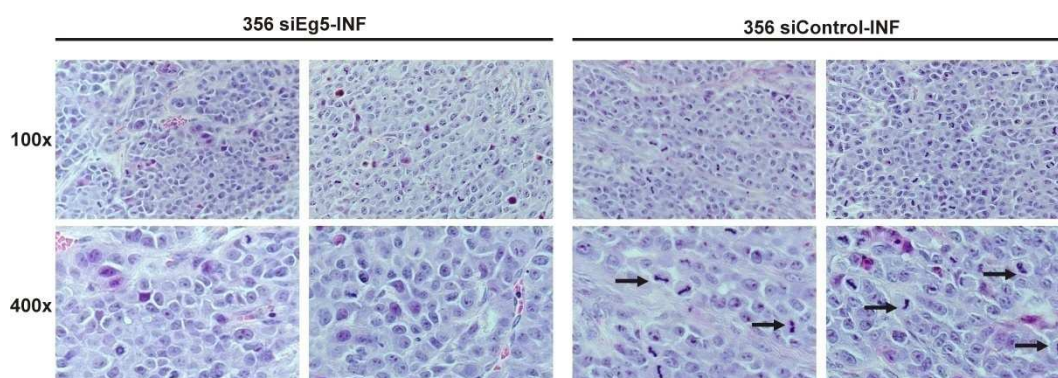


**Figure 54: Mitotic figures after intravenous polyplex injection:** 10 days after subcutaneous injection of  $5 \times 10^6$  KB cells into NMRI mice ( $n = 5$ ) polyplexes were injected intratumorally. Mice were killed 24 h after the treatment and tumors were stored in paraformaldehyde. H&E staining of paraffin sections displayed aster formation mainly in Eg5-Inf7 siRNA containing polyplexes. Experiments were performed with Laura Schreiner (veterinary MD thesis, LMU 2013).

### 3.2.2 Methotrexate linked Targeting Oligomers

After demonstrating successful targeting and siRNA induced gene silencing with folic acid linked targeting oligomer **356**, the targeting ligand was changed to

methotrexate (MTX). MTX has almost the same chemical structure as folic acid apart from the positions marked with red circles in Figure 55. Generally, the ubiquitous expressed reduced folate carrier is responsible for MTX uptake<sup>143</sup>, whereas in cells overexpressing the folic acid receptor MTX may also be taken up through folate receptor mediated endocytosis<sup>144</sup>.

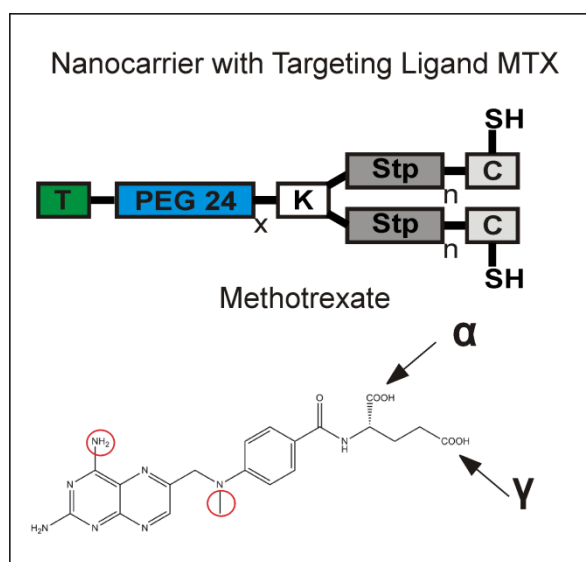


**Figure 55 Chemical structures of the oligomer backbone and methotrexate:** Upper structure shows the standard oligomer with  $n = 4$  and  $x = 1$ . Methotrexate is coupled via  $\gamma$ - (638), like in the case of the folate oligomers, or  $\alpha$ -carboxy group (642) indicated by the arrows. To improve the methotrexate related effects glutamic acid spacer with 2 (639), 4 (640) or 6 (641) glutamic acid molecules between the  $\gamma$ -carboxy group of methotrexate and the PEG spacer were integrated. Oligomers were synthesized by U. Lächelt.

Apart from the use as a targeting ligand, MTX is a well characterized drug applied for the treatment of cancer and rheumatoid arthritis. MTX binds with high affinity to the enzyme dihydrofolate reductase (DHFR) and inhibits the conversion of dihydrofolate to tetrahydrofolate<sup>145</sup>. Tetrahydrofolate is an important 1-carbon carrier, essential for the synthesis of purines, thymidine and methionine. During the 1-carbon transfer, tetrahydrofolate is oxidized to dihydrofoalte which is again reduced by the enzyme DHFR. Specifically, cells during the synthesis phase are harmed by the inhibition of DHFR because of the resulting low levels of thymidine and purine bases for DNA and RNA synthesis. Therefore, MTX targeted oligomers display the efficacy of this antimetabolic drug and allow the delivery of siRNA. MTX targeted oligomers can be combined with therapeutic siRNAs, for example Eg5 and Ran siRNA, with siRNAs targeting drug resistance mechanism, or with anti inflammatory siRNAs like TNF- $\alpha$  siRNA. Combination of MTX and siRNA in one compound ensures the simultaneous active principal inside the targeted cell.

### 3.2.2.1 Sensitivity of Different Cell Lines to MTX

For further oligomer comparison cell lines sensitive and resistant to the treatment with MTX had to be identified. Hence, the IC<sub>50</sub> values of different cell lines were evaluated with pure MTX after 48 h incubation time through an ATP dependent assay.

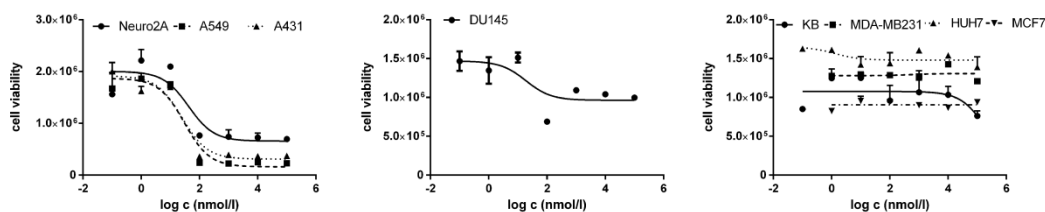


**Figure 56 Sensitivity of different cell lines to the treatment with MTX:** Several cell lines were tested for their sensitivity to MTX treatment. Cell viability was determined by CellTiter Glo measurement 48 h after addition of MTX.

Three cell lines highly sensitive to the treatment with MTX could be identified namely Neuro2A cells, A549 and the human epidermoid carcinoma A431. The human prostate cancer cell line DU145 showed medium sensitivity, whereas HUH7, KB and the human breast cancer cell lines MDA-MB 231 and MCF7 did not react to MTX treatment at all (Figure 56).

### 3.2.2.2 Cytotoxicity of MTX Oligomers

Initially the enzyme affinity of pure MTX and MTX linked oligomers was compared in a cell free system. For this experiment oligomers coupled through a PEG spacer to the  $\alpha$ - or  $\gamma$ -carboxy group of MTX were synthesized. Furthermore, glutamic acid (E) spacers between the  $\gamma$ -carboxy group and the PEG group were integrated, to imitate the naturally occurring addition of glutamic acid molecules after cellular uptake to the free  $\gamma$ -carboxy group<sup>146</sup>. Addition of up to 6 glutamic acid groups, mediated by the enzyme folylpolyglutamate synthetase, was reported to be of utmost importance, as it enhances the enzyme affinity of MTX. In this experimental setting no addition of glutamic acid molecules was possible. Enzyme activity was determined through a photometric assay detecting the amount of NADPH/H<sup>+</sup> at 340 nm. The enzyme activity without inhibitor was set to 100% and compared to the activity after addition of MTX or MTX targeted oligomers (Figure 57).

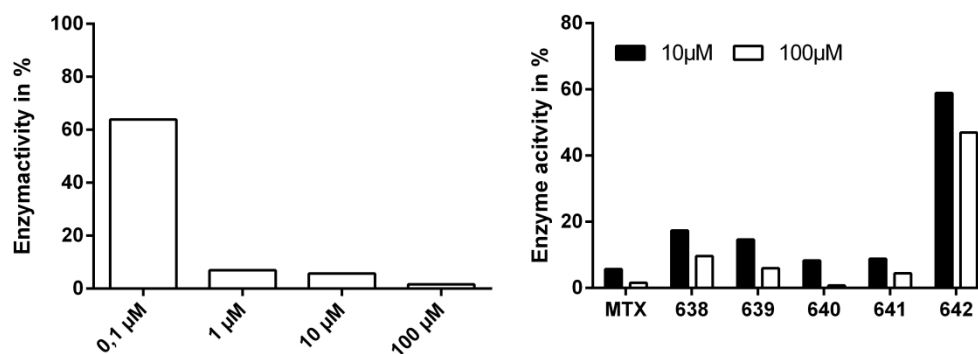


**Figure 57 DHFR activity in a cell free system:** Concentrations of NADPH/H<sup>+</sup> were measured photometrically to determine the enzyme activity. For the evaluation of the assay different MTX concentrations were tested (left panel). Thereafter MTX targeted oligomers **638** (MTX-PEG-STP), **639** (MTX-2E-PEG-STP), **640** (MTX-4E-PEG-STP), **641** (MTX-6E-PEG-STP), **642** ( $\alpha$ MTX-PEG-STP) were compared in the same photometric assay (right panel).

A clear dose dependency was demonstrated for pure MTX in this assay and the highest MTX concentrations were chosen for further oligomer comparison. Pure MTX and oligomers **640** and **641** performed best in this assay, while oligomers **638** and **639** showed reduced activity and oligomer **642** showed the lowest activity. This activity profile demonstrated the negative effect of  $\alpha$ -carboxy coupling and the positive effect of oligoglutamate addition.

Subsequently MTX sensitive A549 cells were treated with pure MTX or MTX linked oligomers (Figure 58). In this instance, coupling through the  $\alpha$ -carboxy group was favorable in comparison to coupling through the  $\gamma$ -carboxy group because the free  $\gamma$ -carboxy group allowed oligoglutamate addition. The increased enzyme affinity after oligoglutamate addition outweighed the negative effect of  $\alpha$ -carboxy coupling in this cellular assay. Consistently, the synthetic addition of oligoglutamates reduced IC<sub>50</sub> 10 fold compared to the unmodified  $\gamma$ -carboxy coupled oligomer **638**.

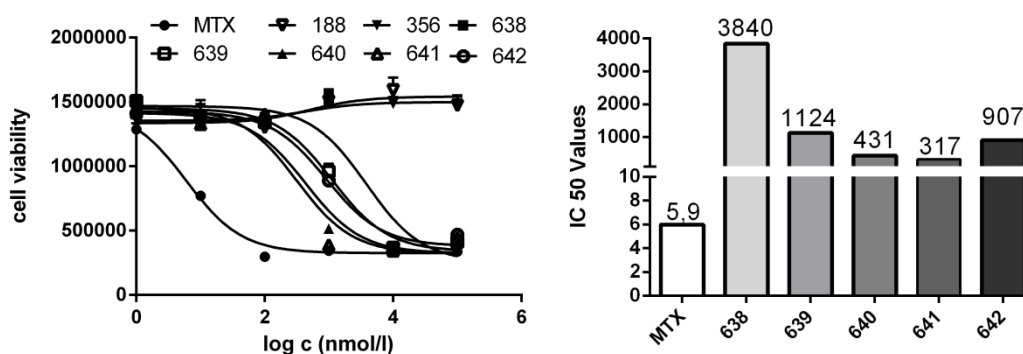


**Figure 58 IC<sub>50</sub> values of MTX and MTX oligomers:** A549 cells were treated with pure MTX or oligomers **638** (MTX-PEG-STP), **639** (MTX-2E-PEG-STP), **640** (MTX-4E-PEG-STP), **641** (MTX-6E-PEG-STP), **642** ( $\alpha$ MTX-PEG-STP) to determine IC<sub>50</sub> values.

In conclusion, coupling via the  $\alpha$ -carboxy group (**642**) improved the IC<sub>50</sub> 4-fold compared to oligomer **638**. The addition of glutamic acid spacers 2E, 4E, 6E improved the IC<sub>50</sub> 3.5-fold, 9-fold and 12-fold respectively. This assay demonstrates the necessity of the free  $\gamma$ -carboxy group or the pre addition of glutamic acid for the effectivity of coupled MTX. The IC<sub>50</sub> values however were still > 50-fold higher than for free MTX.

### 3.2.2.3 Uptake Studies

Targeting efficiency of oligomers **638**, **639**, **640**, **641** and **642** was determined by flow cytometry and compared to oligomer **188** (untargeted) and **356** (targeted by folic acid). Folic acid receptor overexpressing KB cells and minimal folic acid receptor expressing A549 cells were transfected applying MTX targeted oligomers and Cy5 labeled siRNA. After 45 min incubation time, cells were trypsinized, collected in FACS buffer (10% FCS in PBS), and analyzed in a flow cytometric assay. KB cells showed efficient polyplex uptake for all MTX linked oligomers. Uptake efficiency was slightly reduced compared to folic acid targeted oligomers, as expected because of the reduced folate receptor binding affinity of MTX, compensated by the high receptor density. Strongly reduced uptake of MTX linked polyplexes (as compared with folate linked polyplexes) in receptor-low A549 cells demonstrated the receptor mediated uptake of targeted oligomers.

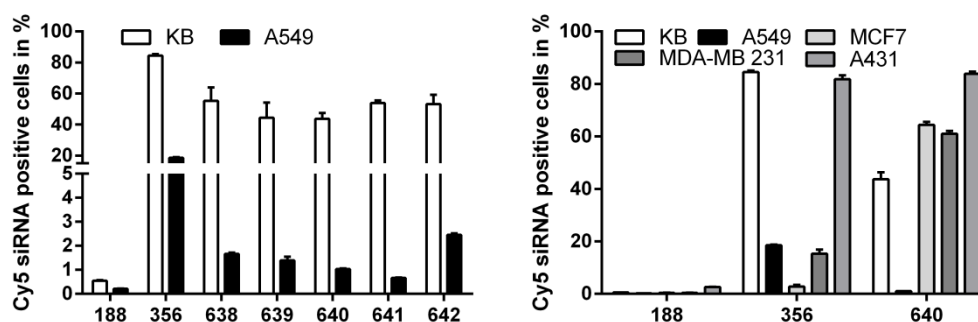


**Figure 59 Polyplex uptake determined by flow cytometry:** In the left graph polyplex uptake into KB cells with high and A549 cells with low folate receptor was compared by flow cytometry. Polyplexes were incubated for 45 min on the cells to compare the receptor binding capacity of different oligomers without targeting ligand, with folic acid or MTX as targeting ligands. In the right graph oligomers **188** (untargeted), **356** (folic acid) and **640** (MTX) were compared in different cell lines to determine uptake either through the folic acid receptor or the reduced folate carrier.

Following KB, A549, MCF7, MDA-MB 231 and A431 cells were compared due to the uptake of polyplexes targeted by MTX (**640**) or folic acid (**356**) (Figure 59 right panel). Efficient uptake of folic acid targeted and moderately reduced uptake of MTX targeted oligomers described for KB cells indicated the involvement of solely folate receptors. In contrast, efficient uptake of both targeted oligomers indicated the presence of folic acid receptors and reduced folate carriers described for A431 cells (right panel, far right lanes). MCF7 and MDA-MB 231 showed superior uptake of MTX targeted oligomer **640**, indicating the absence of folate receptor and uptake solely via the reduced folate carrier. Both targeting assays revealed receptor mediated uptake for MTX targeted oligomers (Figure 59). The experiment in combination with the previous testing of folic acid receptor levels indicated polyplex uptake for the MTX oligomers through the folic acid receptor in KB cells, the reduced folate carrier in MCF7 and MDA-MB 231 cells and a combination of both in A431 cells.

#### 3.2.2.4 GFP Knockdown in KB Cells

For the detection of marker gene silencing, KB-eGFPLuc cells were chosen due to their high expression of folic acid receptors and their moderate susceptibility to the treatment with MTX. Knockdown after GFP siRNA transfection was compared to control siRNA and pure oligomer. To demonstrate efficient targeting MTX targeted and untargeted polyplexes were compared after an incubation time of 45 min.

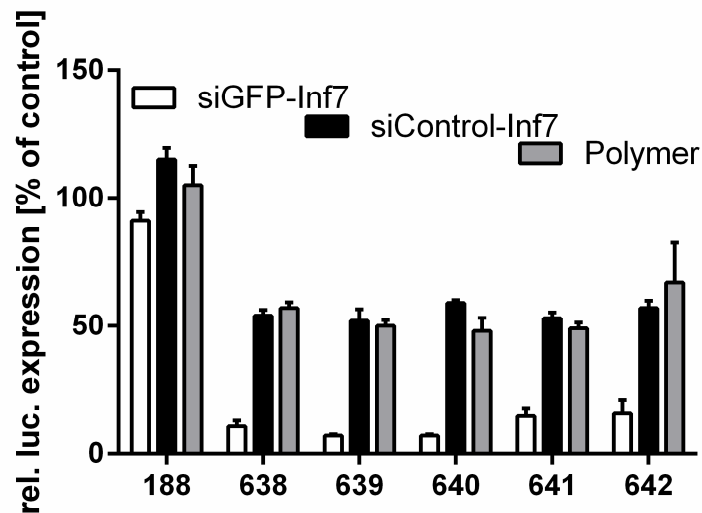


**Figure 60 Transfection experiments:** KB-eGFP<sub>Luc</sub> cells were transfected with MTX targeted (*638*, *639*, *640*, *641*, *642*) and untargeted (*188*) polyplexes. GFP and control siRNAs modified with the lytic peptide Inf7 were used because previous experiments demonstrated the necessity of an endosomolytic siRNA. Polyplexes were mixed at an N/P of 16 with 200 ng siRNA per well and incubated for 45 min.

The results demonstrated efficient target gene knockdown mediated through MTX linked oligomers similar as previously shown for folate linked oligomers, whereas untargeted oligomers did not show eGFP<sub>Luc</sub> silencing (Figure 60). In contrast to folate-linked oligomers, MTX oligomers and control siRNA polyplexes caused comparable unspecific eGFP<sub>Luc</sub> silencing (50% luciferase reduction) due to carrier related toxicity. In conclusion, all MTX linked oligomers showed similar and efficient marker gene knockdown in the GFP siRNA group with moderate toxicity caused by the MTX oligomers.

### 3.2.2.5 Combined Toxicity of MTX/siEG5 Polyplexes

Polyplexes consisting of MTX oligomer *640* and Eg5-Inf7 siRNA were mixed to demonstrate combined toxicity of the carrier and therapeutic siRNA. A431 cells were chosen because of their high susceptibility to MTX treatment and the effective uptake of MTX targeted oligomers demonstrated in the previous experiments. Cell viability of A431 cells after transfection with pure polymer or polyplexes containing either control or Eg5 siRNA was compared.

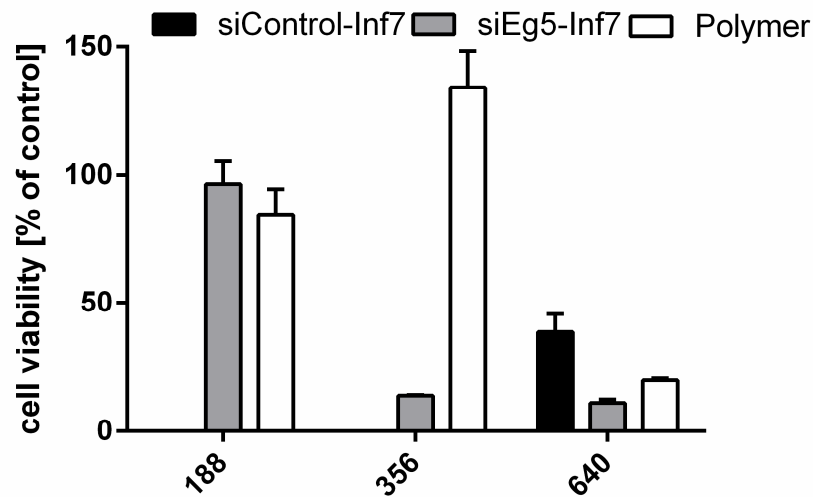


**Figure 61 Cell viability assay:** A431 cells transfected with control oligomer **188**, folate oligomer **356** or MTX oligomer **640** polyplexes containing either Eg5 or control siRNA were compared due to the cell viability. Oligomer concentration of 100  $\mu$ M was calculated and the siRNA concentration was adjusted to result in an N/P of 16.

Transfection with Eg5 siRNA in combination with MTX targeted oligomer **640** and folic acid targeted oligomer **356** resulted in reduced cell viability compared to buffer treatment (Figure 61). The pure MTX oligomer reduced cell viability very effectively, whereas control siRNA polyplexes displayed reduced effects on cell viability. The combination of oligomer **640** and Eg5 siRNA improved the cytotoxic effect indicating the potential of this combination. Consistent with the previous marker gene experiment oligomer **188** did not mediate any effect because of the short incubation time.

## 4 DISCUSSION

### 4.1 Evaluation of Monodisperse, Sequence Defined siRNA Carriers

Technological aspects, such as tumor targeting and insufficient delivery into the cytosol, are hindering the medical application of siRNA in cancer therapy<sup>147</sup>. To overcome this hurdle we built on a large library of sequence defined biodegradable oligomers for siRNA delivery<sup>133</sup>. This approach allowed the comparison of several oligomers to establish structure-activity relations for siRNA carriers<sup>75</sup>. Many modifications of the biodegradable oligomers, improving siRNA binding, cellular uptake and endosomal release of the polyplexes have been reported<sup>136</sup>. For further experiments two lipo-oligomers (**49** with T-shape and **229** with i-shape topology) and a branched oligomer (**386**) were selected. These oligomers fulfil the previously defined requirements for successful siRNA delivery and were compared for silencing of the marker gene eGFPLuc and two therapeutic targets, Ran and Eg5.

#### 4.1.1 Oligomer Evaluation *in vitro* and *in vivo*

Comparison of oligomer **49** to the gold standards Lipofectamine 2000 and PEI-Succ10 displayed comparable high gene silencing efficiency for all carriers. The following comparison of oligomers **49**, **229** and **386** revealed similar knockdown efficiency for the structurally different oligomers. This was an important fact as differences concerning the *in vivo* efficacy of these *in vitro* functional carriers should be demonstrated. Besides eGFPLuc also Eg5 and Ran silencing were evaluated *in vitro* to establish a therapeutic *in vivo* oligomer screening system. The experiments highlighted clear differences between the *in vitro* gene silencing and the corresponding *in vivo* antitumoral efficiencies of these carriers.

Both antitumoral siRNAs, Eg5 and Ran, showed specific target gene knockdown on mRNA and protein level. Interestingly, target gene knockdown only persisted for a short period of time. Reduced mRNA levels were detectable 24 and 48 h after siRNA transfection, whereas after 72 h Eg5 mRNA levels of control and Eg5 siRNA transfected cells were on the same level. Ran knockdown was also detectable after 24 and 48 h, but after 72 h an up-regulation of Ran mRNA was

observed. The fast growth rate of Neuro2A cells and the fact that successful transfection led to removal of cells by cell death, explained the short duration of target gene knockdown compared to other siRNA studies<sup>148</sup>. Eg5 knockdown resulted in aster formation and changed cell cycle stages compared to control siRNA or buffer transfected cells. DAPI and tubulin staining revealed typical mitotic figures, due to the blocked separation of the centrosomes after Eg5 knockdown. Furthermore, increased G2 peaks and increasing sub G1/G0 peaks demonstrated the mitotic arrest, followed by cell death. In contrast, Ran knockdown only led to increased sub G1/G0 peaks. These findings were consistent with the biological mechanism of the target gene inhibition and demonstrated the antitumoral potential of both siRNAs. Furthermore, a cell viability assay confirmed the therapeutic tumor cell killing by both siRNAs *in vitro*. To evaluate the two target genes *in vivo*, three different siRNA concentrations were compared for intratumoral injection<sup>75</sup>. Only oligomer **49** polyplexes with 50 µg siRNA per injection showed significant reduction of tumor growth in the Eg5 siRNA group compared to control siRNA treatment. In contrast, polyplexes with 25 and 12.5 µg siRNA per injection did not result in reduced tumor growth. This relatively high amount of siRNA is required because of the fast tumor growth after subcutaneous injection of  $5 \times 10^6$  Neuro2A cells. Experiments comparing Eg5 and Ran siRNA were performed according to the previous dose finding experiment using oligomer **49**. Mitotic arrest after transfection with Eg5 siRNA and apoptotic TUNEL staining after transfection with Ran siRNA indicated successful target gene knockdown *in vivo*. Both therapeutic siRNAs reduced tumor growth compared to control siRNA treatment. Control siRNA polyplexes had some inhibitory effect on tumor growth compared to buffer treated tumors, but did not result in significant prolonged survival. Ran siRNA polyplexes mediated the best antitumoral effects. Therefore, Ran silencing led to slower tumor growth rates and prolonged survival (28 days) compared to Eg5 mRNA knockdown (25 days). This might be explained by the effects of Ran (role in nuclear transport) knockdown on cells in all cell cycle stages, whereas knockdown of Eg5 (role in mitotic chromosome separation) only affects dividing cells. Due to these findings Ran siRNA was used for further *in vivo* experiments.

For the oligomer comparison the three previously described, diversely shaped carriers were selected because of their high gene silencing efficacy *in vitro*.

Polyplex size and stability varied depending on the applied oligomer. Both lipo-oligomers formed polyplexes in a range of 20-50 nm, whereas the branched oligomer **386** formed large particles with a size of about 600 nm. The lipo-oligomers possess higher polyplex stability than the larger branched oligomer **386** particles. This was confirmed through the findings by imaging polyplexes containing Cy7 labelled siRNA after intratumoral injection. Oligomers **49** and **229** showed high intratumoral Cy7 signals for 48 h after polyplex injection, whereas Cy7 signals for oligomer **386** polyplexes decreased in this time range. The fluorescence signals in the kidneys (indicating slow release of free siRNA) confirm the partial instability of oligomer **386** polyplexes. Polyplex stability however was not critical and apparently sufficient in intratumoral administration with dosing at every 3 days, as antitumoral efficacy did not correlate with polyplex stability. After intravenous injection oligomers **49** and **229** showed accumulation in the liver > kidneys > tumor > lung detected by fluorescence microscopy of organ sections. Oligomer **229** showed superior tumor accumulation compared to oligomer **49**. This could be influenced due to the lower zeta potential of oligomer **229** polyplexes, leading to reduced interaction with blood components and therefore increasing tumor accumulation after intravenous injection.

*In vitro* knockdown efficiencies determined by qPCR and Western blot after Eg5 and Ran silencing were in consistency with the marker gene studies demonstrating the same level of target gene silencing for the three oligomers. Furthermore, the effects on tumor cell viability and the kinetics of target gene knockdown were evaluated. Comparing the three oligomers, different silencing kinetics were detectable on protein level after 24 h, demonstrating the fastest Eg5 and Ran protein silencing mediated by oligomer **386**. In accordance with these findings, oligomer **386** polyplexes containing either Eg5 or Ran siRNA decreased tumor cell viability at 48 h best. After 72 h all polyplexes containing therapeutic Eg5 or Ran siRNA mediated significant tumor cell killing, with oligomer **386** mediating the strongest effects. To compare antitumoral *in vitro* and *in vivo* efficacy of the three oligomers, an intratumoral siRNA treatment was started. Oligomer **229** failed to reduce tumor growth comparing the Ran siRNA and the control siRNA groups. Oligomer **49** Ran siRNA polyplexes showed significantly reduced tumor growth compared to control siRNA polyplexes after 3 but not after 2 intratumoral

polyplex injections per week, indicating the necessity of frequent polyplex dosing in the fast growing Neuro2A tumor model. The best tumor growth reduction was mediated by oligomer **386**. Tumor growth and tumor weights were significantly reduced in the Ran siRNA compared to the control siRNA transfected tumors in two independent experiments. In sum, oligomer **386** reduced tumor volume best, followed by oligomer **49**, whereas oligomer **229** was inactive for local tumor treatment *in vivo*.

The results demonstrate a discrepancy of the three tested oligomers in their *in vitro* and *in vivo* activity. Although all oligomers showed efficient target gene mRNA and protein knockdown in several *in vitro* assays, only oligomer **386** and to some extent oligomer **49** mediated reduced tumor growth *in vivo*. Only the fast knockdown kinetic and the high antitumoral activity of oligomer **386** *in vitro* can be correlated to the high *in vivo* efficiency. Of note, **386** forms the largest siRNA polyplexes with only moderate stability. These findings demonstrated the importance of *in vivo* testing for the development of potent siRNA delivery agents. Future experiments should demonstrate efficient tumor growth reduction after intravenous polyplex injection. For this reason stabilisation through the incorporation of tyrosines<sup>136</sup> or PEGylation and targeting<sup>116,149</sup> will be important factors.

#### 4.1.2 Tyrosine Trimer Stabilized T-shape Oligomers

Improved polyplex stability plays an important role especially for the successful delivery of nucleic acids after intravenous injection<sup>141</sup>. Hence, certain components, like hydrophobic dioleic acid motifs and cysteines, were incorporated in the previous oligomeric structures to ensure polyplex stabilization. To further enhance polyplex stability an oligotyrosine motif was integrated into the sequence defined oligomers<sup>150</sup>. Subsequently, the stability and silencing efficiency of polyplexes containing cysteines, a dioleic acid motif, an oligotyrosine modification or a combination of these components were compared. Oligomers modified with solely tyrosines were less efficient in binding nucleic acid and displayed decreased transfection efficiency. All other oligomers, except the control oligomer **216**, showed efficient eGFPLuc silencing. In conclusion, the efficient siRNA transfection requires the combination of two different stabilizing components.

Additionally, polyplex stability was analyzed in 90% serum and demonstrated superior stability of oligomers with lateral oligotyrosines to oligomers with terminal cysteines. Oligomers combining oligotyrosines and cysteines in the periphery displayed the best polyplex stability. On account of these beneficial properties, the *in vivo* distribution of Cy7 labeled siRNA polyplexes after intravenous injections was monitored. Oligomers **468** and **464** quenched the fluorescent signal of the Cy7-labeled siRNA, making an *in vivo* comparison of these polyplexes impossible due to detection reasons. Even though, the oligomers quenched the signal, no free Cy7-labeled siRNA was detected in the kidneys or the bladder. This allowed the conclusion that the polyplexes were still intact during the first hour. NIR fluorescence imaging revealed short circulation times followed by a fast renal clearance<sup>116,151</sup> for free siRNA with a hydrodynamic radius of approximately 2.3 nm and for oligomer **216** polyplexes. As the sizes of the control polyplexes were larger than the renal filtration limit, dissociation must have occurred before elimination through the kidneys. According to previous stability assays oligomer **333** polyplexes showed partial instability with stable polyplexes accumulating in the liver and free siRNA being detectable in the kidneys after intravenous injection. In contrast, oligomers **49**, **332**, and **454** polyplexes revealed a prolonged presence of complexed siRNA in the circulation compared to free siRNA and control oligomers. The modification with fatty acids increased polyplex accumulation in the liver<sup>152</sup>. Consistent with the high *in vitro* stability, longer circulation times of oligomers **332** and **454** polyplexes were recorded compared to oligomer **49** polyplexes. In summary, the higher serum stability of oligotyrosine modified polyplexes was beneficial for *in vivo* distribution, but oligomer characteristics, like the hydrophobicity, also played an important role.

In accordance with the previously established intratumoral treatment, oligomer **332**, **468**, **454** and **464** polyplexes were compared to oligomer **49** polyplexes. Again Neuro2A tumor bearing NMRI mice were treated with Ran or control siRNA polyplexes twice a week, in total 5 times. Oligomers **49**, **454** and **464** failed to mediate reduced tumor growth in the Ran siRNA group compared to the control siRNA group. Oligomer **464** polyplexes caused tumor necrosis making the bioluminescence evaluation of tumor growth impossible. In contrast, treatment with oligomer **468** and **332** Ran siRNA polyplexes reduced the tumor volume

compared to control siRNA polyplexes. These data confirmed the previous experiment demonstrating the efficacy of less stable polyplexes for the intratumoral treatment of Neuro2A tumor bearing mice. However, these highly stable polyplexes with increased circulation times will improve tumor accumulation after intravenous injection. In conclusion, the incorporation of oligotyrosine motifs improved polyplex stability of T-shaped oligomers and is an important option for the *in vitro* and *in vivo* stabilization of other carriers.

## **4.2 Evaluation of Targeted Nanocarriers for siRNA Delivery**

On the contrary to polyplexes without targeting ligands, incorporation of targeting ligands allows target cell specific polyplex delivery<sup>153</sup>. Specifically shielded particles with low zeta potentials are dependent on targeting ligands, because the incorporation of targeting ligands regains polyplex cell interaction in a receptor specific way. For *in vivo* applications targeted structures with low zeta potentials are favored due to reduced unspecific interactions leading to reduced side effects. Targeted carriers were also synthesized by solid-phase-assisted macromolecule assembly, enabling the incorporation of different building blocks, PEG chains and targeting ligands<sup>116</sup>.

### **4.2.1 Nanocarriers with Targeting Ligand Folic Acid**

The targeted nanocarriers were thoroughly analyzed, and the requirement of every single substructure was demonstrated. A cell line screen revealed only KB and Igrov cells highly expressing the folic acid receptor. Therefore, KB and Igrov cells were chosen for transfection and targeting experiments, demonstrating the high targeting specificity of the nanocarrier. Furthermore, the beneficial effect of influenza-peptide modified siRNA could be demonstrated in a marker gene silencing assay. In contrast to the high amounts of nanocarrier required for efficient endosomal escape the application of influenza peptide modified siRNA enabled efficient siRNA silencing at low N/P ratios. Moreover, the titration of polyplex or siRNA concentrations demonstrated the high efficiency of these nanocarriers down to a siRNA concentration of 6 nM. The comparison with the gold standard Lipofectamine 2000 revealed superior efficiency for the targeted nanocarrier system. In accordance, with the eGFPLuc screen silencing of the therapeutic protein Eg5 demonstrated aster formation only for targeted nanocarriers complexing Eg5-Inf7 siRNA.

For *in vivo* experiments KB cells were chosen because they developed tumors of 200 mm<sup>3</sup> after 10 days incubation time. In contrast, subcutaneous injection of Igrov cells did not result in fast growing tumors. Following *in vivo* experiments demonstrated tumor retention for 120 h after intratumoral injection of folic acid targeted nanocarriers. In contrast, untargeted nanocarriers and free siRNA were washed out of the tumor within 24 h and showed significantly reduced tumor retention. In consistency, with previous *in vitro* experiment this experiment demonstrated the positive effect of folic acid targeting *in vivo*.

After intravenous injection the nanocarriers complexing Cy7 labeled siRNA were detectable by NIR imaging in the circulation without unspecific accumulation in non targeted tissue such as liver, lung, or spleen. However, the nanosized appearance (about 5.8 nm hydrodynamic diameter) of this functionally active carrier caused fast renal clearance, compared to the bigger branched oligomer **386** polyplexes and the very lipophilic polyplexes of oligomer **278**. KB tumors were implanted into the neck of NMRI mice, preventing the interaction of tumor and kidney signals. In this experiment kidney and bladder signals were caused by intact polyplexes and not by pure siRNA. Gel shift assays of urine samples taken 4 h after polyplex injection proved the stability of the nanocarriers as free siRNA was only detectable after heparin and TCEP treatment. To increase circulation times and improve tumor targeting structures with longer PEG spacers, tyrosine, or fatty acid modification were synthesized. However, the resulting nanocarriers did not positively influence the *in vivo* distribution. Incorporation of longer PEG spacers increased particle size but reduced polyplex stability especially for oligomer **647** with 8 x more PEG than the standard oligomer **356**. Oligotyrosines did not influence particle size and circulation time at all, only a moderate liver accumulation in consequence to their lipophilic character was detectable. Nanocarriers with fatty acid modification showed the worst effect with caprylic acid incorporation leading to liver accumulation of the polyplexes and stearic acid modification causing fatal side effects. Hence, the standard oligomer **356** was used for functional *in vivo* studies.

Intravenous injection of targeted and untargeted nanocarriers with Eg5-Inf7 siRNA showed histological aster formation 24 h after polyplex injection. Presumably, very little amounts of the nanocarriers undetectable by NIR imaging reached the tumor and caused target gene knockdown because of their high

efficiency. Apparently, targeted nanocarriers are more efficient as untargeted, but the quantification of aster formation was very complicated because of intense regional differences in this assay.

Consequently, Eg5 knockdown was detected by H&E staining after intratumoral injection. This approach allowed a semi quantitative evaluation of mitotic figures. In contrast to the previously described aster formation, the analysis of mitotic figures is not a positive read out system, because also mitotic cells are detected. The analysis of H&E stained sections revealed a strong increase of mitotic figures after injection of Eg5-Inf7 siRNA incorporating nanocarriers compared to control-Inf7 siRNA nanocarriers. Both assays proved successful siRNA delivery and Eg5 silencing *in vivo*, demonstrating the high potential of this multifunctional nanocarrier.

#### **4.2.2 Nanocarriers with Targeting Ligand Methotrexate**

Pharmaceutically relevant drugs, like methotrexate with high structure similarity to folic acid, can be used for targeting in the multifunctional nanocarrier system. This approach combines the effect of a classical drug with the great potential of siRNA induced gene silencing. Several siRNAs can be included into the nanocarrier addressing targets related to the illness or causing drug resistance. The combination could allow dose reduction of the chemostatic drug yielding in reduced side effects or increased overall efficiency. Chemical synthesis of functionalized nanocarriers was complicated because the coupled drug has to maintain its efficiency.

Several cancer cell lines were screened and three cell lines (A549, A431, Neuro2A) were identified to be highly sensitive to MTX treatment. We utilized the human alveolar A549 cells to screen the IC<sub>50</sub> values of several MTX targeted oligomers either coupled through the  $\alpha$ - or  $\gamma$ -carboxy group. To simulate the addition of glutamic acid and to improve the enzyme affinity after cellular uptake different glutamic acid spacers were introduced into the structure. At first DHFR inhibition was tested in a cell free system, demonstrating successful enzyme inhibition for MTX targeted carriers. Coupling through the  $\alpha$ -carboxy group was unfavorable in a cell free system resulting in reduced enzyme affinity for the  $\alpha$ -carboxy modified carrier. In contrast, the  $\alpha$ -carboxy modification was superior to the  $\gamma$ -carboxy modification in A549 cells, allowing the adhesion of glutamic acid

molecules after cellular uptake. In accordance, the use of glutamic acid spacers for  $\gamma$ -carboxy modified MTX carriers resulted in 10-fold lower IC50 values compared to  $\gamma$ -carboxy modified MTX carriers without glutamic acid spacers. However, the IC50 values of the best performing oligomer **641** with 6 glutamic acid spacers was still 60-fold higher than the IC50 value of pure MTX. Incorporation of acid labile or reducible bonds between PEG spacer and MTX could further reduce the IC50 values and improve the efficiency.

Receptor specificity was demonstrated through flow cytometric experiments. The experiment demonstrated efficient uptake of all MTX linked carriers into folic acid receptor highly expressing KB cells, whereas the uptake in A549 cells with low folic acid receptor level was significantly reduced. In comparison to folic acid linked nanocarriers the uptake was moderately decreased displaying the reduced receptor affinity. Further flow cytometric experiments were performed comparing the uptake of MTX and folic acid linked nanocarriers to distinguish between the uptake through folic acid receptors or the reduced folate carriers. KB cells expressed the folic acid receptor (Figure 41) and preferable took up folic acid targeted carriers<sup>154</sup>. In contrast, MCF7 and MDA-MB 231 cells did not express the folic acid receptor determined in a flow cytometric assay. Therefore, folic acid linked nanocarriers were not taken up and MTX linked nanocarriers were presumably primarily taken up through the reduced folate carrier. A431 cells expressed both, folic acid receptors and reduced folate carriers, and took up folic acid and MTX linked oligomers with equal efficiency.

Transfection experiments were performed in KB cells moderately susceptible to MTX treatment because high carrier mediated toxicity would be unsuitable for the detection of target gene knockdown. All targeted siRNA binding nanocarriers mediated specific eGFPLuc silencing and proved superior efficiency over untargeted nanocarriers. Besides efficient targeting, all MTX nanocarriers mediated MTX specific toxicity detectable after control siRNA and pure carrier transfections. In conclusion, the assays demonstrated successful receptor binding, DHFR inhibition and siRNA delivery for the MTX targeted nanocarriers. Consequently, the most efficient nanocarrier **640** was combined with Eg5-Inf7 siRNA for the transfection of A431 cells. Pure and control siRNA binding nanocarrier **640** significantly reduced cell viability compared to pure and Eg5 binding untargeted nanocarrier **188**, demonstrating the MTX related toxicity.

According to the previous experiments, the combination of Eg5 siRNA and MTX linked nanocarrier **640** showed the strongest effect and evidenced the proof of concept for the combination of MTX linked nanocarriers and therapeutic siRNAs.

## 5 SUMMARY

Nucleic acid therapies, such as siRNA induced gene silencing, are considered as promising options for novel treatments of cancer and several other incurable diseases<sup>5,11,155-157</sup>. Successful siRNA application is hampered due to the difficult applicability of nucleic acids in general and the low serum stability of siRNAs in particular. Advances in carrier design, including polymers<sup>112,133,158</sup> show the potential to overcome these problems and to establish this innovative class of drugs. In this thesis several *in vitro* and *in vivo* assays were established to demonstrate successful application of sequence defined, biodegradable oligomers for siRNA delivery.

Several hundred monodisperse oligomers were synthesized by solid-phase-assisted macromolecule assembly and screened to define structure-activity relationships. Three structurally diverse oligomers were selected and qPCR and Western blot assays were established to demonstrate successful target gene knockdown for the therapeutic relevant Eg5 and Ran siRNAs. In accordance with the previous screening assay, lipo-oligomers **49** (T-shape), **229** (i-shape) and the branched oligomer **386** mediated successful and efficient target gene silencing. Furthermore, flow cytometric, histological, and cell viability assays demonstrated the high therapeutic potential of Eg5 (aster formation, G2 arrest, cell death) and Ran (cell death) siRNA. First *in vivo* assays helped to define the required doses for intratumoral polyplex injections and enabled the comparison of Eg5 and Ran siRNA *in vivo*. Silencing of Ran showed superior therapeutic effects with reduced tumor growth and prolonged survival compared to all other groups. The comparison of different oligomers revealed oligomer **386** as the most *in vivo* effective oligomer although all oligomers showed efficient target gene knockdown *in vitro*. In summary, this demonstrated the difficult correlation of *in vitro* and *in vivo* activity and proved the necessity of *in vivo* experiments for the design of efficient siRNA carriers.

Additional integration of oligotyrosine motifs into the carriers resulted in improved polyplex stability detectable in serum gel shifts *in vitro* and through NIR imaging *in vivo*. After intratumoral injection high polyplex stability was not the most critical parameter. Therefore, this polyplexes did not improve Ran silencing. Exchange of terminal cysteines by oligotyrosine motifs slightly

increased the stability and showed Ran silencing after intratumoral application. In conclusion, the integration of oligotyrosines improves polyplex stability, but very high polyplex stability is not favorable for effective gene silencing after intratumoral injection.

Effective shielding and the addition of folic acid as ligand for targeting in combination with siRNA coupled to the lytic influenza peptide resulted in highly efficient nanocarriers. Several experiments proved the necessity of every single domain like cysteines for stabilisation, folic acid for targeting and influenza peptide for endosomal escape. Further studies revealed the impressive targeting efficiency of this nanocarrier system after intratumoral injection and the short circulation time without any undesired accumulation after intravenous injection. Low tumor accumulation was detected after intravenous injection affected by the poor blood flow in the implanted KB tumors. However, nanocarriers binding Eg5-Inf7 siRNA selectively showed aster formation indicating a low accumulation of nanocarriers in the tumor. Several modifications of the carrier did not result in the desired increased size and stability of the carrier system, but the synthetic approach and the increasing knowledge will allow the integration of further modifications to develop a more efficient nanocarrier.

The synthetic approach also allowed the substitution of folic acid through other targeting ligands. The integration of the drug methotrexate extended targeting to the reduced folate carrier and combined targeting with a cytostatic activity of this ligand. Several chemically modified nanocarriers were tested to demonstrate the inhibition of dihydrofolate reductase and the targeting efficiency. In summary, the integration of a four glutamic acid long spacer between the PEG chain and methotrexate showed the best overall activity. This compound in combination with therapeutic Eg5 siRNA was tested in a cell viability assay and demonstrated superior efficiency compared to all controls. Improved oligomer backbones, as discussed for folic acid targeted nanocarriers, will turn this concept into a highly efficient siRNA carrier with cytostatic activity.

## 6 APPENDIX

### 6.1 Abbreviations

Ago2	Argonaute protein 2
brPEI	Branched PEI
CapA	Caprylic acid
CCD	Charge-coupled Device
Cy3	Cyanine dye (ex. 550 ; em. 570)
Cy5	Cyanine dye (ex. 650 ; em. 670)
Cy7	Cyanine dye (ex. 743; em. 767)
DAPI	4',6-diamidino-2-phenylindole
DHFR	Dihydrofolatereductase
DMEM	Dulbecco`s modified eagle medium
DMSO	Dimethyl sulfoxide
DNA	Deoxyribonucleic acid
DSP	Bifunctional crosslinker
eGFP	Enhanced green fluorescend protein
EDTA	Ethylenediaminetetraacetic acid
EGF/EGFR	Epidermal growth factor/ Epidermal growth factor receptor
Eg5	Eglin 5, or KSP, Kinesin spindle protein
EPR effect	Enhanced permeability and retention effect
EtBr	Ethidium bromide
FCS	Fluorescence correlation spectroscopy
FCS	Fetal calf serum
FoIA	Folic acid
FR	Folic acid receptor
GDP/GTP	Guanosine-diphosphat/ Guanosine-triphosphat
GMP	Good manufacturing practice

---

GTP	Glutaryl-tetraethyl-pentamine
GTT	Glutaryl-triethyl-tetramine
HA-2	Hemagglutinin subunit 2
HBG	Hepes buffered glucose
HEPES	N-(2-hydroxyethyl) piperazine-N'-(2-ethansulfonic acid)
HES	Hydroxyethyl starch
INF7	Subunit of the influenza peptide
i.p.	Intraperitoneal(ly)
i.v.	Intravenous(ly)
kDa	Kilo Dalton
LCA	Leber congenital amaurosis
LF2000	Lipofectamine 2000
IPEI	Linear polyethylenimine
Luc	Luciferin
LSM	Laser scanning microscopy
MDR	Multidrug resistance
miRNA	Micro ribonucleic acid
mRNA	Messenger ribonucleic acid
MDA-5	Melanoma differentiation associated protein
MTT	3-(4,5-dimethylthiazol-2-yl)-2,5-diphenyltetrazolium bromide
MTX	Methotrexate
N/P	Polymer nitrogen to nucleic acid phosphate ratio
NIR	Near infrared
OEI	Oligo ethylene imine
ON	Oligo nucleotide
PAMAM	Polyamidoamine dendrimer
PBS	Phosphate buffered saline
pDNA	Plasmid deoxyribonucleic acid

---

PEG	Polyethylene glycol
PEG <sub>24</sub>	Polyethylene glycol with exactly 24 monomers
PEI-Succ10	Branched polyethyleneimine modified with succinic acid
pHPMA	Polyhydroxypropylmethacrylate
PLL	Polylysine
Ptp	Phthalyl-tetraethyl-pentamine
qPCR	Quantitative polymerase chain reaction
r <sub>h</sub>	Hydrodynamic radius
Ran	RAS related nuclear protein
RIG-1	Retinoic acid inducible protein
RISC	Ribonucleic acid induced silencing complex
RLC	RISC loading complex
RNA	Ribonucleic acid
RNAi	Ribonucleic acid interference
ROI	Region of Interest
S.E.M.	Standard Error of the Mean
SCID	Severe combined immunodeficiency
siRNA	Small interfering ribonucleic acid
SteA	Stearic acid
Stp	Succinyl-tetraethylen-pentamine
TBE-buffer	Tris-Boric acid-EDTA-buffer
TCEP	Tris(2-carboxyethyl)phosphine
TFA	Trifluoroacetic acid
TfR	Transferrin receptor
TLR	Toll like receptor
TRBP	Transactivating response RNA binding protein
Y <sub>3</sub>	Tyrosin-Tyrosin-Tyrosin (Tyrosin trimer)

## 6.2 Publications

### 6.2.1 Original Papers

Schaffert D, Troiber C, Salcher EE, Fröhlich T, Martin I, Badgujar N, Dohmen C, Edinger D, Kläger R, Maiwald G, Farkasova K, Seeber S, Jahn-Hofmann K, Hadwiger P, Wagner E (2011) *Solid-phase synthesis of sequence-defined T-, i-, and U-shape polymers for pDNA and siRNA delivery*. *Angew Chem Int Ed Engl*. 2011 Sep12;50(38):8986-9

Noga M, Edinger D, Rödl W, Wagner E, Winter G, Besheer A (2012) *Controlled shielding and deshielding of gene delivery polyplexes using hydroxyethyl starch (HES) and alpha-amylase*. *J Control Release*. 2012 Apr 10;159(1):92-103

Fröhlich T\*, Edinger D\*, Kläger R, Troiber C, Salcher E, Badgujar N, Martin I, Schaffert D, Cengizeroglu A, Hadwiger P, Vornlocher HP, Wagner E (2012) *Structure-activity relationships of siRNA carriers based on sequence-defined oligo (ethane amino) amides*. *J Control Release*. 2012 Jun 28;160(3):532-41

Dohmen C, Edinger D, Fröhlich T, Schreiner L, Lächelt U, Troiber C, Rädler J, Hadwiger P, Vornlocher HP, Wagner E (2012) *Nanosized multifunctional polyplexes for receptor-mediated siRNA delivery*. *ACS Nano*. 2012 Jun 26;6(6):5198-208

Fröhlich T, Edinger D, Russ V, Wagner E (2012) *Stabilization of polyplexes via polymer crosslinking for efficient siRNA delivery*. *Eur J Pharm Sci*. 2012 Dec 18;47(5):914-20

Troiber C, Edinger D, Kos P, Schreiner L, Kläger R, Herrmann A, Wagner E (2013) *Stabilizing effect of tyrosine trimers on pDNA and siRNA polyplexes*. *Biomaterials*. 2013 Feb;34(5):1624-33

Noga M, Edinger D, Kläger R, Wegner SV, Spatz JP, Wagner E, Winter G, Besheer A (2013) *The effect of molar mass and degree of hydroxyethylation on the controlled shielding and deshielding of hydroxyethyl starch-coated polyplexes*. *Biomaterials*. 2013 Mar;34(10):2530-8

Daniel Edinger, Raphaela Kläger, Christina Troiber, Christian Dohmen, Ernst Wagner (2013) *Gene Silencing and Antitumoral Effects of Eg5 or Ran siRNA Oligoaminoamide Polyplexes*. Drug Delivery and Translational Research **Accepted**

Matthäus Noga, Daniel Edinger, Ernst Wagner, Gerhard Winter, Ahmed Besheer (2013) *Characterization and biocompatibility of hydroxyethyl starch-polyethylenimine copolymers for DNA delivery*. European Journal of Pharmaceutics and Biopharmaceutics **Submitted**

### **6.2.2 Review**

Edinger D, Wagner E (2011) *Bioresponsive polymers for the delivery of therapeutic nucleic acids*. Wiley Interdiscip Rev Nanomed Nanobiotechnol. 2011 Jan-Feb;3(1):33-46

### **6.2.3 Patent**

Ahmed Besheer, Matthäus Noga, Gerhard Winter, Ernst Wagner, Daniel Edinger *Method for the controlled intracellular delivery of nucleic acids* International Patent Application (WO2013021056A1)

### **6.2.4 Poster Presentations**

Daniel Edinger, Alexander Philipp, Katarina Farkasova and Ernst Wagner *Succinylated PEI as carrier for siRNA delivery in tumor xenograft models: evaluation by RT-qPCR*. 4th Annual Symposium on Nanobiotechnology (NIM), October 5-7, 2010 LMU, Munich, Germany and 17th Annual Meeting German Society for Gene Therapy (DG-GT e.V.), October 7–9, 2010, LMU, Munich, Germany

Raphaela Kläger\*, Daniel Edinger\*, Thomas Fröhlich, Christina Troiber and Ernst Wagner *Development of oligo (aminoethane) amides for in vivo delivery of siRNA*. 18th Annual Meeting German Society for Gene Therapy (DG-GT e.V.), March 15–17, 2012, Frankfurt, Germany

## 7 REFERENCES

- 1 Ginn, S. L., Alexander, I. E., Edelstein, M. L., Abedi, M. R. & Wixon, J. Gene therapy clinical trials worldwide to 2012 - an update. *J Gene Med*, doi:10.1002/jgm.2698 (2013).
- 2 Wagner, E. *et al.* Coupling of adenovirus to transferrin-polylysine/DNA complexes greatly enhances receptor-mediated gene delivery and expression of transfected genes. *Proc.Natl.Acad.Sci.U.S.A* **89**, 6099-6103 (1992).
- 3 Kay, M. A., Glorioso, J. C. & Naldini, L. Viral vectors for gene therapy: the art of turning infectious agents into vehicles of therapeutics. *Nat.Med* **7**, 33-40 (2001).
- 4 Vijayanathan, V., Thomas, T. & Thomas, T. J. DNA nanoparticles and development of DNA delivery vehicles for gene therapy. *Biochemistry* **41**, 14085-14094 (2002).
- 5 Fire, A. *et al.* Potent and specific genetic interference by double-stranded RNA in *Caenorhabditis elegans*. *Nature* **391**, 806-811 (1998).
- 6 Elmen, J. *et al.* LNA-mediated microRNA silencing in non-human primates. *Nature* **452**, 896-899, doi:nature06783 [pii] 10.1038/nature06783 (2008).
- 7 Nimjee, S. M., Rusconi, C. P., Harrington, R. A. & Sullenger, B. A. The potential of aptamers as anticoagulants. *Trends Cardiovasc Med* **15**, 41-45, doi:S1050-1738(05)00003-4 [pii] 10.1016/j.tcm.2005.01.002 (2005).
- 8 Summerton, J. & Weller, D. Morpholino antisense oligomers: design, preparation, and properties. *Antisense Nucleic Acid Drug Dev* **7**, 187-195 (1997).
- 9 Schaffert, D. *et al.* Poly(I:C)-Mediated Tumor Growth Suppression in EGF-Receptor Overexpressing Tumors Using EGF-Polyethylene Glycol-Linear Polyethylenimine as Carrier. *Pharm Res* [**Epub ahead of print**], doi:10.1007/s11095-010-0225-4 (2010).
- 10 Zamore, P. D., Tuschl, T., Sharp, P. A. & Bartel, D. P. RNAi: double-stranded RNA directs the ATP-dependent cleavage of mRNA at 21 to 23 nucleotide intervals. *Cell* **101**, 25-33 (2000).
- 11 Elbashir, S. M. *et al.* Duplexes of 21-nucleotide RNAs mediate RNA interference in cultured mammalian cells. *Nature* **411**, 494-498 (2001).
- 12 Elbashir, S. M., Lendeckel, W. & Tuschl, T. RNA interference is mediated by 21- and 22-nucleotide RNAs 2. *Genes Dev.* **15**, 188-200 (2001).
- 13 Liu, Q. *et al.* R2D2, a bridge between the initiation and effector steps of the *Drosophila* RNAi pathway. *Science* **301**, 1921-1925, doi:10.1126/science.1088710 301/5641/1921 [pii] (2003).
- 14 Wang, H. W. *et al.* Structural insights into RNA processing by the human RISC-loading complex. *Nat Struct Mol Biol* **16**, 1148-1153, doi:nsmb.1673 [pii] 10.1038/nsmb.1673 (2009).
- 15 Rand, T. A., Petersen, S., Du, F. & Wang, X. Argonaute2 cleaves the anti-guide strand of siRNA during RISC activation. *Cell* **123**, 621-629, doi:S0092-8674(05)01107-4 [pii] 10.1016/j.cell.2005.10.020 (2005).
- 16 Rand, T. A., Ginalski, K., Grishin, N. V. & Wang, X. Biochemical identification of Argonaute 2 as the sole protein required for RNA-induced silencing complex activity. *Proc Natl Acad Sci U S A* **101**, 14385-14389,

- doi:10.1073/pnas.0405913101  
0405913101 [pii] (2004).
- 17 Matranga, C., Tomari, Y., Shin, C., Bartel, D. P. & Zamore, P. D. Passenger-strand cleavage facilitates assembly of siRNA into Ago2-containing RNAi enzyme complexes. *Cell* **123**, 607-620, doi:S0092-8674(05)00922-0 [pii] 10.1016/j.cell.2005.08.044 (2005).
- 18 Joshua-Tor, L. siRNAs at RISC. *Structure* **12**, 1120-1122, doi:10.1016/j.str.2004.06.008 S0969212604002199 [pii] (2004).
- 19 Lewis, B. P., Shih, I. H., Jones-Rhoades, M. W., Bartel, D. P. & Burge, C. B. Prediction of mammalian microRNA targets. *Cell* **115**, 787-798, doi:S0092867403010183 [pii] (2003).
- 20 Bartel, D. P. MicroRNAs: target recognition and regulatory functions. *Cell* **136**, 215-233, doi:S0092-8674(09)00008-7 [pii] 10.1016/j.cell.2009.01.002 (2009).
- 21 Wittmann, J. & Jack, H. M. Serum microRNAs as powerful cancer biomarkers. *Biochim Biophys Acta* **1806**, 200-207, doi:S0304-419X(10)00052-1 [pii] 10.1016/j.bbcan.2010.07.002 (2010).
- 22 Petrocca, F. & Lieberman, J. Micromanipulating cancer: microRNA-based therapeutics? *RNA Biol* **6**, 335-340, doi:9013 [pii] (2009).
- 23 Shukla, S., Sumaria, C. S. & Pradeepkumar, P. I. Exploring chemical modifications for siRNA therapeutics: a structural and functional outlook. *ChemMedChem* **5**, 328-349, doi:10.1002/cmcd.200900444 (2010).
- 24 Stenvang, J., Silaharoglu, A. N., Lindow, M., Elmen, J. & Kauppinen, S. The utility of LNA in microRNA-based cancer diagnostics and therapeutics. *Semin Cancer Biol* **18**, 89-102, doi:S1044-579X(08)00005-9 [pii] 10.1016/j.semcancer.2008.01.004 (2008).
- 25 Wilton, S. D. *et al.* Antisense oligonucleotide-induced exon skipping across the human dystrophin gene transcript. *Mol Ther* **15**, 1288-1296, doi:6300095 [pii] 10.1038/sj.mt.6300095 (2007).
- 26 Elmen, J. *et al.* Antagonism of microRNA-122 in mice by systemically administered LNA-antimiR leads to up-regulation of a large set of predicted target mRNAs in the liver. *Nucleic Acids Res* **36**, 1153-1162, doi:gkm1113 [pii] 10.1093/nar/gkm1113 (2008).
- 27 Pei, Y. & Tuschl, T. On the art of identifying effective and specific siRNAs. *Nat Methods* **3**, 670-676, doi:nmeth911 [pii] 10.1038/nmeth911 (2006).
- 28 Allerson, C. R. *et al.* Fully 2'-modified oligonucleotide duplexes with improved in vitro potency and stability compared to unmodified small interfering RNA. *J Med Chem* **48**, 901-904, doi:10.1021/jm049167j (2005).
- 29 Harborth, J. *et al.* Sequence, chemical, and structural variation of small interfering RNAs and short hairpin RNAs and the effect on mammalian gene silencing. *Antisense Nucleic Acid Drug Dev* **13**, 83-105, doi:10.1089/108729003321629638 (2003).
- 30 Prakash, T. P. *et al.* Positional effect of chemical modifications on short interference RNA activity in mammalian cells. *J Med Chem* **48**, 4247-4253, doi:10.1021/jm050044o (2005).
- 31 Elmen, J. *et al.* Locked nucleic acid (LNA) mediated improvements in siRNA stability and functionality. *Nucleic Acids Res* **33**, 439-447, doi:33/1/439 [pii] 10.1093/nar/gki193 (2005).
- 32 Braasch, D. A. *et al.* RNA interference in mammalian cells by chemically-modified RNA. *Biochemistry* **42**, 7967-7975, doi:10.1021/bi0343774 (2003).

- 33 Robbins, M., Judge, A. & MacLachlan, I. siRNA and innate immunity. *Oligonucleotides* **19**, 89-102, doi:10.1089/oli.2009.0180 (2009).
- 34 Lima, W. F. *et al.* Single-stranded siRNAs activate RNAi in animals. *Cell* **150**, 883-894, doi:S0092-8674(12)01009-4 [pii] 10.1016/j.cell.2012.08.014 (2012).
- 35 Yu, D. *et al.* Single-stranded RNAs use RNAi to potently and allele-selectively inhibit mutant huntingtin expression. *Cell* **150**, 895-908, doi:S0092-8674(12)00947-6 [pii] 10.1016/j.cell.2012.08.002 (2012).
- 36 Frohlich, T. & Wagner, E. Peptide- and polymer-based delivery of therapeutic RNA. *Soft Matter* **6**, 226-234, doi:10.1039/b916053a (2010).
- 37 Schaffert, D. & Wagner, E. Gene therapy progress and prospects: synthetic polymer-based systems. *Gene Ther* **15**, 1131-1138 (2008).
- 38 Kukowska-Latallo, J. F. *et al.* Intravascular and endobronchial DNA delivery to murine lung tissue using a novel, nonviral vector 999. *Hum. Gene Ther.* **11**, 1385-1395 (2000).
- 39 Hartmann, L., Hafele, S., Peschka-Suss, R., Antonietti, M. & Borner, H. G. Tailor-Made Poly(amidoamine)s for Controlled Complexation and Condensation of DNA. *Chemistry*. **14**, 2025-2033 (2008).
- 40 Wang, X. L., Nguyen, T., Gillespie, D., Jensen, R. & Lu, Z. R. A multifunctional and reversibly polymerizable carrier for efficient siRNA delivery. *Biomaterials* **29**, 15-22 (2008).
- 41 Schaffert, D. *et al.* Solid-Phase Synthesis of Sequence-Defined T-, i-, and U-Shape Polymers for pDNA and siRNA Delivery. *Angew. Chem. Int. Ed.* **50**, 8986-8989, doi:10.1002/anie.201102165 (2011).
- 42 de Bruin, K. *et al.* Cellular dynamics of EGF receptor-targeted synthetic viruses. *Mol Ther* **15**, 1297-1305 (2007).
- 43 Buyens, K. *et al.* A fast and sensitive method for measuring the integrity of siRNA-carrier complexes in full human serum. *J Control Release* **126**, 67-76 (2008).
- 44 Chen, H. H. *et al.* Quantitative Comparison of Intracellular Unpacking Kinetics of Polyplexes by a Model Constructed From Quantum Dot-FRET. *Molecular Therapy* **16**, 324-332, doi:doi:10.1038/sj.mt.6300392 (2008).
- 45 Matsumoto, Y., Itaka, K., Yamasoba, T. & Kataoka, K. Intranuclear fluorescence resonance energy transfer analysis of plasmid DNA decondensation from nonviral gene carriers. *J Gene Med* **11**, 615-623 (2009).
- 46 Edinger, D. & Wagner, E. Bioresponsive polymers for the delivery of therapeutic nucleic acids. *Wiley Interdiscip Rev Nanomed Nanobiotechnol* **3**, 33-46, doi:10.1002/wnan.97 (2011).
- 47 Huth, S. *et al.* Interaction of polyamine gene vectors with RNA leads to the dissociation of plasmid DNA-carrier complexes. *J. Gene Med.* **8**, 1416-1424 (2006).
- 48 Leonetti, J. P., Degols, G. & Lebleu, B. Biological activity of oligonucleotide-poly(L-lysine) conjugates: mechanism of cell uptake 381. *Bioconjug Chem* **1**, 149-153 (1990).
- 49 Rozema, D. B. *et al.* Dynamic PolyConjugates for targeted in vivo delivery of siRNA to hepatocytes. *Proc. Natl. Acad. Sci. U.S.A* **104**, 12982-12987 (2007).
- 50 Meyer, M. *et al.* Synthesis and Biological Evaluation of a Bioresponsive and Endosomolytic siRNA-Polymer Conjugate. *Mol Pharm* **6**, 752-762, doi:10.1021/mp9000124 (2009).
- 51 Dohmen, C. *et al.* Defined Folate-PEG-siRNA Conjugates for Receptor-specific Gene Silencing. *Mol Ther Nucleic Acids* **1**, e7, doi: 10.1038 (2012).

- 52 Midoux, P. & Monsigny, M. Efficient gene transfer by histidylated polylysine/pDNA complexes. *Bioconjug.Chem.* **10**, 406-411 (1999).
- 53 Behr, J. P., Demeneix, B., Loeffler, J. P. & Perez-Mutul, J. Efficient gene transfer into mammalian primary endocrine cells with lipopolyamine-coated DNA. *Proc.Natl.Acad.Sci.U.S.A* **86**, 6982-6986 (1989).
- 54 Zintchenko, A., Philipp, A., Dehshahri, A. & Wagner, E. Simple Modifications of Branched PEI Lead to Highly Efficient siRNA Carriers with Low Toxicity. *Bioconjug Chem* **19**, 1448-1455 (2008).
- 55 Kukowska-Latallo, J. F. *et al.* Efficient transfer of genetic material into mammalian cells using Starburst polyamidoamine dendrimers. *Proc.Natl.Acad.Sci.U.S.A* **93**, 4897-4902 (1996).
- 56 Tang, M. X. & Szoka, F. C. The influence of polymer structure on the interactions of cationic polymers with DNA and morphology of the resulting complexes 2. *Gene Ther* **4**, 823-832 (1997).
- 57 Fant, K., Esbjorner, E. K., Lincoln, P. & Norden, B. DNA condensation by PAMAM dendrimers: self-assembly characteristics and effect on transcription. *Biochemistry* **47**, 1732-1740, doi:10.1021/bi7017199 (2008).
- 58 Zhou, J. *et al.* PAMAM dendrimers for efficient siRNA delivery and potent gene silencing. *Chem Commun (Camb)*, 2362-2364, doi:10.1039/b601381c [doi] (2006).
- 59 Prevette, L. E., Kodger, T. E., Reineke, T. M. & Lynch, M. L. Deciphering the role of hydrogen bonding in enhancing pDNA-polycation interactions. *Langmuir* **23**, 9773-9784 (2007).
- 60 Philipp, A., Zhao, X., Tarcha, P., Wagner, E. & Zintchenko, A. Hydrophobically modified oligoethylenimines as highly efficient transfection agents for siRNA delivery. *Bioconjug Chem* **20**, 2055-2061, doi:10.1021/bc9001536 (2009).
- 61 Creusat, G. & Zuber, G. Self-assembling polyethylenimine derivatives mediate efficient siRNA delivery in mammalian cells. *Chembiochem* **9**, 2787-2789, doi:10.1002/cbic.200800540 (2008).
- 62 Grayson, A. C., Doody, A. M. & Putnam, D. Biophysical and structural characterization of polyethylenimine-mediated siRNA delivery in vitro. *Pharm.Res.* **23**, 1868-1876 (2006).
- 63 Buyens, K. *et al.* Monitoring the disassembly of siRNA polyplexes in serum is crucial for predicting their biological efficacy. *J Control Release* **141**, 38-41, doi:S0168-3659(09)00613-0 [pii] 10.1016/j.jconrel.2009.08.026 (2010).
- 64 Bolcato-Bellemin, A. L., Bonnet, M. E., Creusat, G., Erbacher, P. & Behr, J. P. Sticky overhangs enhance siRNA-mediated gene silencing. *Proc.Natl.Acad.Sci U.S.A* **104**, 16050-16055 (2007).
- 65 Forrest, M. L., Koerber, J. T. & Pack, D. W. A degradable polyethylenimine derivative with low toxicity for highly efficient gene delivery. *Bioconjug.Chem.* **14**, 934-940 (2003).
- 66 Kloeckner, J., Bruzzano, S., Ogris, M. & Wagner, E. Gene carriers based on hexanediol diacrylate linked oligoethylenimine: effect of chemical structure of polymer on biological properties. *Bioconjug Chem* **17**, 1339-1345 (2006).
- 67 Zugates, G. T. *et al.* Rapid optimization of gene delivery by parallel end-modification of poly(beta-amino ester)s. *Mol Ther* **15**, 1306-1312 (2007).
- 68 Knorr, V., Russ, V., Allmendinger, L., Ogris, M. & Wagner, E. Acetal linked oligoethylenimines for use as pH-sensitive gene carriers. *Bioconjug Chem* **19**, 1625-1634 (2008).
- 69 Knorr, V., Ogris, M. & Wagner, E. An acid sensitive ketal-based polyethylene

- glycol-oligoethylenimine copolymer mediates improved transfection efficiency at reduced toxicity. *Pharm.Res* **25**, 2937-2945 (2008).
- 70 Read, M. L. *et al.* Vectors based on reducible polycations facilitate intracellular release of nucleic acids. *J.Gene Med.* **5**, 232-245 (2003).
- 71 Hoon, J. J. *et al.* Reducible poly(amido ethylenimine) directed to enhance RNA interference. *Biomaterials* **28**, 1912-1917 (2007).
- 72 Lin, C. *et al.* Bioreducible poly(amido amine)s with oligoamine side chains: Synthesis, characterization, and structural effects on gene delivery. *Journal of Controlled Release* **126**, 166-174, doi:DOI: 10.1016/j.jconrel.2007.11.012 (2008).
- 73 Russ, V. *et al.* Improved in vivo gene transfer into tumor tissue by stabilization of pseudodendritic oligoethylenimine-based polyplexes. *J Gene Med* **12**, 180-193, doi:10.1002/jgm.1430 (2010).
- 74 Fröhlich, T., Edinger, D., Russ, V. & Wagner, E. Stabilization of polyplexes via polymer crosslinking for efficient siRNA delivery. *Eur J Pharm Sci* **47**, 914-920, doi:S0928-0987(12)00358-2 [pii] 10.1016/j.ejps.2012.09.006 (2012).
- 75 Fröhlich, T. *et al.* Structure-activity relationships of siRNA carriers based on sequence-defined oligo (ethane amino) amides. *J Control Release*, doi:S0168-3659(12)00206-4 [pii] 10.1016/j.jconrel.2012.03.018 [doi] (2012).
- 76 Lukacs, G. L. *et al.* Size-dependent DNA mobility in cytoplasm and nucleus. *J.Biol Chem* **275**, 1625-1629 (2000).
- 77 Lechardeur, D., Verkman, A. S. & Lukacs, G. L. Intracellular routing of plasmid DNA during non-viral gene transfer. *Adv Drug Deliv.Rev.* **57**, 755-767 (2005).
- 78 Saito, G., Amidon, G. L. & Lee, K. D. Enhanced cytosolic delivery of plasmid DNA by a sulfhydryl-activatable listeriolysin O/protamine conjugate utilizing cellular reducing potential. *Gene Ther* **10**, 72-83 (2003).
- 79 Boeckle, S., Wagner, E. & Ogris, M. C- versus N-terminally linked melittin-polyethylenimine conjugates: the site of linkage strongly influences activity of DNA polyplexes. *J Gene Med* **7**, 1335-1347 (2005).
- 80 Chen, C. P., Kim, J. S., Steenblock, E., Liu, D. & Rice, K. G. Gene transfer with poly-melittin peptides. *Bioconjug Chem* **17**, 1057-1062 (2006).
- 81 Lai, S. K., Hida, K., Chen, C. & Hanes, J. Characterization of the intracellular dynamics of a non-degradative pathway accessed by polymer nanoparticles. *J Control Release* **125**, 107-111 (2008).
- 82 Chen, X., Kube, D. M., Cooper, M. J. & Davis, P. B. Cell surface nucleolin serves as receptor for DNA nanoparticles composed of pegylated polylysine and DNA. *Mol Ther* **16**, 333-342, doi:6300365 [pii] 10.1038/sj.mt.6300365 (2008).
- 83 Sonawane, N. D., Szoka, F. C., Jr. & Verkman, A. S. Chloride Accumulation and Swelling in Endosomes Enhances DNA Transfer by Polyamine-DNA Polyplexes. *J.Biol.Chem.* **278**, 44826-44831 (2003).
- 84 Plank, C., Oberhauser, B., Mechtler, K., Koch, C. & Wagner, E. The influence of endosome-disruptive peptides on gene transfer using synthetic virus-like gene transfer systems. *J Biol.Chem.* **269**, 12918-12924 (1994).
- 85 Nishikawa, M. *et al.* Hepatocyte-targeted in vivo gene expression by intravenous injection of plasmid DNA complexed with synthetic multi- functional gene delivery system. *Gene Ther.* **7**, 548-555 (2000).
- 86 Zauner, W., Blaas, D., Kuechler, E. & Wagner, E. Rhinovirus-mediated endosomal release of transfection complexes. *J Virol.* **69**, 1085-1092 (1995).
- 87 Wyman, T. B. *et al.* Design, synthesis, and characterization of a cationic

- peptide that binds to nucleic acids and permeabilizes bilayers. *Biochemistry* **36**, 3008-3017 (1997).
- 88 Kursa, M. *et al.* Novel Shielded Transferrin-Polyethylene Glycol-Polyethylenimine/DNA Complexes for Systemic Tumor-Targeted Gene Transfer. *Bioconjug.Chem.* **14**, 222-231 (2003).
- 89 Walker, G. F. *et al.* Toward synthetic viruses: endosomal pH-triggered deshielding of targeted polyplexes greatly enhances gene transfer in vitro and in vivo. *Mol Ther* **11**, 418-425 (2005).
- 90 Malek, A., Czubayko, F. & Aigner, A. PEG grafting of polyethylenimine (PEI) exerts different effects on DNA transfection and siRNA-induced gene targeting efficacy. *J Drug Target* **16**, 124-139 (2008).
- 91 Zhang, X. *et al.* Poly(ethylene glycol)-block-polyethylenimine copolymers as carriers for gene delivery: effects of PEG molecular weight and PEGylation degree. *J Biomed Mater Res A* **84**, 795-804 (2008).
- 92 Brus, C., Petersen, H., Aigner, A., Czubayko, F. & Kissel, T. Physicochemical and biological characterization of polyethylenimine-graft-poly(ethylene glycol) block copolymers as a delivery system for oligonucleotides and ribozymes. *Bioconjug Chem* **15**, 677-684, doi:10.1021/bc034160m (2004).
- 93 Oishi, M., Nagasaki, Y., Itaka, K., Nishiyama, N. & Kataoka, K. Lactosylated Poly(ethylene glycol)-siRNA Conjugate through Acid-Labile  $\beta$ -Thiopropionate Linkage to Construct pH-Sensitive Polyion Complex Micelles Achieving Enhanced Gene Silencing in Hepatoma Cells. *Journal of the American Chemical Society* **127**, 1624-1625, doi:10.1021/ja044941d (2005).
- 94 Kim, W. J. *et al.* Anti-angiogenic inhibition of tumor growth by systemic delivery of PEI-g-PEG-RGD/pCMV-sFlt-1 complexes in tumor-bearing mice. *J.Control Release* **114**, 381-388 (2006).
- 95 Beh, C. W. *et al.* Efficient delivery of Bcl-2-targeted siRNA using cationic polymer nanoparticles: downregulating mRNA expression level and sensitizing cancer cells to anticancer drug. *Biomacromolecules* **10**, 41-48, doi:10.1021/bm801109g  
10.1021/bm801109g [pii] (2009).
- 96 Fella, C., Walker, G. F., Ogris, M. & Wagner, E. Amine-reactive pyridylhydrazone-based PEG reagents for pH-reversible PEI polyplex shielding. *Eur.J Pharm.Sci* **34**, 309-320 (2008).
- 97 Taratula, O. *et al.* Surface-engineered targeted PPI dendrimer for efficient intracellular and intratumoral siRNA delivery. *J Control Release* **140**, 284-293, doi:S0168-3659(09)00440-4 [pii]  
10.1016/j.jconrel.2009.06.019 (2009).
- 98 Fisher, K. D. *et al.* A versatile system for receptor-mediated gene delivery permits increased entry of DNA into target cells, enhanced delivery to the nucleus and elevated rates of transgene expression. *Gene Ther.* **7**, 1337-1343 (2000).
- 99 Carlisle, R. C. *et al.* Polymer-coated polyethylenimine/DNA complexes designed for triggered activation by intracellular reduction. *J Gene Med* **6**, 337-344 (2004).
- 100 Hornof, M., de la, F. M., Hallikainen, M., Tammi, R. H. & Urtti, A. Low molecular weight hyaluronan shielding of DNA/PEI polyplexes facilitates CD44 receptor mediated uptake in human corneal epithelial cells. *J Gene Med.* **10**, 70-80 (2008).
- 101 Noga, M. *et al.* Controlled shielding and deshielding of gene delivery polyplexes using hydroxyethyl starch (HES) and alpha-amylase. *J Control Release* **159**, 92-103, doi:S0168-3659(12)00011-9 [pii]  
10.1016/j.jconrel.2012.01.006 (2012).

- 102 Noga, M. *et al.* The effect of molar mass and degree of hydroxyethylation on the controlled shielding and deshielding of hydroxyethyl starch-coated polyplexes. *Biomaterials* **34**, 2530-2538, doi:S0142-9612(12)01405-6 [pii] 10.1016/j.biomaterials.2012.12.025 (2013).
- 103 Hatakeyama, H. *et al.* Development of a novel systemic gene delivery system for cancer therapy with a tumor-specific cleavable PEG-lipid. *Gene Ther* **14**, 68-77 (2007).
- 104 Knorr, V., Allmendinger, L., Walker, G. F., Paintner, F. F. & Wagner, E. An acetal-based PEGylation reagent for pH-sensitive shielding of DNA polyplexes. *Bioconjug Chem* **18**, 1218-1225 (2007).
- 105 Li, Z. *et al.* Identification and characterization of a novel peptide ligand of epidermal growth factor receptor for targeted delivery of therapeutics. *Faseb J* **19**, 1978-1985 (2005).
- 106 Kircheis, R. *et al.* Polyethylenimine/DNA complexes shielded by transferrin target gene expression to tumors after systemic application. *Gene Ther* **8**, 28-40 (2001).
- 107 Wagner, E., Zenke, M., Cotten, M., Beug, H. & Birnstiel, M. L. Transferrin-polycation conjugates as carriers for DNA uptake into cells. *Proc.Natl.Acad.Sci.U.S.A* **87**, 3410-3414 (1990).
- 108 Bellocq, N. C., Pun, S. H., Jensen, G. S. & Davis, M. E. Transferrin-containing, cyclodextrin polymer-based particles for tumor-targeted gene delivery. *Bioconjug.Chem.* **14**, 1122-1132 (2003).
- 109 Tietze, N. *et al.* Induction of apoptosis in murine neuroblastoma by systemic delivery of transferrin-shielded siRNA polyplexes for downregulation of Ran. *Oligonucleotides* **18**, 161-174 (2008).
- 110 Heidel, J. D. *et al.* Administration in non-human primates of escalating intravenous doses of targeted nanoparticles containing ribonucleotide reductase subunit M2 siRNA. *Proc.Natl.Acad.Sci U.S.A* **104**, 5715-5721 (2007).
- 111 Hu-Lieskovan, S., Heidel, J. D., Bartlett, D. W., Davis, M. E. & Triche, T. J. Sequence-specific knockdown of EWS-FLI1 by targeted, nonviral delivery of small interfering RNA inhibits tumor growth in a murine model of metastatic Ewing's sarcoma. *Cancer Res.* **65**, 8984-8992 (2005).
- 112 Davis, M. E. The first targeted delivery of siRNA in humans via a self-assembling, cyclodextrin polymer-based nanoparticle: from concept to clinic. *Mol Pharm* **6**, 659-668, doi:10.1021/mp900015y (2009).
- 113 Davis, M. E. *et al.* Evidence of RNAi in humans from systemically administered siRNA via targeted nanoparticles. *Nature* **464** 1067-1070, doi:nature08956 [pii] 10.1038/nature08956 (2010).
- 114 Xia, W. & Low, P. S. Folate-targeted therapies for cancer. *J Med Chem* **53**, 6811-6824, doi:10.1021/jm100509v (2010).
- 115 Thomas, M. *et al.* Ligand-Targeted Delivery of Small Interfering RNAs to Malignant Cells and Tissues. *Annals of the New York Academy of Sciences* **1175**, 32-39, doi:10.1111/j.1749-6632.2009.04977.x (2009).
- 116 Dohmen, C. *et al.* Nanosized Multifunctional Polyplexes for Receptor-Mediated SiRNA Delivery. *ACS Nano* **6**, 5198-5208, doi:10.1021/nn300960m (2012).
- 117 Thomas, T. P. *et al.* Polyvalent dendrimer-methotrexate as a folate receptor-targeted cancer therapeutic. *Mol Pharm* **9**, 2669-2676, doi:10.1021/mp3002232 (2012).
- 118 Soutschek, J. *et al.* Therapeutic silencing of an endogenous gene by systemic administration of modified siRNAs. *Nature* **432**, 173-178 (2004).

- 119 Zimmermann, T. S. *et al.* RNAi-mediated gene silencing in non-human primates. *Nature* **441**, 111-114 (2006).
- 120 Judge, A. D. *et al.* Confirming the RNAi-mediated mechanism of action of siRNA-based cancer therapeutics in mice. *J Clin Invest* **119**, 661-673, doi:37515 [pii] 10.1172/JCI37515 (2009).
- 121 Harborth, J., Elbashir, S. M., Bechert, K., Tuschl, T. & Weber, K. Identification of essential genes in cultured mammalian cells using small interfering RNAs. *J Cell Sci* **114**, 4557-4565 (2001).
- 122 Valentine, M. T., Fordyce, P. M. & Block, S. M. Eg5 steps it up! *Cell Div* **1**, 31, doi:1747-1028-1-31 [pii] 10.1186/1747-1028-1-31 (2006).
- 123 Kapoor, T. M., Mayer, T. U., Coughlin, M. L. & Mitchison, T. J. Probing spindle assembly mechanisms with monastrol, a small molecule inhibitor of the mitotic kinesin, Eg5. *J Cell Biol* **150**, 975-988 (2000).
- 124 Castillo, A., Morse, H. C., 3rd, Godfrey, V. L., Naeem, R. & Justice, M. J. Overexpression of Eg5 causes genomic instability and tumor formation in mice. *Cancer Res* **67**, 10138-10147, doi:67/21/10138 [pii] 10.1158/0008-5472.CAN-07-0326 (2007).
- 125 Quimby, B. B. & Dasso, M. The small GTPase Ran: interpreting the signs. *Curr Opin Cell Biol* **15**, 338-344 (2003).
- 126 A. Cervantes, M. A., J. Tabernero, J. R. Infante, P. LoRusso, G. Shapiro, L. G. Paz-Ares, R. Falzone, J. Hill, J. Cehelsky, A. White, I. Toudjarska, D. Bumcrot, R. Meyers, G. Hinkle, N. Svrzikapa, D. W. Sah, A. Vaishnav, J. Gollob, H. A. Burris. in *ASCO Annual Meeting* (Chicago, 2011).
- 127 Sazer, S. & Dasso, M. The ran decathlon: multiple roles of Ran. *J Cell Sci* **113** ( Pt 7), 1111-1118 (2000).
- 128 Dasso, M. Running on Ran: nuclear transport and the mitotic spindle. *Cell* **104**, 321-324 (2001).
- 129 Abe, H. *et al.* High expression of Ran GTPase is associated with local invasion and metastasis of human clear cell renal cell carcinoma. *Int.J.Cancer* **122**, 2391-2397 (2008).
- 130 Xia, F., Lee, C. W. & Altieri, D. C. Tumor cell dependence on Ran-GTP-directed mitosis. *Cancer Res* **68**, 1826-1833, doi:68/6/1826 [pii] 10.1158/0008-5472.CAN-07-5279 (2008).
- 131 Akinc, A. *et al.* A combinatorial library of lipid-like materials for delivery of RNAi therapeutics. *Nat.Biotechnol.* **26**, 561-569 (2008).
- 132 Schaffert, D., Badgular, N. & Wagner, E. Novel Fmoc-polyamino acids for solid-phase synthesis of defined polyamidoamines. *Org Lett* **13**, 1586-1589, doi:10.1021/ol200381z (2011).
- 133 Schaffert, D. *et al.* Solid-phase synthesis of sequence-defined T-, i-, and U-shape polymers for pDNA and siRNA delivery. *Angew Chem Int Ed Engl* **50**, 8986-8989, doi:10.1002/anie.201102165 (2011).
- 134 Hartmann, L., Krause, E., Antonietti, M. & Borner, H. G. Solid-phase supported polymer synthesis of sequence-defined, multifunctional poly(amidoamines). *Biomacromolecules*. **7**, 1239-1244 (2006).
- 135 Ziebarth, J. D. & Wang, Y. Understanding the protonation behavior of linear polyethylenimine in solutions through Monte Carlo simulations. *Biomacromolecules* **11**, 29-38, doi:10.1021/bm900842d (2010).
- 136 Troiber, C. *et al.* Stabilizing effect of tyrosine trimers on pDNA and siRNA polyplexes. *Biomaterials* **34**, 1624-1633, doi:S0142-9612(12)01265-3 [pii] 10.1016/j.biomaterials.2012.11.021 (2013).

- 137 Salcher, E. E. *et al.* Sequence-defined four-arm oligo(ethan amino)amides for pDNA and siRNA delivery: Impact of building blocks on efficacy. *J Control Release*, doi:S0168-3659(12)00523-8 [pii] 10.1016/j.jconrel.2012.06.023 (2012).
- 138 Morgan-Lappe, S. E. *et al.* Identification of Ras-Related Nuclear Protein, Targeting Protein for Xenopus Kinesin-like Protein 2, and Stearoyl-CoA Desaturase 1 as Promising Cancer Targets from an RNAi-Based Screen. *Cancer Res* **67**, 4390-4398 (2007).
- 139 Pecot, C. V., Calin, G. A., Coleman, R. L., Lopez-Berestein, G. & Sood, A. K. RNA interference in the clinic: challenges and future directions. *Nat Rev Cancer* **11**, 59-67, doi:nrc2966 [pii] 10.1038/nrc2966 (2011).
- 140 Pai, S. I. *et al.* Prospects of RNA interference therapy for cancer. *Gene Ther* **13**, 464-477 (2006).
- 141 Merkel, O. M. *et al.* Stability of siRNA polyplexes from poly(ethylenimine) and poly(ethylenimine)-g-poly(ethylene glycol) under in vivo conditions: effects on pharmacokinetics and biodistribution measured by Fluorescence Fluctuation Spectroscopy and Single Photon Emission Computed Tomography (SPECT) imaging. *J Control Release* **138**, 148-159, doi:S0168-3659(09)00305-8 [pii] 10.1016/j.jconrel.2009.05.016 (2009).
- 142 Zaghoul, E. M., Viola, J. R., Zuber, G., Smith, C. I. & Lundin, K. E. Formulation and delivery of splice-correction antisense oligonucleotides by amino acid modified polyethylenimine. *Mol Pharm* **7**, 652-663, doi:10.1021/mp900220p (2010).
- 143 Kremer, J. M. Toward a better understanding of methotrexate. *Arthritis & Rheumatism* **50**, 1370-1382, doi:10.1002/art.20278 (2004).
- 144 Turk, M. J. *et al.* Folate-targeted imaging of activated macrophages in rats with adjuvant-induced arthritis. *Arthritis Rheum* **46**, 1947-1955, doi:10.1002/art.10405 (2002).
- 145 McGuire, J. J. Anticancer Antifolates: Current Status and Future Directions. *Current Pharmaceutical Design* **9**, 2593-2613 (2003).
- 146 McGuire, J. J., Mini, E., Hsieh, P. & Bertino, J. R. Role of methotrexate polyglutamates in methotrexate- and sequential methotrexate-5-fluorouracil-mediated cell kill. *Cancer Res* **45**, 6395-6400 (1985).
- 147 Zhang, Y., Satterlee, A. & Huang, L. In vivo gene delivery by nonviral vectors: overcoming hurdles? *Mol Ther* **20**, 1298-1304, doi:mt201279 [pii] 10.1038/mt.2012.79 (2012).
- 148 Bartlett, D. W. & Davis, M. E. Insights into the kinetics of siRNA-mediated gene silencing from live-cell and live-animal bioluminescent imaging. *Nucleic Acids Res* **34**, 322-333 (2006).
- 149 Martin, I. *et al.* Solid-phase-assisted synthesis of targeting peptide-PEG-oligo(ethane amino)amides for receptor-mediated gene delivery. *Org Biomol Chem* **10**, 3258-3268, doi:10.1039/c2ob06907e (2012).
- 150 Creusat, G. *et al.* Proton sponge trick for pH-sensitive disassembly of polyethylenimine-based siRNA delivery systems. *Bioconjug Chem* **21**, 994-1002, doi:10.1021/bc100010k [doi] (2010).
- 151 Huang, Y. *et al.* Elimination pathways of systemically delivered siRNA. *Mol Ther* **19**, 381-385, doi:mt2010266 [pii] 10.1038/mt.2010.266 (2011).
- 152 Zhang, Y., Bradshaw-Pierce, E. L., Delille, A., Gustafson, D. L. & Anchoroquy, T. J. In vivo comparative study of lipid/DNA complexes with different in vitro serum stability: effects on biodistribution and tumor

- accumulation. *J Pharm Sci* **97**, 237-250, doi:10.1002/jps.21076 (2008).
- 153 Ogris, M. & Wagner, E. To be targeted: is the magic bullet concept a viable option for synthetic nucleic Acid therapeutics? *Human gene therapy* **22**, 799-807, doi:10.1089/hum.2011.065 (2011).
- 154 Spinella, M. J., Brigle, K. E., Sierra, E. E. & Goldman, I. D. Distinguishing between folate receptor-alpha-mediated transport and reduced folate carrier-mediated transport in L1210 leukemia cells. *J Biol Chem* **270**, 7842-7849 (1995).
- 155 de Fougerolles, A., Vornlocher, H. P., Maraganore, J. & Lieberman, J. Interfering with disease: a progress report on siRNA-based therapeutics. *Nat Rev Drug Discov* **6**, 443-453, doi:nrd2310 [pii] 10.1038/nrd2310 [doi] (2007).
- 156 Schroeder, A. *et al.* Treating metastatic cancer with nanotechnology. *Nat Rev Cancer* **12**, 39-50, doi:nrc3180 [pii] 10.1038/nrc3180 (2012).
- 157 Bumcrot, D., Manoharan, M., Koteliansky, V. & Sah, D. W. RNAi therapeutics: a potential new class of pharmaceutical drugs. *Nat.Chem Biol* **2**, 711-719 (2006).
- 158 Urban-Klein, B., Werth, S., Abuharbeid, S., Czubayko, F. & Aigner, A. RNAi-mediated gene-targeting through systemic application of polyethylenimine (PEI)-complexed siRNA in vivo. *Gene Ther.* **12**, 461-466 (2005).

## 8 ACKNOWLEDGMENT

Many people turned the 4 years of my PhD thesis into a prosperous and great time. Your assistance and advices made my work successful. For this reason I want to say Thank You.

Foremost, I want to thank my supervisor Prof. Dr. Ernst Wagner for offering me the opportunity to join his research group. I really appreciate your scientific guidance and the trust you put in me creating this atmosphere of creativity and individual freedom.

Special thanks go to Flo who was a really good friend before my PhD thesis and the best friend and much valued colleague during this thesis. Due to the great atmosphere in our group and because of several social events, like the skiing trip, several colleagues became friends. I want to mention Raphaela, Laura, Petra, Rebekka, Alex, Christian, Kevin, Andi and Thomas who were excellent colleagues and turned into good friends. All of you were either “inhabitants” of the PhD room or joined us regularly for a chat or a beer making the work easier. There are so many stories, like the Frankfurt trip, Pharma Parties and PhD celebrations we experienced together making this period of my life unforgettable.

I am also very grateful for the perfect collaboration and the great discussions in the “siRNA group” during the Roche project. Christina, Christian, David, Naresh, Claudia, Edith and Uli supported me with the basis of my work the oligomers. Thanks go to Thomas and Petra for their assistance and great collaboration in cell culture and to Raphaela, Laura and Katarina for introducing me into mouse experiments. Big thanks also go to Wolfgang the good soul of our research group. Also Miriam, Anna, Ursula and Markus did a great job and always kept the lab running. Many thanks go to Martina who patiently helped me to understand the plant anatomy. After supervising the PB1 practical course for 8 times I am still not sure how I could pass the test when I was a student. Many thanks go also to my collaboration partners especially to my college friend Matthäus.

As life is not just about work I want to thank my friends and my girlfriend Caro reminding me to keep work and life in balance. “Super” thanks go also to my father for free habitation and to the whole family for always supporting me!